

Review

Not peer-reviewed version

---

# Titanium Dioxide and Photocatalysis: a Detailed Overview of the Synthesis, Applications, Challenges, Advances and Prospects for Sustainable Development

---

[Dilshod Nematov](#)<sup>\*</sup>, Anushervon Ashurov, Mufazzala Umarzoda

Posted Date: 29 November 2024

doi: 10.20944/preprints202408.1733.v2

Keywords: TiO<sub>2</sub>, thin films; catalytic reactions; photocatalysis; photocatalyst; surface interaction; nanomaterials; water purification; sustainable development



Preprints.org is a free multidisciplinary platform providing preprint service that is dedicated to making early versions of research outputs permanently available and citable. Preprints posted at Preprints.org appear in Web of Science, Crossref, Google Scholar, Scilit, Europe PMC.

Copyright: This open access article is published under a Creative Commons CC BY 4.0 license, which permit the free download, distribution, and reuse, provided that the author and preprint are cited in any reuse.

Review

# TiO<sub>2</sub> for Photocatalysis and Energy Conversion: A Detailed Overview of the Synthesis, Applications, Challenges, Advances and Prospects for Sustainable Development

Dilshod Nematov \*, Anushervon Ashurov, Sayfiddin Giesov and Mufazzala Umarzoda

S.U. Umarov Physical-Technical Institute of NAST, 734042 Dushanbe, Tajikistan

\* Correspondence: Dilshod Nematov, PhD, Head of Laboratory, S.U. National Academy of Sciences of Tajikistan, Umarov Institute of Physics and Technology, 33 Rudaca Street, Dushanbe, 734042, Tajikistan; Email: dilnem@mail.ru

**Abstract:** The term “photocatalysis” has recently gained high popularity, and various products using photocatalytic functions have been commercialized. Of all the materials that may be used as photocatalysts, titanium dioxide (TiO<sub>2</sub>) is virtually the only one that is now and most likely will remain appropriate for industrial application. Water and air purification systems, sterilization, hydrogen evolution, self-cleaning surfaces, and photoelectrochemical conversion are just a few of the products and applications in the environmental and energy domains that make extensive use of TiO<sub>2</sub> photocatalysis. This is due to the fact that TiO<sub>2</sub> has the lowest cost, most stability, and most effective photoactivity. Furthermore, history attests to its safety for both people and the environment because it has been used as a white pigment since antiquity. This review discusses some important aspects and issues concerning different synthesis methods and their influence on the structure and properties of TiO<sub>2</sub>, as well as the concept of photocatalysis based on it as a promising biocompatible functional material that has been widely used in recent years. The advantages of TiO<sub>2</sub> applications in various fields of science and technology are discussed, including environmental protection, photocatalysis including self-cleaning surfaces, water and air purification systems, hydrogen liberation, photovoltaic energy, cancer diagnosis and therapy, coatings and dental products, etc. Information on the structure and properties of TiO<sub>2</sub> phases is presented, as well as modern methods of synthesizing functional materials based on it. A detailed review of the basic principles of TiO<sub>2</sub> photocatalysis is then given, with a brief introduction to the modern concept of TiO<sub>2</sub> photocatalysis. Recent advances in the fundamental understanding of TiO<sub>2</sub> photocatalysis at the atomic-molecular level are highlighted, and advances in TiO<sub>2</sub> photocatalysis from the perspective of design and engineering of new materials are discussed. The challenges and prospects of TiO<sub>2</sub> photocatalysis are briefly discussed.

**Keywords:** TiO<sub>2</sub>; thin films; catalytic reactions; photocatalysis; photocatalyst; surface interaction; nanomaterials; water purification; sustainable development

## 1. Introduction

Fossil fuel usage is rising quickly due to the expansion of human society and unchecked industrial progress. The development of clean, safe, and sustainable energy technologies is therefore one of the most pressing issues facing humanity today, especially for researchers in related physical and chemical sciences. Otherwise, the world population may face future pollution (e.g., toxic emissions and industrial waste), resource and energy scarcity[1–4]. Solar energy is easily turned into chemical and electrical energy, making it one of the most significant clean and renewable energy sources on Earth[5]. One way to produce pure hydrogen (H<sub>2</sub>) is through solar water splitting[6,7]. To address the global energy and environmental issues, solar-powered clean energy solutions have to be extensively researched and implemented. Of all the energy technologies, one of the most significant developments in this regard is photocatalysis, which uses solar energy to regulate energy and chemical reactions[8–11].

Back in 1901, the Italian chemist Giacomo Chamizian conducted experiments on the systematic study of the effect of light on chemical reactions[12,13]. However, photocatalyst was not used in these experiments. Only in 1911, the key word “photocatalysis” appeared in scientific literature for the first time[14,15]. Then it was reported that ZnO was a photocatalyst for the bleaching of Prussian blue and other reactions, including the reduction of  $\text{Ag}^+$  to Ag[16]. In 1932, titanium dioxide ( $\text{TiO}_2$ ) and  $\text{Nb}_2\text{O}_5$  were found to be active in the photocatalytic reduction of  $\text{AuCl}_3$  and  $\text{AgNO}_3$  to Au and Ag, respectively[17]. Later, in 1938,  $\text{TiO}_2$  was first used as a photosensitizer for the bleaching of O<sub>2</sub> dyes[18], but at that time, researchers did not pay much attention to photocatalysis due to the lack of practical applications. In the early 1970s, the “oil crisis” and the environmental impact of industrial plants led scientists to search for alternative and renewable energy sources[19–22]. Just since that time, several pioneering works in this direction have been reported. In 1968, it was discovered that O<sub>2</sub> is formed on  $\text{TiO}_2$  in an electrolytic cell under ultraviolet (UV) light[22,23]. In 1972, Fujishima and Honda[22] experimentally showed that photoelectrochemical cleavage of H<sub>2</sub>O to produce O<sub>2</sub> and H<sub>2</sub> on  $\text{TiO}_2$  on platinum black dye electrode and can be achieved by irradiating  $\text{TiO}_2$  electrode with UV light. The photocatalytic splitting of H<sub>2</sub>O on  $\text{TiO}_2$  powder to form H<sub>2</sub> and O<sub>2</sub> with a molar ratio of 2:1 in an argon atmosphere was also reported in 1977[24,25]. A little later, it became known that methanol ( $\text{CH}_3\text{OH}$ ), as a sacrificial reagent, can significantly enhance the photocatalytic production of H<sub>2</sub> from  $\text{CH}_3\text{OH}$ -H<sub>2</sub>O mixture[26]. In addition, photocatalytic reduction of CO<sub>2</sub> using different types of semiconductors as photocatalysts has been reported[27–30]. These pioneering works have shown that photocatalysis will be used in many fields in the future, and tremendous research attention has been paid to similar reactions using  $\text{TiO}_2$  as a photocatalyst in recent years. Besides  $\text{TiO}_2$ , various other materials such as  $\text{Ta}_2\text{O}_5$ ,  $\text{Ta}_3\text{N}_5$ ,  $\text{SrTiO}_3$ ,  $\text{Ag}_3\text{PO}_4$ ,  $\text{BiVO}_4$ ,  $\text{MoS}_2$ ,  $\text{WSe}_2$ ,  $\text{LaTiO}_3$ ,  $\text{SrTaO}_2\text{N}$ ,  $\text{CdS}$ ,  $\text{TaON}$ ,  $\text{RuO}_2$ ,  $\text{Nb}_2\text{O}_5$  and their nanoparticles, have been applied directly to enable the utilization of solar energy for various photocatalytic reactions[31–58]. Due to the rapid increase in the use of heterogeneous photocatalysis, the literature describing this field has been summarized in numerous publications that not only review the development of photocatalysts and the characterization of photocatalytic processes, but also point out the challenges and opportunities encountered in heterogeneous photocatalysis[59–68].

For example, the main problems due to which  $\text{TiO}_2$  still does not recommend itself very well in mastabic applications for water disinfection and detoxification[59–61] have been studied and the influence of morphology on the photocatalytic reaction, the rate and yield of the photocatalysis product have been studied for some materials[62–67]. It has been shown that the creation of heterojunctions including doping, modification of oxygen vacancies, loading the heterojunction with support components and controlling the crystal face will positively affect the photocatalytic properties of the photocatalyst [68–73].

Among various photocatalysts,  $\text{TiO}_2$ , as the most widely used “promising” photocatalyst, has been widely used in heterogeneous photocatalysis because of its chemical stability, non-toxicity and low cost[68–79].

$\text{TiO}_2$ -based photocatalysts exhibit good biocompatibility, and are widely used for the efficient removal of pharmaceutical contaminants in water and other liquids[74]. Metal-free thiophene-based organic frameworks have also been shown to provide efficient photocatalytic hydrogen release by accelerating interfacial charge transfer [75]. Perovskite photocatalysts and carbon quantum dots also showed good activity in the photocatalytic reaction of CO<sub>2</sub> reduction and water purification[76–79]. In the past two decades, heterogeneous photocatalysis of  $\text{TiO}_2$  has spread very rapidly, undergoing various energy and environmental challenges such as direct solar splitting of H<sub>2</sub>O into H<sub>2</sub> and decomposition of pollutants[80]. Although much progress has been made in heterogeneous  $\text{TiO}_2$  photocatalysis, much remains unknown, which poses an interesting challenge not only to engineers but also to basic research scientists. Generally, a typical  $\text{TiO}_2$  photocatalytic reaction contains many fundamental processes, including charge carrier formation, separation, relaxation, trapping, transport, recombination and transport, and bond breaking/forming, which need to be thoroughly investigated. Only when all these fundamental processes are clearly identified can a better

understanding of TiO<sub>2</sub> photocatalysis be achieved[81–83], which is vital for the development of new photocatalysts and the characterization of new photocatalytic processes.

Ideally, investigating the fundamental processes of TiO<sub>2</sub> photocatalysis under real environmental conditions (e.g., in solution) is the best way to gain a deep understanding of TiO<sub>2</sub> photocatalysis. At present, the processes of charge carrier formation, separation, relaxation, capture, recombination and transport, as well as the stages of single charge transfer in TiO<sub>2</sub> photocatalysis have been systematically investigated by various methods using appropriate electron acceptors or electron donors under real environmental conditions[84–87]. However, in TiO<sub>2</sub> photocatalysis, the whole reaction is usually completed by several charge transfer and bond breaking / bond formation steps. In addition, most of the reactants are neither good electron acceptors nor good electron donors. This makes it very difficult to identify mechanistic studies of TiO<sub>2</sub> photocatalysis under real environmental conditions. To achieve this goal, a number of surface science methods (including desorption-oriented methods, spectroscopy and electron spectroscopy) have been used to investigate the photocatalytic reactions on single crystal TiO<sub>2</sub> surfaces to provide important information for TiO<sub>2</sub> photocatalysis and gain an in-depth understanding of TiO<sub>2</sub> photocatalysis[88–91]. Therefore, fundamental studies of photocatalytic reactions on various TiO<sub>2</sub> single crystal surfaces (rutile and anatase) have been mainly carried out in recent years. Due to the chemical stability and ease of preparation of rutile TiO<sub>2</sub> (110), this surface has become one of the most widely studied surfaces to gain a fundamental understanding of adsorption, thermal and photochemical reactions of adsorbates on TiO<sub>2</sub> surfaces[92–98]. Using scanning tunneling microscopy (STM) and other ensemble averaging techniques (electron / photon / desorption spectroscopy), the adsorption, diffusion and reaction of various adsorbates in TiO<sub>2</sub> photocatalysis can be clearly identified at the molecular level on TiO<sub>2</sub> model surfaces[99–106], which can provide important information for understanding the photocatalysis of TiO<sub>2</sub> under real environmental conditions. As a result, a considerable amount of research has focused on the fundamental processes of TiO<sub>2</sub> photocatalysis, and many studies in this area have been summarized in a large number of reviews[32–56,107–116]. Photocatalytic processes in TiO<sub>2</sub> are due to the formation of photogenerated charge carriers (holes and electrons), which occurs upon absorption of ultraviolet (UV) light corresponding to the band gap[35–39]. The photogenerated holes in the valence band diffuse to the TiO<sub>2</sub> surface and react with adsorbed water molecules to form hydroxyl radicals (radical •OH)[38,55,56]. The photogenerated holes and hydroxyl radicals oxidize nearby organic molecules on the TiO<sub>2</sub> surface[41–47]. At the same time, electrons in the conduction band are usually involved in reductive processes, which usually react with molecular oxygen in air to form superoxide radical anions (radical O<sub>2</sub>•)[48–54].

TiO<sub>2</sub> surfaces have been shown to become superhydrophilic with a contact angle of less than 5° when irradiated with UV light[107–110]. The study showed that the superhydrophilicity is due to chemical conformational changes in the surface [107–110]. It is assumed that most of the holes are subsequently consumed by direct reaction with adsorbed organics or adsorbed water, forming •OH radicals as previously described [112]. However, a small fraction of the holes are trapped at lattice oxygen sites and can react with TiO<sub>2</sub> itself, weakening the bonds between titanium and lattice oxygen ions. Water molecules can break these bonds, forming new hydroxyl groups[107–114]. Single-coordinated OH-groups formed under UV irradiation are thermodynamically less stable and have high surface energy, which again leads to the formation of a superhydrophilic surface[115,116]. It is generally believed that the bond breaking / forming stages in TiO<sub>2</sub> photocatalysis are induced by photogenerated electrons / holes[117–121].

However, a complete understanding of how photogenerated charge carriers contribute to bond formation / breaking in TiO<sub>2</sub> photocatalysis is still lacking, which is crucial to unravel the nature of TiO<sub>2</sub> photocatalysis. Fundamental studies of these processes using surface science techniques are needed to achieve a thorough understanding of these processes. In this review, we aim to provide a comprehensive overview of TiO<sub>2</sub> photocatalysis and its applications.

## 2. TiO<sub>2</sub>, Synthesis, Characterization and Properties

### 2.1. Brief Introduction and Applications of TiO<sub>2</sub>



TiO<sub>2</sub>, also known as titanium (IV) oxide, is the inorganic compound derived from titanium with the chemical formula TiO<sub>2</sub>. TiO<sub>2</sub> as a white inorganic powder, has been industrially produced and used in a wide variety of industries for more than a century[122–127]. Due to its non-toxic properties, light scattering ability, UV resistance and ultra-white color, TiO<sub>2</sub> is used in a thousand different products, because it enhances the whiteness, brightness and attractiveness of products. In nature, TiO<sub>2</sub> is found in the form of the minerals rutile, anatase and brookite. TiO<sub>2</sub> production is steadily increasing worldwide, as the demand for it is constantly growing. TiO<sub>2</sub> is extracted in several countries from titanium-containing raw materials, primarily from ilmenite ore, which contains up to 60% TiO<sub>2</sub>. [128]. It should be noted that only 5% of raw materials are used to produce pure titanium, and the rest is used to produce its oxides[129].

In terms of properties, TiO<sub>2</sub> is a versatile semiconductor material that has attracted considerable attention in recent years due to its potential in photocatalytic applications and environmental sensing. Due to its large surface area, chemical stability, unique electronic and optical properties, TiO<sub>2</sub> has been investigated for the determination of various volatile organic compounds (VOCs) in air and water[131,132]. TiO<sub>2</sub>-based sensors have been developed for the detection of various VOCs, including benzene, toluene, xylene, and formaldehyde, with high sensitivity and selectivity. TiO<sub>2</sub>-based sensors are also used to detect gases such as nitrogen dioxide and ozone, which are major air pollutants. In addition, the application of TiO<sub>2</sub> photocatalysis to decompose organic pollutants in water and air makes it a promising material for environmental remediation[133–135].

Having a specific gravity of 3.9-4.2, a melting point of 1,854°C, and a hardness of 5.5-6.5, titanium oxide (TiO<sub>2</sub>) is soluble in hot sulfuric and hydrofluoric acids, but insoluble in water, organic acids, and dilute alkaline solutions[136,137]. Titanium dioxide is a wide bandgap semiconductor. Its anatase structure, located in the UV region of the spectrum (100-400nm), has an optical gap of 3.2eV and an absorption edge of 388nm[138]. In the visible region of the spectrum (400-700nm), rutile has a lower optical gap of 3.02eV with an absorption edge of 410nm, while the brookite phase absorbs light in the near visible region with an energy gap of 2.96eV[139]. TiO<sub>2</sub> thin films absorb UV light well but show good transparency in the visible wavelength range[139]. At  $\lambda=550\text{nm}$ , the rutile phase of TiO<sub>2</sub> thin films has a refractive index of 2.8, while the anatase phase has a refractive index of 2.49. TiO<sub>2</sub> used in industry is shown in Figure 1[140]. With a high dielectric coefficient of 80-110 for the rutile phase and 50-60 for the anatase phase, TiO<sub>2</sub> is electrically insulating. Its electrical resistance to breakdown voltage is 4kVmm<sup>-1</sup> [140–143]. Compared to semiconductors such as SnO<sub>2</sub>, which has a resistivity of 30  $\Omega\cdot\text{cm}$ , the surface electrical resistivity of thin films for anatase and rutile structures is 1,012  $\Omega\cdot\text{cm}$ , which is a high resistivity[144].

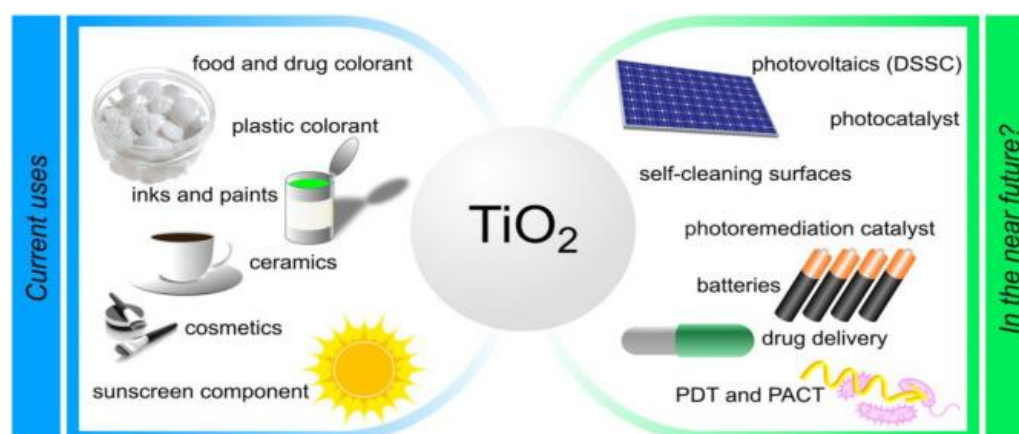


**Figure 1.** Current applications and potential future use of TiO<sub>2</sub>.

Due to its high dielectric coefficient, this material has several applications including anti-reflection surfaces and metal-oxide-semiconductor field-effect transistors as a dielectric gate material[145]. An electron is excited from the valence bands (VB) to the conduction band (CB) of a semiconductor when a photon with energy equal to or greater than the gate energy (greater than 3eV

for TiO<sub>2</sub>) hits the semiconductor[146]. As a result, an electron-hole pair is formed. These charge carriers can react with an electron donor or acceptor, becoming trapped, or recombine with radiation and dissipate energy as heat when indirect gap semiconductors (or direct gap semiconductors) are used[147]. Due to its excellent advantages, TiO<sub>2</sub>-based materials are attracting more and more attention every day, and hundreds of studies are devoted to their properties and applications every year. However, despite numerous works in this field, many aspects and problems still remain insufficiently studied and relevant. This statement highlights the need for an in-depth study of TiO<sub>2</sub> and emphasizes the significance of our review article.

2.2. Crystal Structures of TiO<sub>2</sub>

TiO<sub>2</sub> belongs to the class of transition metal oxides and has several modifications: anatase, rutile, brookite, TiO<sub>2</sub> (B), TiO<sub>2</sub> (II), and TiO<sub>2</sub> (H)[148–152]. It is worth noting that the first three are widely distributed in nature. TiO<sub>2</sub> (B), with monoclinic structure is also found in nature, but rarely. TiO<sub>2</sub> (II) with the structure of PbO<sub>2</sub> and TiO<sub>2</sub> (H) with the structure of hollandite were obtained artificially from rutile under high-pressure conditions. In this review, only the main three crystal structures, anatase, rutile, and brookite, are discussed and their characteristics are summarized in Table 1[150–153].

Table 1. Characteristics of the Crystalline Structure of TiO<sub>2</sub>.

| Parameter                    | Anatase                | Rutile                 | Brookite                         |
|------------------------------|------------------------|------------------------|----------------------------------|
| Crystal structure            | Tetragonal             | Tetragonal             | Rhombic                          |
| Lattice parameters (nm)      | a=0.3784<br>c=0.9515   | a=0.45936<br>c=0.29587 | a=0.9184<br>b=0.5447<br>c=0.5154 |
| Density (g/cm <sup>3</sup> ) | 3.79                   | 4.13                   | 3.99                             |
| Space group                  | L4/amd                 | P4/mnm                 | Pbca                             |
| Number of units in cell      | 2                      | 2                      | 4                                |
| O-Ti-O bond angle            | 77.7°, 92.6°           | 81.2°, 90.0°           | 77.0°-105°                       |
| Ti-O bond length (nm)        | 0.1937(4)<br>0.1965(2) | 0.1949(4)<br>0.1980(2) | 0.187-0.204                      |

Each of these crystal structures has a unique arrangement of atoms and lattice parameters, but the basis of the crystal structure of these polymorphic modifications are TiO<sub>6</sub> octahedrons (see Figure 2)[154]. The octahedrons are arranged in such a way that they may share common vertices or edges. In anatase there are 4 common edges per octahedron, in rutile there are 2[148]. Anatase has a tetragonal lattice with space group L4/amd and rutile P4/mnm, while the space group number of anatase and rutile is 141 and 136, respectively. This is the reason for the difference of their characteristics. TiO<sub>2</sub> with the structure of brookite belongs to the rhombic crystal system, with space group Pbca (space group number 29). In brookite, each octahedron shares common edges with two neighboring octahedrons, and they have a shorter length than the others. The unit cell consists of 8 TiO<sub>2</sub> units and is formed from TiO<sub>6</sub> octahedra (see Figure 2C). Brookite has a more complex unit cell structure, larger volume, and is also the least dense of the 3 considered forms and is not often used for experimental studies[148].

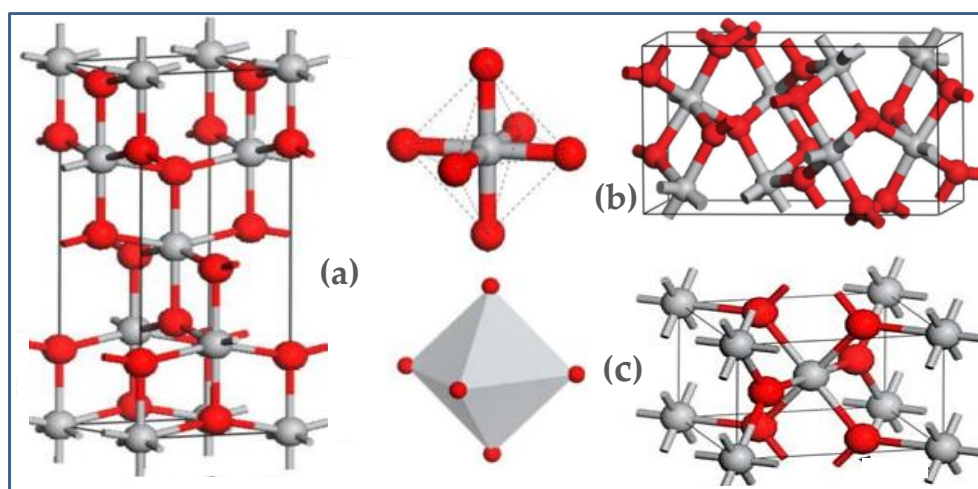


**Figure 2.** Crystal structure of  $\text{TiO}_2$ : anatase (A), brookite (B), rutile (C) during thermal treatment, anatase and brookite change to rutile at temperatures of 400-1000°C and ~750°C, respectively.

### 2.3. Electronic Properties and Band Structure

The electronic structure of  $\text{TiO}_2$  has been well studied using various approaches[155–157]. The  $\text{TiO}_2$  phases described above often have  $\text{O}_2\text{p}$  and  $\text{Ti}3\text{d}$  states near their band edges, respectively, in their VBs (VB) and CB. A large bandgap (BG) makes stoichiometric  $\text{TiO}_2$  an excellent electrical insulator[158]. However, all of the  $\text{TiO}_2$  crystalline materials contain point defects, such as Ovs, interstitial titanium ions ( $\text{Ti}^{3+}$ ), and substituted ions. Within crystalline materials, interstitial ions and vacancies are intrinsic imperfections that can have a substantial impact on the materials' electrical conduction, mass transport, and catalytic properties. New electronic states, referred to as defect states, are introduced by point defects into the  $\text{TiO}_2$  bandgap (Figure 3)[159]. The phases and surface features of  $\text{TiO}_2$  influence the locations of defect states in the BG. R- $\text{TiO}_2$  (110) defect states, for instance, are situated roughly 0.8-1.0eV below the CB edge[160]. On the other hand, A- $\text{TiO}_2$  (101) defect states are situated approximately 0.4-1.1eV below the CB edge[161].

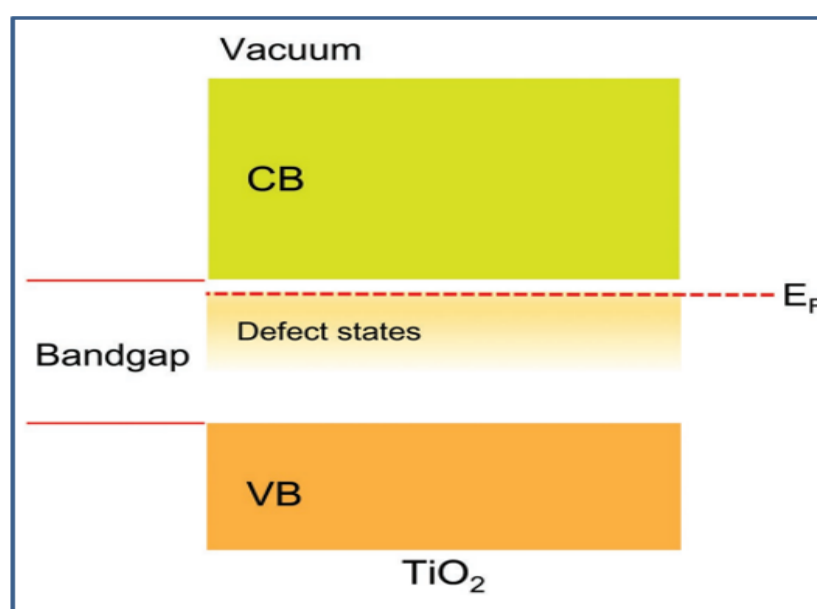


**Figure 3.** Schematic diagram of the electronic structure of  $\text{TiO}_2$ . Reprinted with permission from [159]. Copyright 2019, WILEY-VCH Verlag GmbH & Co. KGaA, Weinheim.

Photoemission experiments[162] report no band bending on the stoichiometric defect-free  $\text{TiO}_2$  surfaces (e.g., R- $\text{TiO}_2$ (110) and R- $\text{TiO}_2$ (100)).  $\text{TiO}_2$  is actually an n-type semiconductor due to point

defects that can occur in the bulk or on the surface. When surface lattice oxygen atoms are removed during the preparation process, unpaired electrons (in the  $Ti_{3d}$  orbitals) remain on the surfaces, which is how defects on  $TiO_2$  surfaces often appear as Ovs[163]. This is one of the BG's defect states' sources. As seen in Figure 4, the extra electrons given up by Ovs (which function as donor states) will collect in the near-surface region and cause a downward bending of the band[164]. In practical scenarios, charge transfer between the surface and adsorbates will occur when electron-rich  $TiO_2$  surfaces adsorb different adsorbates. This could potentially change the direction of the band bend and further influence the chemistry of the  $TiO_2$  surface. The VB of  $TiO_2$  is formed by external p - electrons of oxygen, and the bottom of the CB is predominantly formed by excited titanium ions[156]. Of particular importance for the electronic properties of  $TiO_2$  is the presence of partially reduced titanium ( $Ti^{3+}$ ), the level of which is located  $\sim 0.2-0.8eV$  below the CB[157] and acts as donors. The presence of  $Ti^{3+}$  determines in many cases the conductivity of  $TiO_2$ . The resistivity of pure anatase and rutile are in the range of  $10^4-10^7\Omega\cdot cm$ , but when  $Ti^{3+}$  is formed, it decreases to  $10^{-1}\Omega\cdot cm$  for anatase and  $10^2\Omega\cdot cm$  for rutile[165]. With the nanotube structure of  $TiO_2$ , its conductivity is important because it determines the efficiency with which electrons can be transferred along the length of the nanotubes. Thus, the electronic properties of  $TiO_2$  are mainly determined by the crystal structure and the presence of  $Ti^{3+}$ .  $TiO_2$  has an inherent bend in the space charge region at the semiconductor / electrolyte interface, which is characteristic of a group of semiconductors. This bend is formed spontaneously on the surface and has a steeper bend in anatase than in rutile[166].

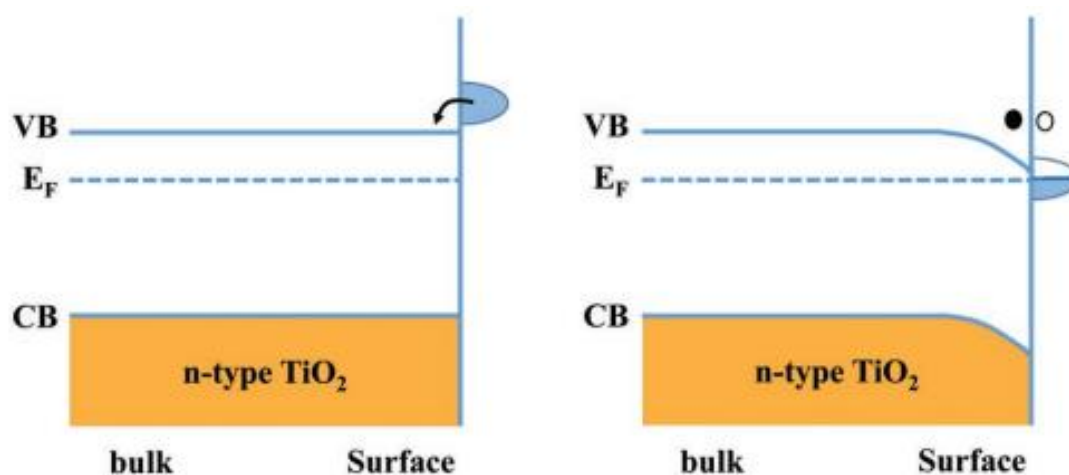


**Figure 4.** Scheme of surface band bending on a clean  $TiO_2$  surface under vacuum conditions, induced by the donor - like surface defect states (●, electron; ○, hole). Reprinted with permission from [159]. Copyright 2019, WILEY-VCH Verlag GmbH & Co. KGaA, Weinheim.

In  $TiO_2$  with anatase structure, the process of hole capture by the surface dominates, since the spatial charge separation is achieved due to the transfer of photogenerated holes to the particle surface through a steep upward bend of the zones. In this case, in the rutile phase there is a bulk recombination of electrons and holes, and only holes generated very close to the surface are transferred to the surface. It is known that the concentration of charge carriers determines the depth of the bulk charge region[167]. The presence of impurities in the  $TiO_2$  structure can contribute to an increase or decrease in the concentration of electrons and holes. Therefore, the presence of impurity compounds has a significant effect on the depth of the volume charge region bending and the photocatalytic activity of  $TiO_2$ .

#### 2.4. Optical Properties of $TiO_2$

$TiO_2$  belongs to semiconductors with a wide BG width. According to literature data, the forbidden band width for anatase structure is 3.2eV, brookite is 3.3eV, and rutile is 3.0eV[156]. Figure 5 shows the absorption spectrum of  $TiO_2$  with anatase structure.



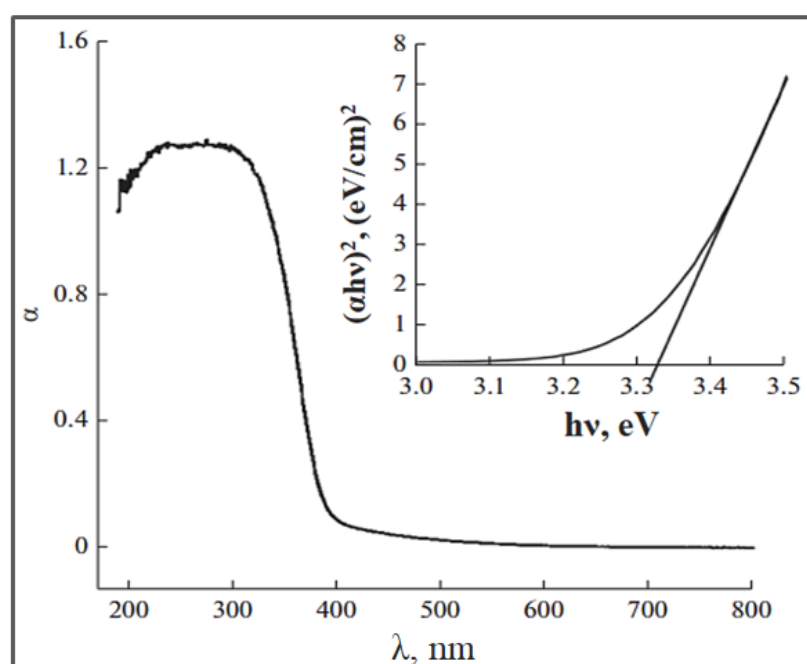


**Figure 5.** Absorption spectrum of TiO<sub>2</sub> with anatase structure.

As can be seen from Figure 5, the absorption spectrum of TiO<sub>2</sub> is limited to the UV region of solar radiation. Consequently, pure TiO<sub>2</sub> exhibits photocatalytic activity only when irradiated with UV light whose wavelength is less than 400nm. In the solar spectrum, the share of UV light does not exceed 7%[168,169]. To utilize the energy of visible radiation, it is necessary to expand the absorption spectrum of TiO<sub>2</sub>. This would allow the utilization of solar radiation for photocatalytic processes. In the last 5 years, there have been many studies based on the idea of extending the wavelength range of photoactivation of TiO<sub>2</sub> in the visible light region and improving the efficiency of solar energy utilization. Activation and optimization of TiO<sub>2</sub> by visible light can be done by implanting metal ions, doping non-metallic atoms or sensitizing TiO<sub>2</sub> with dyes. Therefore, many efforts have been directed to overcome the drawbacks and optimize the absorptivity and photocatalytic properties of TiO<sub>2</sub>, especially in the visible light range. Among them, ionic and cationic doping with the formation of structure defects is an effective approach[170,171]. The possibility of using these approaches is precisely due to the fact that the energy levels of such defects can be located in the forbidden zone, so that the absorption of light by defects (impurity absorption) is also possible in the longer wavelength region[171]. In many works, it has been shown that modified TiO<sub>2</sub> has a higher efficiency compared to pure TiO<sub>2</sub>, but the conversion efficiency depends on many other parameters, such as the concentration of the doping additive, the energy levels of the additive in the TiO<sub>2</sub> lattice, the distribution of doping atoms in the unit cell, etc.[169–174]. According to the literature[173], the presence of metal ion in the TiO<sub>2</sub> matrix significantly affects the absorption spectrum, the recombination rate of charge carriers and their dynamics, on the surface. At doping with metal ions often observed bathochromic effect, due to the emergence of additional levels in the forbidden zone. Doping of ions with stable configuration, such as Fe<sup>3+</sup>, Gd<sup>3+</sup>, Ru<sup>3+</sup> and Os<sup>3+</sup> leads to the narrowing of the forbidden zone or the appearance of additional energy levels[174], which improve charge transfer to the semiconductor surface and contribute to the absorption of visible light, improving their optoelectronic properties.

In most cases, TiO<sub>2</sub> doped with nonmetallic elements in the anionic site shows an increase in absorption in the UV-visible part of the spectrum. For example, N-doped TiO<sub>2</sub> has recently been shown to be more active than pure TiO<sub>2</sub> (Figure 6)[175].

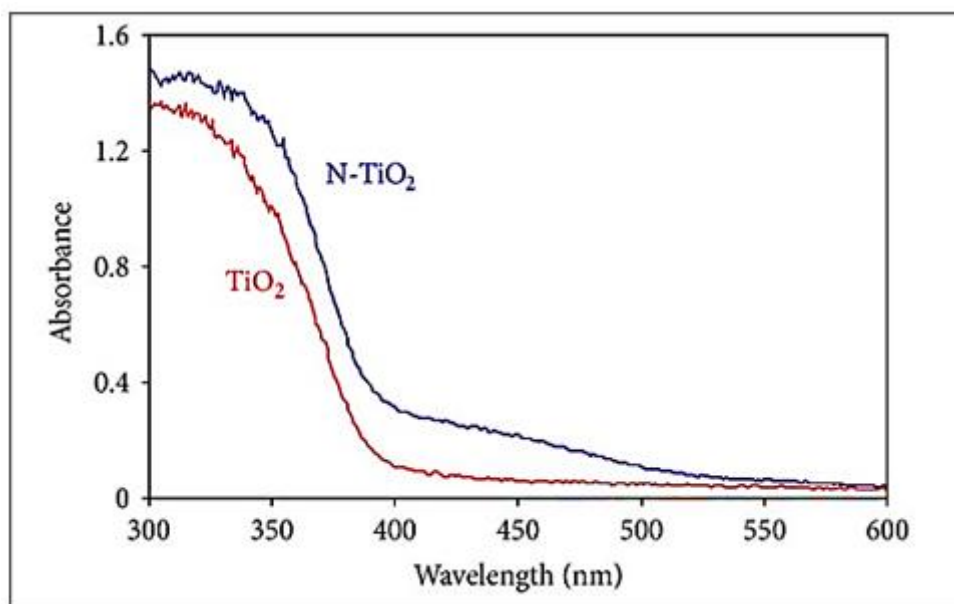


**Figure 6.** Ultraviolet-visible absorption spectrum of  $\text{TiO}_2$  and  $\text{N-TiO}_2$ . Reprinted with permission from [175]. Copyright 2013 WILEY-VCH. Source: <https://onlinelibrary.wiley.com/doi/10.1155/2013/104019>.

The study shows that doping nitrogen at the titanium position shifts the absorption edge to lower energies and increases the absorption capacity of the material in the visible region by reducing the forbidden band width[176,177]. Moreover, it is shown that doping nitrogen in the oxygen position is highly optimal due to comparable atom size, small ionization energy, and stability as well as shallow donor and acceptor levels in the CB and VB due to oxygen vacancy[177]. It has also been reported that  $\text{TiO}_2$  (anatase and rutile) containing nitrogen in the interstitials of the crystal lattice has isolated impurity levels in the forbidden zone[178].

### 3. Efficient Methods OF $\text{TiO}_2$ Synthesis

#### 3.1. Hydrothermal Method of $\text{TiO}_2$ Preparation

$\text{TiO}_2$  can be obtained by high-temperature hydrolysis of various precursors directly in the autoclave or by hydrothermal treatment[179]. For example, nanosized  $\text{TiO}_2$  powders are obtained by adding a 0.5M solution of titanium butylate in isopropanol to deionized water ( $[\text{H}_2\text{O}]/[\text{Ti}]=50$ ). Then peptization is carried out at  $70^\circ\text{C}$  for 1h in the presence of hydroxycitratealkylammonium[180]. This method is also widely used for the synthesis of monodisperse  $\text{TiO}_2$  nanoparticles. In Wahi et al.'s study[181],  $\text{TiO}_2$  nanorods were obtained by hydrothermal treatment of a dilute  $\text{TiCl}_4$  solution in the temperature range of 333-423K with a synthesis duration of 12h. In the study by Wahi et al.[181],  $\text{TiO}_2$  nanotubes were synthesized by hydrothermal treatment of commercial photocatalyst P25 in a 10M aqueous NaOH solution at  $130^\circ\text{C}$  and 24h of synthesis.

In the research by Kobayashi et al., the glycolate-oxo-peroxo-titanium complex was subjected to hydrothermal treatment to obtain  $\text{TiO}_2$ [182]. In an ice bath at room conditions, 20mmol of titanium metal powder was dissolved in a combination of 40mL of hydrogen peroxide solution and 10mL of ammonia solution. After two hours, all of the titanium powder dissolved and a yellow solution containing the peroxo-titanium complex was formed. Then 30mmol of glycolic acid was immediately added and the mixture was heated to 353K to promote complexation and remove excess hydrogen peroxide and ammonia until it formed an orange gel. To obtain an aqueous solution of the ammonium salt of the glycolate-oxo-peroxo- titanium complex, it was dissolved in distilled water. Using 2, 4, 8, 12 and 16cm<sup>3</sup> of stock solution and the required amount of distilled water, 40cm<sup>3</sup> of titanium solutions with Ti=12.5, 25.0, 50.0, 50.0, 75.0 and 100mM concentration were created in the next step. After the solution was placed in a 50cm<sup>3</sup> jar, it was sealed with a stainless steel shroud and heated in an oven for 1-168h at 473K. The autoclaves were then allowed to cool to ambient temperature. Centrifugation was used to separate the precipitate formed, which was then washed

thoroughly three times with deionised water. After drying overnight at 353K in an oven, the sample was extracted. The particle sizes of TiO<sub>2</sub> polymorphs in the samples that were extracted from the Ti complex solution with a concentration of 50.0mM as a function of the procedure duration are shown in Table 2[182].

Table 2. Particle Sizes of TiO<sub>2</sub>

| Processing Time (h) | Crystal Size (nm) |          |        |
|---------------------|-------------------|----------|--------|
|                     | Anatase           | Brookite | Rutile |
| 2                   | 4.9               | 7.7      | 29.1   |
| 3                   | 5.7               | 9.7      | 34.8   |
| 12                  | 8.6               | 14.0     | 51.7   |
| 24                  | 10.0              | 15.6     | 57.4   |
| 72                  | 12.9              | 19.8     | 63.7   |
| 168                 | 16.6              | 23.5     | 67.2   |

Govindaraj et al.[183] used the hydrothermal method to efficiently grow TiO<sub>2</sub> nanorods. To reduce hydrolysis and condensation, an equal volume of acetylacetone was combined with tetrabutyl orthotitanate. The mixture was then gradually stirred for 5min at room temperature by adding 40mL of water. 30mL of 28-30% aqueous ammonia solution was gradually added to the mixture dropwise with continuous stirring. The solution was then transferred to a 250mL stainless steel autoclave and immersed in a silicone oil bath. The precursor solution was then heated to 170°C and stirred continuously at this temperature for 24h. The autoclave was then spontaneously cooled down to ambient temperature. The final product was repeatedly thoroughly purified with aqueous HCl, 2-propanol and water. It was then dried for 12h at 120°C. Finally, the collected samples were incinerated for one hour in a high temperature furnace at 450°C. X-ray examination of the samples showed that they contained a large number of anatase nanorods with an average pore width of 3.1nm and a specific surface area of about 34.82m<sup>2</sup>/g. To enhance the charge transfer ability, the authors of another work[184] obtained TiO<sub>2</sub> nanorods/nanoparticles using hydrothermal method. The obtained nanoparticles have a specific surface area of 84.83m<sup>2</sup>/g and a pore diameter of 5.7nm.

Using surfactant-assisted hydrothermal technology, TiO<sub>2</sub> with different morphologies including nanosheets, nanorods, nanotubes and nanoflowers were produced by adjusting the pH during the preparation process. The experimental results showed that the pH value is critical for controlling the shape of the generated TiO<sub>2</sub>, as it can change the adsorption potential of surfactant on the surface of TiO<sub>2</sub> and its charge state in solution. The experimental protocols are summarised below: A solution resistant to hydrolysis at room temperature was created by mixing titanium isopropoxide and TEOA in the following ratio: titanium tetraisopropoxide (TTIP): TEOA = 1:2. DI water was added to create solution A. Dodecanediamine was mixed with DI water to create solution B, which acts as a shape adjuster. Next, solution A and solution B were mixed. The pH of the mixed solution was adjusted by adding HClO<sub>4</sub> or NaOH. It was then placed in a 100mL Teflon autoclave and incubated at 100°C for 24 h, after which the temperature was raised to 140°C for 72h for nucleation and growth of TiO<sub>2</sub> particles. TiO<sub>2</sub> nanospheres with particle sizes ranging from 30 to 60nm were formed under acidic conditions at pH=5.6. When the pH was increased, most of the prepared TiO<sub>2</sub> particles transformed from ellipsoids to nanorods. When the pH of the solution was changed to a value greater than 11, TiO<sub>2</sub> nanoflowers were formed. In the process of creating these structures, TiO<sub>2</sub> nanosheets were initially formed and then folded to form the final structures at different pH values[185].

Hollow TiO<sub>2</sub> nanospheres can be obtained by hydrothermal method with the addition of aggressive chemicals, and they usually have large surface area and low density[185–187]. For example, the hydrothermal method was used to obtain porous hollow TiO<sub>2</sub> aggregates with a BET surface area of 168m<sup>2</sup>/g and an average pore size of 12nm. Ti(SO<sub>4</sub>)<sub>2</sub> and NH<sub>4</sub>F were dissolved in DI

water for Liu preparation, then the resulting mixture was stirred and placed in a Teflon-lined autoclave. The hydrothermal synthesis was carried out in an electric furnace for six hours at 160°C. The appearance of the products is shown in Figure 7A-D[187]. Despite having a greater estimated BG of 3.36eV than P25 (~3.18eV), the porous TiO<sub>2</sub> products exhibited double the activity of P25 when it came to the photodegradation of Rhodamine B[187]. The HF produced by NH<sub>4</sub>F during the hydrothermal process is responsible for the production of porous, hollow TiO<sub>2</sub> aggregates. HF, a chemical etchant that is corrosive, will erode the inside of TiO<sub>2</sub> to create TiF<sub>4</sub>, which will ultimately result in hollow nanospheres. Using a similar hydrothermal technique, their subsequent investigation employed the metallic Ti powder as reactants together with a specific quantity of NH<sub>4</sub>F and H<sub>2</sub>O<sub>2</sub> (30 wt.%). With a diameter of about 1µm, a shell thickness of 150nm and a cavity size of about 600nm, the obtained anatase TiO<sub>2</sub> resembled hollow spheres. The critical factors for the creation of TiO<sub>2</sub> hollow spheres from metallic Ti powders were reaction time, NH<sub>4</sub>F concentration and H<sub>2</sub>O<sub>2</sub> concentration. The H<sub>2</sub>O<sub>2</sub> served as both an oxidant and a bubble generator, creating O<sub>2</sub> bubbles that served as the aggregation centre when combined with Ti particles. After that, as shown in Figure 7E,F[186], TiO<sub>2</sub> nanoparticles gradually aggregated at the gas-liquid interface to form hollow TiO<sub>2</sub> spheres.

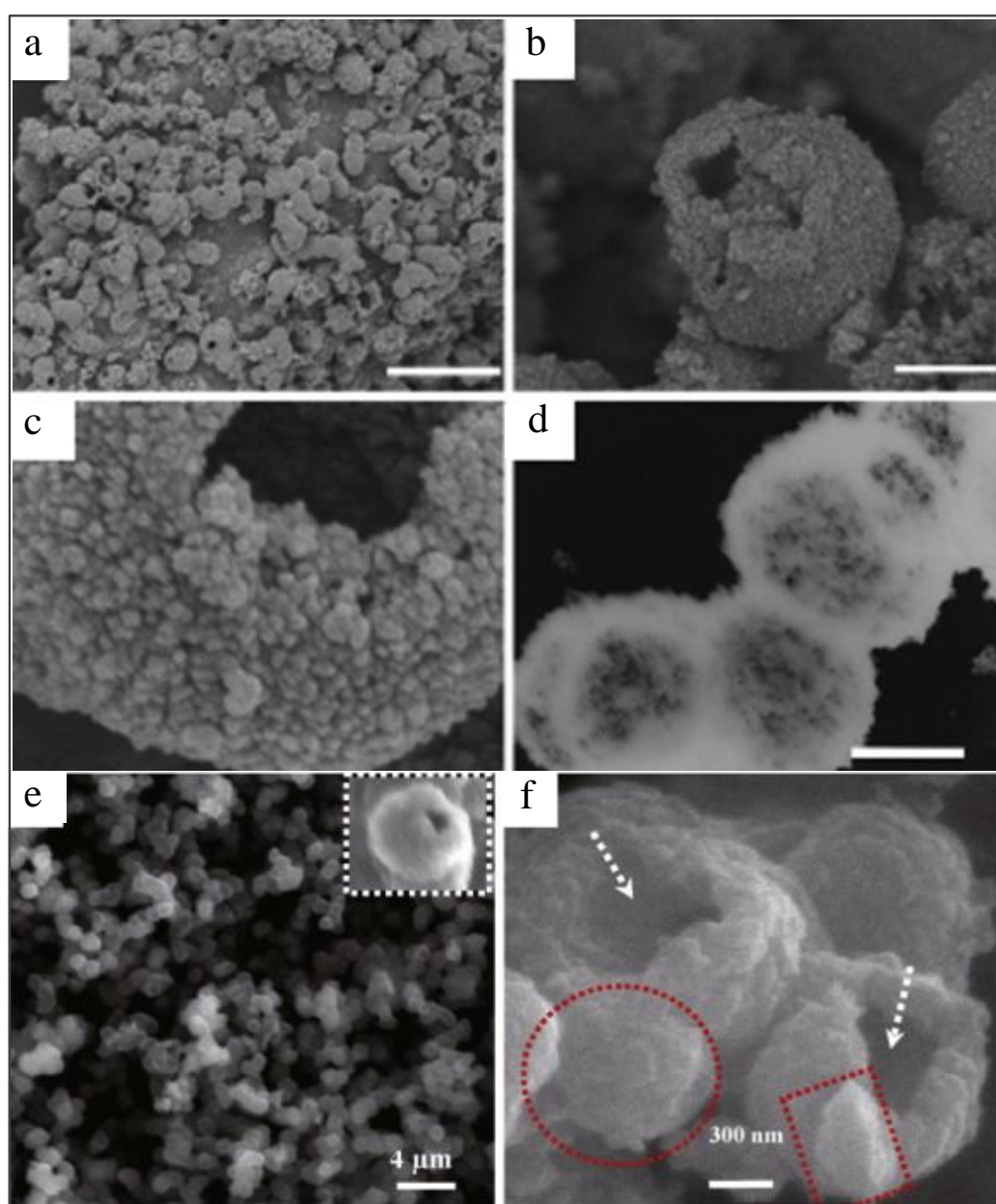




**Figure 7.** (A-C) FESEM and (D) TEM images of the porous, hollow TiO<sub>2</sub> aggregates prepared by the hydrothermal treatment at 160°C for 6 h. Reprinted with permission from [187], Copyright © 2007 WILEY-VCH Verlag GmbH & Co. KGaA, Weinheim; (E, F) SEM overviews of the TiO<sub>2</sub> hollow spheres synthesized by the hydrothermal method at 423K for 10h. The scale bars for (A-D) are 5mm, 500nm, 100nm, and 500nm, respectively. Reprinted with permission from [186], Copyright © 2009 Elsevier B.V. .

The hydrothermal method can be used to create rutile-brucite TiO<sub>2</sub> nanocomposite by replacing NaOH with HCl. The obtained TiO<sub>2</sub> was used for photooxidation of methyl blue as well as for photocatalytic conversion of CO<sub>2</sub>. In Lei et al.'s study [186], titanium chloride was combined with 2mol/L HCl to obtain a clear solution. The solution was then combined with 1.0mL of 5V/V% Triton X-100 in ethanol (EtOH). After transfer to a flask, the prepared solution was refluxed for 22h at 100°C. The final rutile-brucite nanocomposite structures were obtained by centrifuging the obtained products, washing them in water, drying them at room temperature and then calcination at 500°C [187].

### 3.2. Solvothermal Synthesis of TiO<sub>2</sub>

The solvothermal and hydrothermal methods are practically identical except that the solvothermal method uses a non-aqueous solvent. The temperature of the solvothermal process can be much higher because some organic solvents have higher boiling points [188]. Usually, the size, shape and crystal structure of the obtained TiO<sub>2</sub> nanoparticles can be well controlled using the solvothermal method. The method is a versatile way to synthesize various nanoparticles with narrow size and dispersity distributions. Using the solvothermal method, TiO<sub>2</sub> nanoparticles with a characteristic size of less than 5nm can be obtained [189].

The alcohol solvothermal method was first applied to obtain TiO<sub>2</sub> by Kang et al [190]. In Kang's study, 1,4-butanediol was used as a solvent and titanium isopropoxide was used as a source of TiO<sub>2</sub>. The 1,4-butanediol was mixed with titanium isopropoxide at 300°C for 50min to facilitate the synthesis. The obtained TiO<sub>2</sub> powder was cleaned repeatedly with acetone and then left to dry for five hours at 100°C without calcination. The obtained anatase TiO<sub>2</sub> nanoparticles of size 20-50nm were highly hydrophilic and were much more efficient in photocatalytic decomposition of chloroform than TiO<sub>2</sub> nanoparticles obtained by sol-gel method [190]. Subsequently, Nam and Han used the obtained TiO<sub>2</sub> for photodegradation of methyl orange and investigated the effect of several alcoholic solvents under the same conditions [191]. They got ready in the following ways: Titanium isopropoxide (0.1mol) was added to glycerol, 1-butanol, and 1,4-butanediol, in that order. The combinations were heated to 300°C and kept there for an hour under auto-generated pressure. The findings demonstrated that the kinds of solvents employed during the reaction had a significant impact on the physical characteristics of the produced TiO<sub>2</sub>, including crystal size, shape, and structure. Figure 8A-C displays the SEM pictures of the TiO<sub>2</sub> that they produced [191].

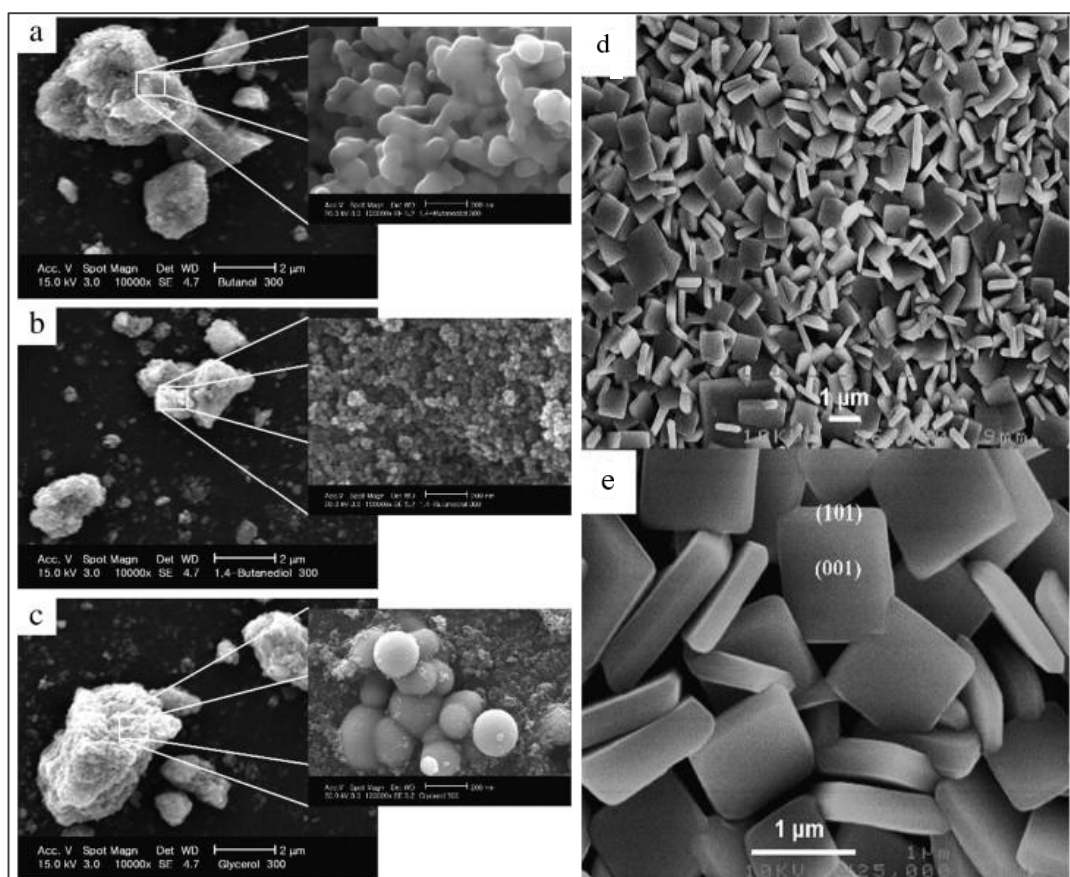


**Figure 8.** (A-C) SEM images for the TiO<sub>2</sub> prepared by the solvothermal method in various alcohol solutions: (A) 300°C, butanol, (B) 300°C, 1,4-butanediol, and (C) 300°C, glycerol. Reprinted with permission from [191], Copyright © 2003, Korean Institute of Chemical Engineering; (D, E) SEM images of the anatase TiO<sub>2</sub> nanosheets synthesized with a reaction time of 11h. Reprinted with permission from [192], Copyright © 2009, American Chemical Society.

Yang et al. [192] synthesized anatase TiO<sub>2</sub> nanosheets with pronounced {001} facets using an alcohol solvothermal technique. This procedure is a common method for fabricating nanosheets and can provide insight into subsequent methods. In a typical experiment, the pH was set to 1.8 and sufficient TiF<sub>4</sub> was added to a combination of hydrochloric acid and DI water to create a TiF<sub>4</sub> solution. Then 14.5 mL of the above aqueous solution of TiF<sub>4</sub>, 13.38 mL of 2-propanol, and 0.5 mL of HF were placed in a Teflon-coated stainless steel autoclave. The autoclave was kept at 180°C for 5.5–44 h in an electric oven. Monocrystalline anatase TiO<sub>2</sub> nanosheets were obtained by centrifugation after the reaction, then washed three times with DI water and dried under vacuum overnight. Heat treatment at 600°C for 90 min was used to remove fluorine from the surface of anatase TiO<sub>2</sub>. They showed that 2-propanol and HF promoted the isotropic development of single-crystalline TiO<sub>2</sub> nanosheets and that 2-propanol could enhance the stabilizing effect associated with fluorine adsorption on the (001) surface using first-order theoretical calculations. Figure 8D,E [192] shows the SEM images of the anatase TiO<sub>2</sub> nanosheets. TiO<sub>2</sub> nanosheets have the potential to remove organic pollutants by photocatalysis because they can produce five times more oxidative hydroxyl radicals (OH) than P25 upon irradiation [193].

Huang et al. [194] prepared highly crystalline TiO<sub>2</sub> hollow spheres by alcohol solvothermal method without corrosion additives and shape controllers at 350°C, as shown in Figure 9 [194]. Although the surface area of the TiO<sub>2</sub> hollow spheres was only 28.2 m<sup>2</sup>/g by BET, they possessed good ability for photocatalytic degradation of methyl orange. Titanium n-butoxide (TNB) and EtOH were used for their synthesis [195]. A mixed solution of TNB and EtOH was prepared by slowly adding TNB to EtOH with a certain volume ratio.

After stirring for 30min, the mixture was transferred to a stainless steel autoclave for the solvothermal reaction at 350°C for 4h. The precipitate was then washed three times with anhydrous ethanol and dried overnight. The precipitate was then washed three times with anhydrous ethanol and dried overnight. The prepared anatase TiO<sub>2</sub> spheres consisted of nanoparticles with an average diameter of 30.2nm. According to their observations, pure TNB can decompose into TiO<sub>2</sub> nanoparticles at temperatures above 350°C to form 1-butene as in the reaction  $\text{Ti}(\text{OBu})_4 \rightarrow \text{TiO}_2 + \text{CH}_3\text{CH}_2\text{CHCHCHCH}_3$ , which can serve as bubble templates for growing hollow TiO<sub>2</sub> microspheres from nanoparticles[194].

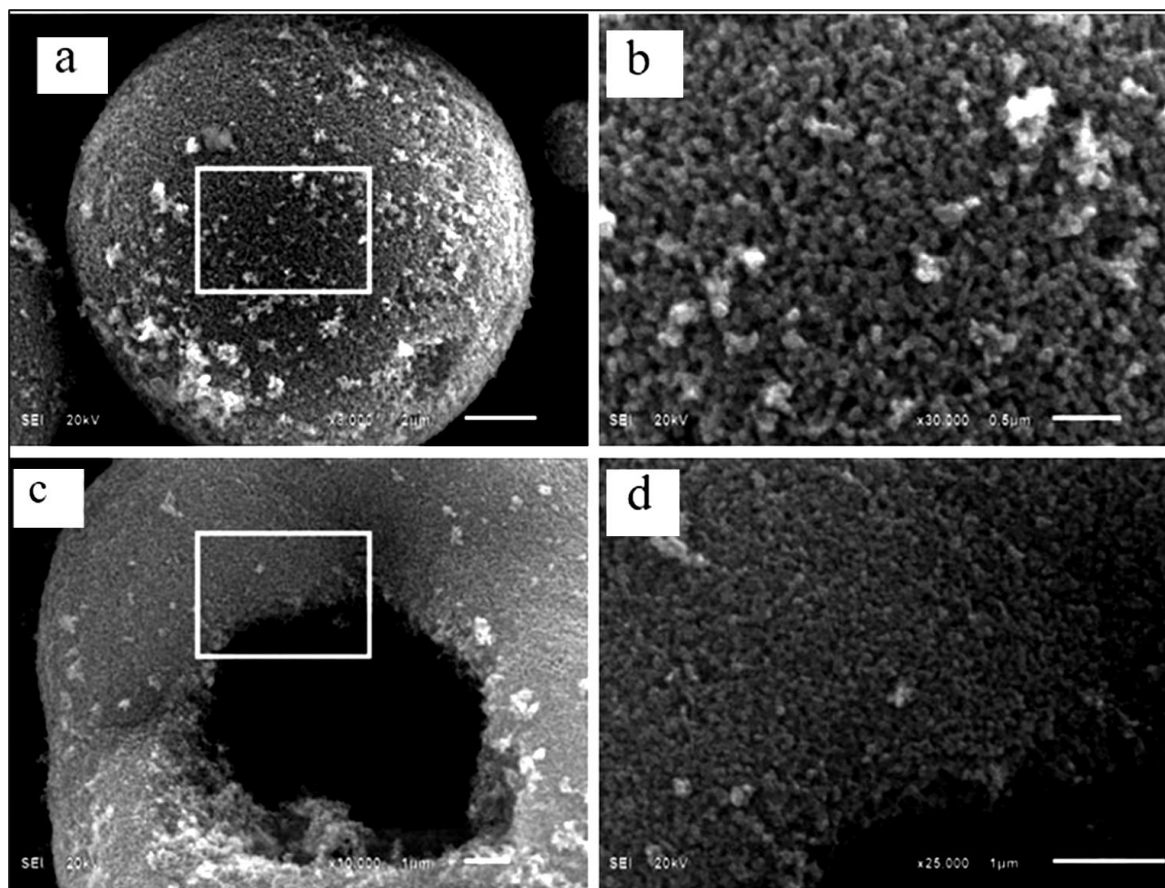


**Figure 9.** SEM images of the TiO<sub>2</sub> samples made by the solvothermal method: (A) a whole sphere, (B) magnified image of the selected part in (A), (C) a broken hollow sphere, (D) magnified image of the selected part in (C). Reprinted with permission from[194]. Copyright © 2011 WILEY-VCH Verlag GmbH & Co. KGaA, Weinheim.

With LA serving as a suitable coordination surfactant to promote the anisotropic crystal growth of TiO<sub>2</sub>, nanorods would be formed. If controlling NH<sub>4</sub>HCO<sub>3</sub> and LA in a desired mole ratio, TiO<sub>2</sub> with different morphologies could be acquired. Figure 10[196–198] are the TEM images of the TiO<sub>2</sub> nanoparticles and nanorods prepared. Adding a small amount of metal chloride or nitrate into the mixed solution of NH<sub>4</sub>HCO<sub>3</sub>, LA, triethylamine, cyclohexane and Ti(OBu)<sub>4</sub>, metal-doped (Fe<sup>3+</sup>, Co<sup>2+</sup>, Sn<sup>4+</sup>, Ni<sup>2+</sup>) TiO<sub>2</sub> nanocrystallines can be obtained[196].



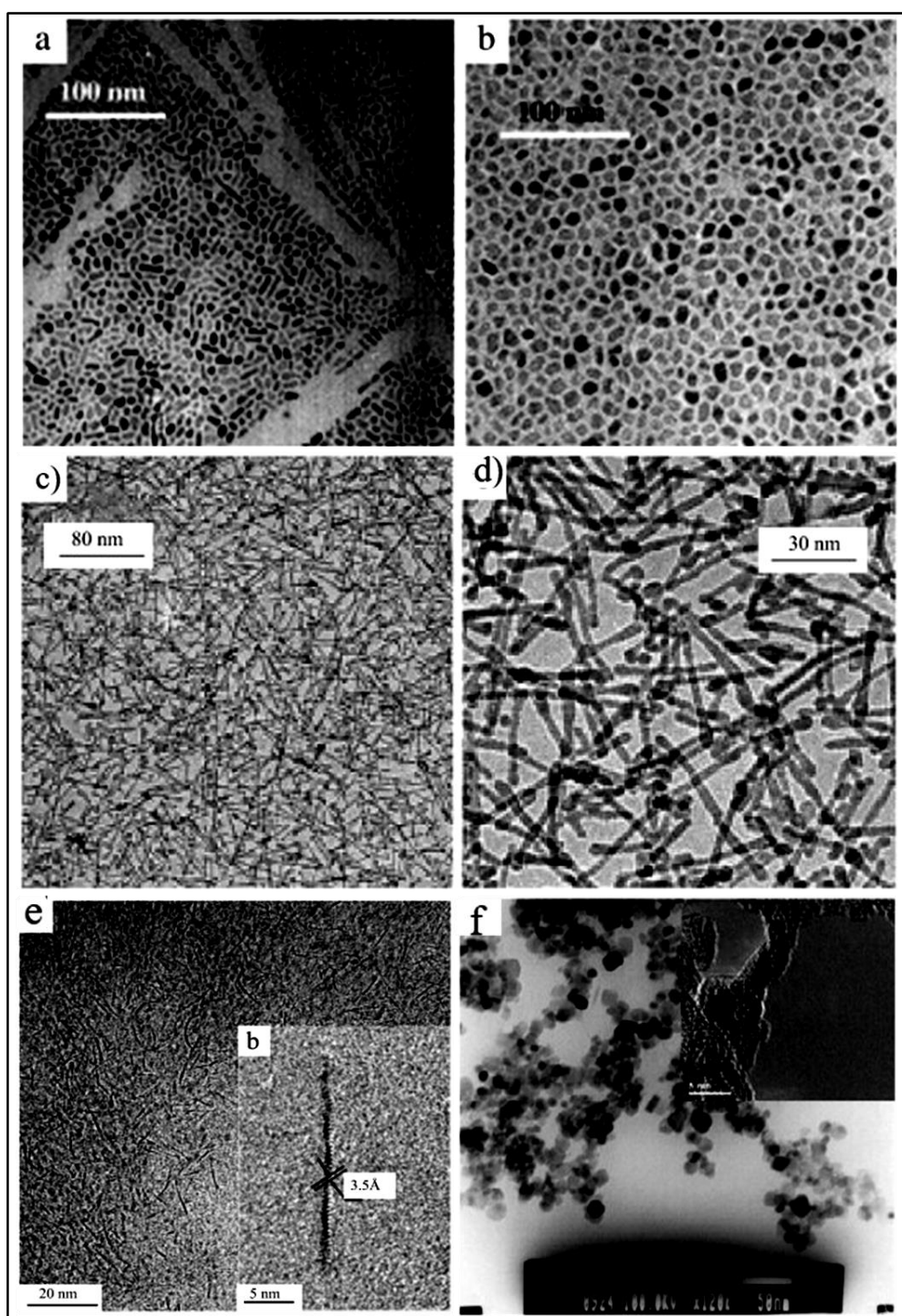


**Figure 10.** TEM images of TiO<sub>2</sub> nanoparticles (A, B) and TiO<sub>2</sub> nanorods (C, D). Reprinted with permission from [187], Copyright © 2007 WILEY-VCH Verlag GmbH & Co. KGaA, Weinheim; (E) TEM image of atomically thin N-TiO<sub>2</sub> wires grown at 180°C for 1h. Reprinted with permission from [197], Copyright © 2010 WILEY-VCH Verlag GmbH & Co. KGaA, Weinheim; (F) TEM image of as-prepared. Reprinted with permission from [198], Copyright © 2007 Elsevier B.V.

Atomically thin anatase TiO<sub>2</sub> wires with a diameter of 4.5 Å were prepared by the carboxylic acid solvothermal process. These diameter-tunable, ultrathin TiO<sub>2</sub> nanowires were obtained as a result of optimized reaction temperature and reaction time. In Yang's synthesis [196], a certain amount of oleic acid and cyclohexane were mixed, and then Ti(OBu)<sub>4</sub> was added dropwise to the mixed solution. The resulting solution was heated to 150°C for 25h in a Teflon-lined stainless steel autoclave. The precipitation was extracted with an excess of ethanol. The titanium complex precursor was then



redispersed in a mixture of octadecene, oleic acid, and oleylamine. The solution was heated to 180°C under stirring and maintained at that temperature for 1h to acquire N-doped TiO<sub>2</sub>. Their research results suggested that a uniform mixture of oleic acid and oleylamine solution favors self-assembly of the wires. In addition, an increase in reaction temperature mainly increased the wire diameter, whereas prolongation of the precursor treatment time mainly caused an increase in the wire length. Their characterization data indicated that N-doping originated from the oxidative coupling of oleylamine on the surfaces of the atomically thin wires, forming the N–O–Ti surface structures. UV-vis absorption spectra indicated that the light absorption edge was 257nm for the atomically thin TiO<sub>2</sub> wires, whereas it shifted to 600nm with N doping. Figure 10 (e) is a TEM image of the N-TiO<sub>2</sub> obtained[197]. To further investigate the capping roles of oleic acid and oleylamine in the solvothermal system, Dinh found out that oleic acid and oleylamine had different binding strengths in controlling the growth of TiO<sub>2</sub> nanoparticles. By varying the ratio of them, TiO<sub>2</sub> with different shapes such as spherical, dog-bone, truncated and elongated rhombic was prepared. The thus-obtained TiO<sub>2</sub> was ascertained to be an excellent support for the synthesis of metal/TiO<sub>2</sub> photocatalyst in which metal clusters could be uniformly deposited on the surface of TiO<sub>2</sub>[199].

Thermal decomposition of titanium alkoxides by the solvothermal reaction in inert organic solvents, such as toluene and acetone, can produce crystallized TiO<sub>2</sub> nanoparticles[198,200]. In Prasertthdam's research, nanocrystalline TiO<sub>2</sub> was prepared by toluene using the solvothermal method. In their synthesis, TNB was used as the starting material and was suspended in toluene in a test tube, which was then placed in a 300mL autoclave. The autoclave was purged by nitrogen, after which it was heated up to 300°C and was held at 300°C for 2h before cooling down to room temperature. The obtained TiO<sub>2</sub> was washed by CH<sub>3</sub>OH several times and quenched in air at 77K. The as-prepared anatase powders were of spherical shape with a size of 8-15nm. The quenching in their research contributed to the formation of Ti<sup>3+</sup> surface defects due to the thermal shock effect and promoted the photocatalytic ethylene decomposition ability of TiO<sub>2</sub>. Figure 10F displays a TEM image of the TiO<sub>2</sub> as prepared[198].

The preparation of TiO<sub>2</sub> microspheres is usually promoted by the addition of surfactants[201–204], while prepared TiO<sub>2</sub> microspheres (Figure 11)[204] with the solvothermal method in acetone without surfactants. Acetone itself might serve as a shape controller, but it hasn't been confirmed yet. In their preparation, a certain volume of TiCl<sub>4</sub> was added dropwise to acetone under vigorous stirring at 0°C. The concentration of TiCl<sub>4</sub> was adjusted to 0.3mol/L. This mixed solution was transferred into an autoclave afterwards and was maintained at 120°C for 12h in an oven for solvothermal treatment. After reaction, the mixture was cooled to room temperature naturally. The resulting precipitates were filtered and thoroughly washed with excessive acetone and then dried at 120°C for 12h under vacuum. The precipitate was calcined under 500°C for 5h in air. The diameter of the layered microspheric anatase TiO<sub>2</sub> was about 3μm with each layer around 300[204]. On the contrary, the solvothermal preparation of TiO<sub>2</sub> in Chen's work also used acetone as a solvent, but TiO<sub>2</sub> nanoparticles were formed instead of microspheres.

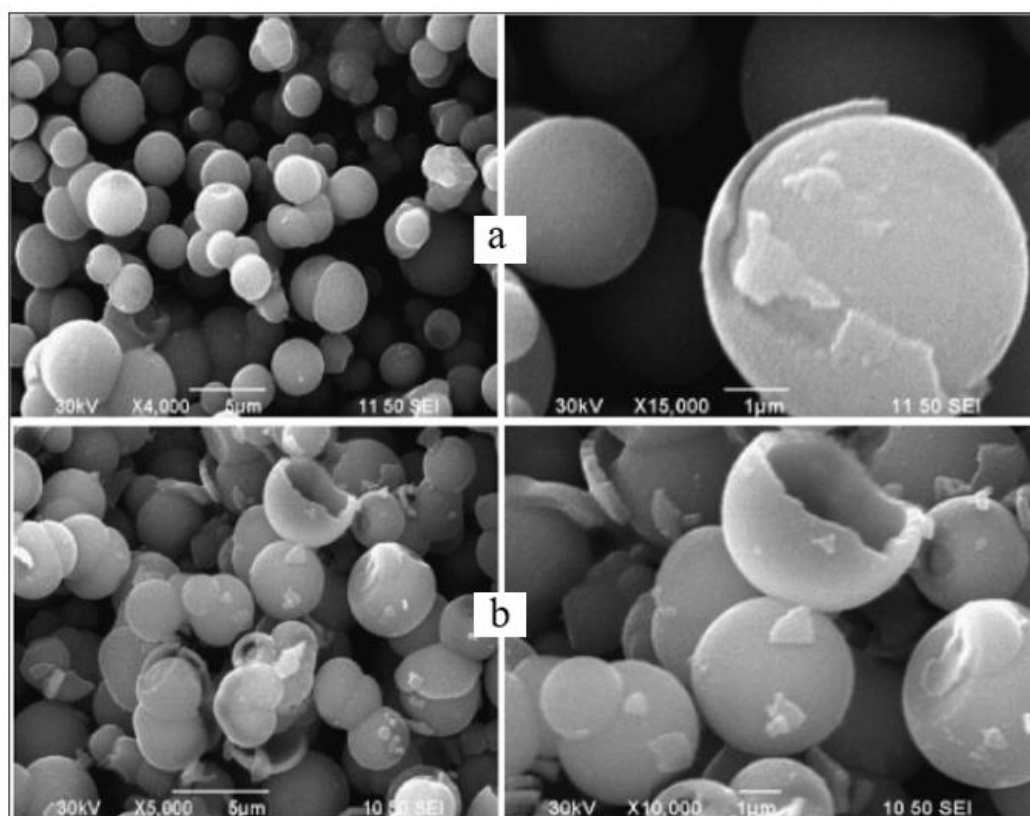


**Figure 11.** TEM images of the anatase samples treated at 120°C (a), and calcined at 500°C for 5h (b) with different magnifications. Reprinted with permission from[204], Copyright © 2009 Elsevier Ltd.

### 3.3. Sol-gel Method of $\text{TiO}_2$ Production

Nanoscale  $\text{TiO}_2$  particles are synthesized by sol-gel method using hydrolysis of titanium precursors[205]. Titanium alkoxide or titanium tetrachloride ( $\text{TiCl}_4$ ) are used as precursor. At the first stage of sol-gel process hydrolysis of IV precursor is carried out with subsequent polycondensation, which leads to the formation of colloidal solution -sol of hydroxide particles, the size of which does not exceed several tens of nanometers. Low water content (low level of hydrolysis) and excess of titanium alkoxide in the reaction mixture contribute to the development of Ti-O-Ti bond chains. Chain formation leads to the formation of a three-dimensional polymer skeleton with a near-ordered degree. The high rate of hydrolysis promotes the formation of  $\text{Ti}(\text{OH})_4$ , which interrupts the development of the Ti-O-Ti skeleton. The presence of a large number of Ti-OH groups and insufficient development of the three-dimensional polymer skeleton leads to loose packing of particles[205–207].

The use of low processing temperatures ( $<100^\circ\text{C}$ ) and molecular level composition uniformity makes the sol-gel technique very promising for the synthesis and manufacture of inorganic and organic-inorganic hybrid nanomaterials, as compared to the previously stated approaches[207]. The sol-gel process makes it simple to adjust the size and form of the particles.

The sol-gel technique, which is commonly used to create  $\text{TiO}_2$  materials, generates fine, spherical powders of uniform size and typically starts with an acid-catalyzed stage involving titanium alkoxides[208,209]. The ability to mold the resultant material into desired shapes, such as fiber, film, and monodispersed powder, is one of the most appealing aspects of the sol-gel process. Figure 12[210] illustrates how a sol-gel technique, as proposed by Mehrotra and Singh[208], applies a number of variables and phases to regulate the final morphology.

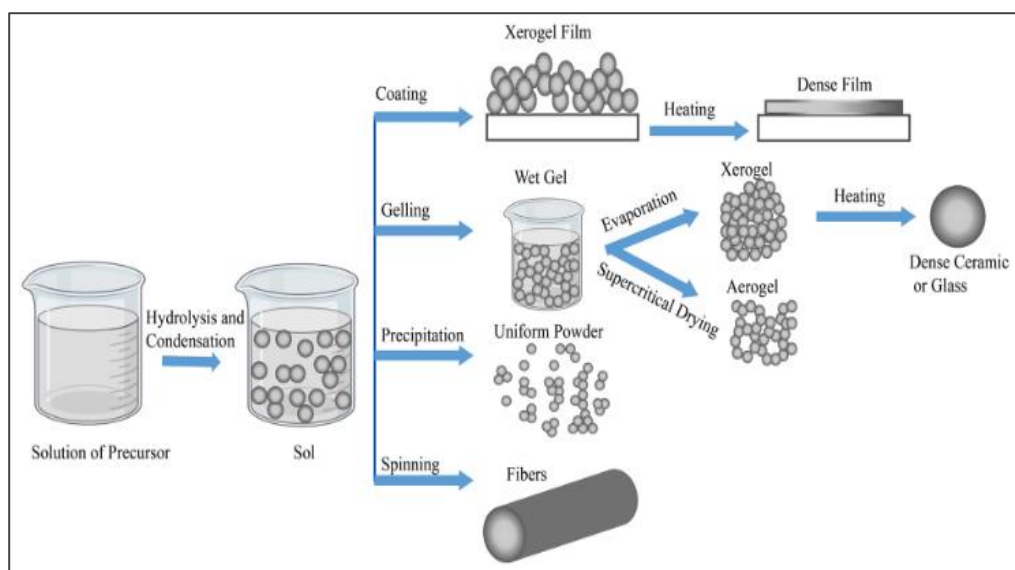


**Figure 12.** Different sol-gel process steps to control the final morphology of the product. Reprinted with permission from [210], Copyright © 2009 Elsevier Ltd. Copyright © 2023, Iranian Chemical Society.

Metal oxides and metal chlorides are common precursors. The compound  $M-O-R$ , where  $M$  is metal,  $O$  is oxygen, and  $R$  is an alkyl group, is a metal alkoxide. The  $M-O$  bond is polarised, making it vulnerable to nucleophilic attack. Hydrolysis is a process in which an alkoxide in the presence of water undergoes a nucleophilic substitution reaction in which hydroxyl groups from water replace alkoxy groups ( $OR$ ). Condensation is a process in which metal hydroxide groups combine with each other to form a hydrated metal-oxide network in which tiny nuclei are eventually formed.

The reactivity of metal alkoxides used in the sol-gel process needs to be controlled to obtain sols and gels with desired properties. This can be done by adding chelating ligands such as  $\beta$ -diketones, carboxylic acids or other complex ligands, or by using modifiers. To improve the control of the hydrolysis-condensation process in sol-gel fabrication, modifiers react with alkoxides to form new molecular precursors. These new precursors reduce functionality and reactivity, inhibit condensation and induce smaller species. The potential of acetylacetone to improve sol-gel processing of metal alkoxides was studied by Livage et al. in 1988[209]. Susceptibility to hydrolysis is reduced when modifiers change the number of  $M-OR$  bonds available for hydrolysis. Since  $\beta$ -diketones are surface capping reagents and polymerisation fixatives, their use reduces nuclearity and results in the formation of fine particles. Acetic acid and other carboxylate ligands mainly act as bridging chelating ligands.

The sol-gel method has several advantages, which include [210]: (I) low-temperature preparation; (II) easy and efficient control of particle size, shape and properties; (III) improve the homogeneity of the raw materials; (IV) increase the purity of the starting material; and (V) create the structure and properties of the material by appropriate choice of precursor.

### 3.4. Sonochemical and Microwave-assisted Methods of $TiO_2$ Synthesis

The sonochemical strategy has been applied to deliver exceptionally photoactive  $TiO_2$  nanoparticles by the hydrolysis of TTIP in unadulterated water or in an ethanol / water blend under ultrasonic radiation [211]. Acoustic cavitation, or the formation, growth, and collapse of bubbles within a liquid medium, is the basis for sonochemistry. Heat ( $\sim 5000K$ ) and high tensions ( $\sim 1000atm$ ) are delivered by cavitation breakdown [212]. Microwaves, which are electromagnetic waves with wavelengths ranging from 1mm to 1m and frequencies ranging from 0.3 to 300GHz, are utilized in microwave-assisted techniques. As indicated by Zhu and Chen [213], microwave warming includes two principal systems to be specific dipolar polarization and ionic conduction. Any materials that contain versatile electric charges, for example, polar particles or leading particles are by and large intensity by microwaves. When polar molecules attempt to align themselves with the rapidly shifting

alternating electric field in the microwave, they generate heat through rotation, friction, and collision. Assuming particles are available in arrangement, they will travel through the arrangement and continually taking an alternate route in view of the direction of the electric field bringing about nearby temperature climb because of erosion and impact[214].

Microwave warming is as an elective intensity hotspot for quick warming with more limited response time and higher response rate, selectivity and yield when contrasted with the regular warming techniques[213]. Pulsed microwave heating and continuous microwave heating are the two types of microwave heating. In 1995, Jacob et al. came up with two models for how microwaves increase reaction rates. However, although the microwave response time is significantly reduced, the energy or component of the composite response does not change, suggesting that the increase in response speed is due to heating effects[215]. The second proposed system makes a supposition that there are “nonthermal microwave impacts” notwithstanding the warm impacts thus the impacts of microwave light in substance responses are because of both warm impacts and nonthermal impacts[216]. The nonthermal impacts are because of direct communication of microwaves with specific particles in the response medium.

Microwave radiations can likewise be applied to deliver different  $\text{TiO}_2$  nanomaterials[217]. This method has the advantage of rapid heat transfer and selective heating for industrial processing. This procedure gives uniform conveyance of energy inside the example, better reproducibility and amazing control of exploratory boundaries. When compared to the several hours required for the conventional methods of forced hydrolysis at high temperatures ( $195^\circ\text{C}$ ), the colloidal  $\text{TiO}_2$  nanoparticles can be prepared in a short amount of time (within 5-60min)[218].  $\text{TiO}_2$  nanotubes which are unassuming and multi-walled with breadths of 8-12nm and lengths somewhere in the range of 200 and 1000nm were additionally pre-arranged utilizing this technique[219].  $\text{TiO}_2$  nanoparticles in the anatase stage were ready by Baldassari et al.[220] utilizing microwave-helped hydrolysis of  $\text{TiCl}_4$  in a weaken acidic watery medium. Under microwave-hydrothermal conditions, they discovered that the product nearly crystallized within 30min. Because the sulfate prevented brookite from crystallizing, they used  $\text{H}_2\text{SO}_4$  as the acid to produce a pure anatase phase. In another review, they likewise pre-arranged  $\text{TiO}_2$  nanoparticles in the rutile stage from  $\text{TiCl}_4$  by a microwave-aqueous cycle at various temperatures somewhere in the range of 100 and  $160^\circ\text{C}$  for 5-120min[220]. The morphology and size of the subsequent nanoparticles can be fluctuated by changing the hour of response, microwave power and reactant fixation.

In another study, titanium slags were converted into rutile  $\text{TiO}_2$  powder by microwave activation (Figure 13)[221]. Then, the effects of the  $\text{Na}_2\text{CO}_3$  additive on the calcined product's surface functional groups, crystallinity, phase transformation, and surface microstructure were examined. The following is the makeup of titanium slag: 9.72% Fe, 5.87%  $\text{Al}_2\text{O}_3$ , 5.23%  $\text{SiO}_2$ , 1.23%  $\text{MgO}$ , 1.81%  $\text{CaO}$ , 75.34%  $\text{TiO}_2$ , and other trace elements, such S and P. Using a planetary ball mill (model: QM-3SP4), the material was first processed into a powder for 180min in order to improve the specific surface area of the slag. The obtained titanium slag sample, weighing 100g, was then equally divided into five pieces, each of which was mixed with  $\text{Na}_2\text{CO}_3$  in an agate mortar for 10min.





**Figure 13.** Scheme of the microwave synthesis of rutile TiO<sub>2</sub>. Reprinted with permission from[221], Copyright © 2020 The Society of Powder Technology Japan.

For the mixes, the mass ratios of Na<sub>2</sub>CO<sub>3</sub> to titanium slag were 0.2, 0.3, 0.4, 0.5, and 0.6, respectively. After that, the mixture was put in a corundum crucible and heated to 850°C for 30min using a 1kW microwave heating power in a microwave box reactor. With the use of a magnetic stirrer, 10g of calcined slag was leached for 4h at 92-95°C using 20% HCl (mass ratio of liquid/solid: 4:1). Following three rounds of water washing, the residue from the leaching process was collected and put in a corundum crucible for high-temperature annealing in a microwave box reactor set at 900°C for 60min with a 1kW microwave heating power. The calcined product was then cooled and put to use in an analysis. The findings demonstrated that the ideal mass ratio of Na<sub>2</sub>CO<sub>3</sub> was 0.4, at which point the average size of the crystallites was 43.5nm and the rutile TiO<sub>2</sub> crystallinity attained its maximum value of 99.21%.

### 3.5. Synthesis of TiO<sub>2</sub> by Oxidation Method

These methods involve the oxidation of titanium metal using oxidants or anodization. Anodization of titanium sheet under a voltage between 10 and 20V in 0.5% hydrogen fluoride leads to the formation of aligned TiO<sub>2</sub> nanotubes whose diameter is controlled by varying the applied voltage[212]. In another study, crystallized TiO<sub>2</sub> nanotubes were obtained when anodized titanium plate was heat treated at 500°C for 6h in an oxygen environment[211]. Direct oxidation of the titanium metal with hydrogen peroxide has also been found to lead to the formation of TiO<sub>2</sub> nanorods. The TiO<sub>2</sub> can be obtained by placing a cleaned Ti metal plate in a 50mL solution of 30wt% H<sub>2</sub>O<sub>2</sub> at 353K for 72h[222]. Formation of crystalline TiO<sub>2</sub> occurs via mechanism of dissolution precipitation and this phase can be controlled by addition of NaX (X = F<sup>-</sup>, Cl<sup>-</sup>, SO<sub>4</sub><sup>2-</sup>) inorganic salts. Addition of Na<sub>2</sub>SO<sub>4</sub> and NaF results in the formation of anatase phase and when rutile phase is needed, NaCl can be added during dissolution precipitation[223].

Acetone, pure oxygen and a mixture of oxygen and argon can be used as sources of oxygen for oxidation of titanium metal. Acetone is a good source of oxygen and when used at high temperatures, it results in nanorods which are well aligned and highly dense. Use of pure oxygen or a mixture of oxygen and argon results in crystal grain films and morphology of the nanoparticles can be controlled by the diffusion competition of oxygen and titanium[223,224].

### 3.6. Synthesis of TiO<sub>2</sub> by Chemical Vapor Deposition (CVD)

In these methods, materials in the vapor state are condensed to form a solid phase material. The process is normally carried out in a vacuum chamber and if a chemical reaction takes place, it is called CVD and physical vapor deposition if no reaction occurs. Examples of CVD include electrostatic spray hydrolysis, diffusion flame pyrolysis, thermal plasma pyrolysis, ultrasonic spray pyrolysis, laser-induced pyrolysis and ultrasonic-assisted hydrolysis. TiO<sub>2</sub> films with grain size less than 30nm and TiO<sub>2</sub> nanoparticles with sizes less than 10nm were synthesized by pyrolysis of TTIP in a helium / oxygen atmosphere[225]. Thermal plasma synthesis[226] and spray pyrolysis[227] have been used in some studies but they are complex, capital and energy-intensive and the properties of the powder are not easy to control.

CVD is a method of producing thin films or powders by means of high-temperature decomposition reactions and / or gas-vapor interactions. is a method of producing thin films or powders by high-temperature decomposition reactions and / or interactions of gaseous precursors on a substrate (producing films) or in a reactor volume (producing powders)[228]. To date, it has been established that the nature of the substrate affects the size and distribution of crystals in TiO<sub>2</sub> films[229]. This method is used to obtain TiO<sub>2</sub> at 300-750°C, using titanium tetraisopropoxide as a precursor[230].

### 3.7. Green Synthesis of TiO<sub>2</sub>

An ecologically benign substitute for the chemical method of creating nanomaterials is the “green” synthesis of TiO<sub>2</sub> functional materials. Using biological agents including bacteria, fungus, actinomycetes, yeast, and plants, the biological technique offers a multitude of resources for the production of nanoparticles[231,232]. The pace at which metal ions are reduced with the aid of biological agents is substantially quicker than it is because of the surrounding pressure and temperature. Significant advancements in “green” synthesis techniques for the creation of many nanoparticles have resulted from the extraction of TiO<sub>2</sub> from plant extracts[233]. Green tea extract was used by Saikumari et al.[234] to create mesoporous TiO<sub>2</sub> nanoparticles using the sol-gel technique. A mixture of 9mL of titanium isopropoxide and 60mL of isopropanol was stirred continuously with a magnetic stirrer at room temperature for 1h. Then green tea extract was added in various ratios (0.5, 1, and 1.5g in 30mL of distilled water) and stirred slowly for 3h in order to obtain a colloidal solution. It was found that the pH of the solution was 6.0 during the TiO<sub>2</sub> nanoparticles synthesis. The resulting sol was kept at rest for 10h to obtain a gel. Then the gel was filtered, dried at 110°C for 3h and calcined at 500°C for 10h. The calcined samples were designated as NTG0.5, NTG1, and NTG1.5, which corresponded to mass ratios in samples 1:0.06, 1:0.12, and 1:0.18 TiO<sub>2</sub>:GTE (extract), respectively. TiO<sub>2</sub> nanoparticles prepared without extract were monitored and were designated as NT. The mild, non-toxic, and inexpensive green tea extract, which has active organic components, limited agglomeration, and promoted the growth of TiO<sub>2</sub> nanoparticles. In Sundrarajan et al.’s work[235], the authors have synthesized TiO<sub>2</sub> nanoparticles by an improved hydrothermal method using *Morinda citrifolia* leaf extract. 50mL of *M. Citrifolia* leaf extract was added to 0.1M TiCl<sub>4</sub> solution. The solution was transferred to a 100mL stainless steel autoclave at 120°C for 8h and then cooled to room temperature. A white suspension was obtained, which was centrifuged at 5,000rpm/min for 10min to remove unreacted chemicals. The resulting suspension was filtered and washed several times with deionized water and ethanol. The filtered suspension was dried in an oven at 100°C for 5h. Titanium hydroxide was calcined at 400°C for 4h in a muffle furnace, resulting in quasi-microspheres of TiO<sub>2</sub> nanoparticles. X-ray diffraction patterns showed the presence of rutile phase TiO<sub>2</sub> and confirmed an average crystallites size of 10nm. Hariharan et al.[236] synthesized TiO<sub>2</sub> nanoparticles by the hydrothermal method using Aloe Vera gel for use as a photocatalyst in the degradation of picric acid. Aloe Vera was peeled and the gel was washed seven times under running water. 10mL of the gel was added to 100mL of deionized water and stirred for 1h. To this aqueous solution was added dropwise 0.1M titanium isopropoxide. The reaction mixture was stirred continuously for 1h at 20°C. The solution was kept in an autoclave at a temperature of 180°C for 4h. Then the solution was heated on a hot plate at a temperature of 80°C. The resulting product was ground and calcined in a muffle furnace at a temperature of 500°C for 5h. The size of the synthesized TiO<sub>2</sub> nanoparticles ranged from 6 to 13nm. In a study[237], TiO<sub>2</sub> nanoparticles were efficiently synthesized using aqueous extracts of *Parthenium hysterophorus* leaves by microwave irradiation. The collected leaves were washed with distilled water to remove dust particles and contaminants. About 20g of leaves were weighed and crushed into small pieces with a mortar and pestle. The samples were added to 100mL of distilled water and boiled for 10min at 60°C in a microwave oven. After boiling, the extract left to cool at room temperature.

### 3.8. Electrodeposition and Ionic Liquid-assisted Methods

Electrodeposition is a plating process in which ions in a solution migrate under the influence of an electric field (electrophoresis) and are deposited onto an electrode. In a normal process, components containing one or more dissolved metal salts are immersed in electrolytes, and the metallic ions are attracted to the cathode to be deposited. Electrodeposition is easily controlled, can produce tight coating with uniform thickness and is able to coat complex fabricated objects[238,239]. Electrodeposition of TiO<sub>2</sub> nanoparticles onto multiwalled carbon nanotube arrays was conducted in an electrolyte consisting of 3mol/L KCl solution, 10mmol/L H<sub>2</sub>O<sub>2</sub>, and 10mmol/L Ti(SO<sub>4</sub>)<sub>2</sub>. Multiwalled carbon nanotube arrays were used as the working electrode, an Ag/AgCl electrode as the reference electrode, and Pt as the counter electrode. The working potential was – 0.10V and the deposition time was 30min[240].

Ionic liquids refer to salts in the liquid state. Actually, when heated to a high temperature, almost all salts can become ionic liquids. The ionic liquid referred to here is a kind of salt that is in liquid states at low temperatures ( $< 100^{\circ}\text{C}$ ) or even room temperature. The ion size of these liquids is usually large and poorly coordinated, resulting in a low bounding force and a loose structure, thus forming a liquid rather than a solid at a relatively low temperature. Ionic liquids have many merits, they exhibit excellent thermal stability, powerful solubility, good electrical conducting ability, low viscosity, and have almost no vapor pressure. Usually, the low temperature ionic liquids have at least an organic cation (such as methylimidazolium and pyridinium ions) and an inorganic anion (such as halide, tetrafluoro-borate, and hexafluoro-phosphoric ions). Despite the fact that the ionic liquid is usually poisonous, it has found its way into the research of pharmaceuticals, gas treatment, cellulose processing, solar thermal energy, etc., and is recently used to modify the preparation process of  $\text{TiO}_2$ [241–243].

Different binary ionic liquids were applied to synthesize  $\text{TiO}_2$  hollow spheres. It was found out that the shape, size and crystallinity were different by varying the binary ionic liquid composition, which is a result of different interface interactions. In a typical process, 3.6mL of binary ionic liquids were mixed with 0.4mL of anhydrous toluene solution containing 0.2mol/L titanium isopropoxide. 6mL  $\text{CH}_3\text{OH}$  was then added and centrifuged. The final mesoporous  $\text{TiO}_2$  was obtained after filtration and calcination at  $500^{\circ}\text{C}$ . They tested all the binary mixtures of six different ionic liquids, which were 1-butyl-3-methylimidazolium hexafluorophosphate ([Bmim][PF<sub>6</sub>]), 1-hexyl-3-methylimidazolium hexafluorophosphate ([Hmim][PF<sub>6</sub>]), 1-butyl-3-methylimidazolium tetrafluoroborate ([Bmim][BF<sub>4</sub>]), 1-octyl-3-methylimidazolium hexafluorophosphate ([Omim][PF<sub>6</sub>]), 1-hexyl-3-methylimidazolium tetrafluoroborate ([Hmim][BF<sub>4</sub>]), and 1-octyl-3-methylimidazolium tetrafluoroborate ([Omim][BF<sub>4</sub>]) and discovered that [Bmim][BF<sub>4</sub>] + [Omim][PF<sub>6</sub>] mixtures were the most effective group and would make anatase  $\text{TiO}_2$  with a surface area of about  $100\text{m}^2/\text{g}$  after calcination[244]. Ionic liquid-assisted hydrothermal synthesis was reported by using 3-carboxymethyl-1-methylimidazolium bisulfate ([CMIM][HSO<sub>4</sub>]), titanium isopropoxide, concentrated HCl and  $\text{H}_2\text{O}$  to fabricate rutile  $\text{TiO}_2$  nanorod films. In a typical process, 0.5mL titanium isopropoxide was added to a mixed solution of DI water, concentrated HCl and 0.5mL [CMIM][HSO<sub>4</sub>]. The resulting transparent mixture was then transferred to a hydrothermal autoclave with a piece of glass immersed in the solution. The autoclave was heated to  $180^{\circ}\text{C}$  for 3h. When ionic liquids were not used in the process, the diameter of  $\text{TiO}_2$  was about 250nm, but when [CMIM][HSO<sub>4</sub>] was used, the diameter of  $\text{TiO}_2$  nanorods decreased to 62nm. This was not only due to the effective prevention of the gathering of the nanoparticles by the surfactant-acted ionic liquids, but also because of the extended hydrogen bonding and ionic strength which favored the formation of small crystals. Figure 14 A[190,245,256] is an FESEM image of  $\text{TiO}_2$  nanorods in Mali's work.

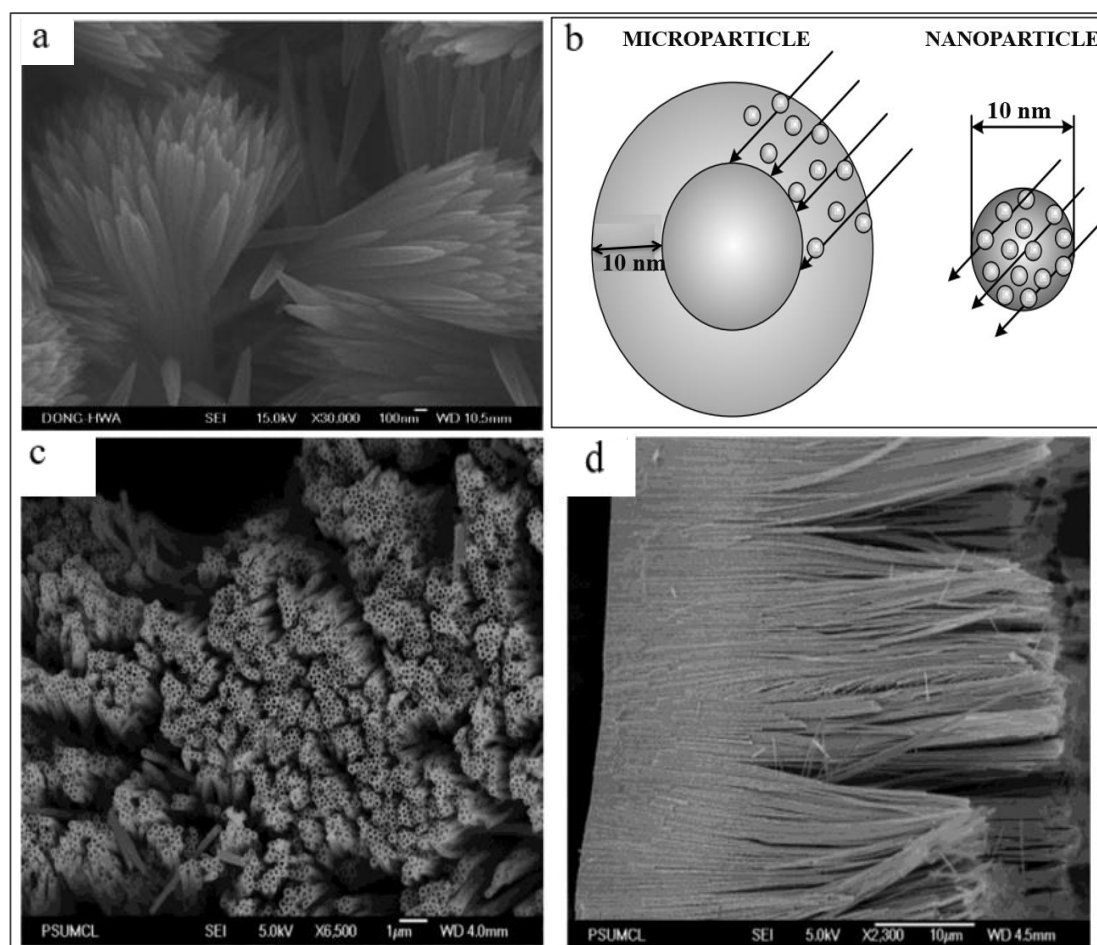


**Figure 14.** (A) An FESEM image of TiO<sub>2</sub> nanorods in Mali's work. Reprinted with permission from [245], Copyright © 2020 ROYAL SOCIETY OF CHEMISTRY; (B) absorption of light quanta in TiO<sub>2</sub> micro- and nanoparticles. Reprinted with permission from [190], Copyright © 2021, Pleiades Publishing, Ltd.; Microphotographs of the TiO<sub>2</sub> coating obtained by anodizing titanium in a fluoride-containing electrolyte: (C)-surface, (D)-slip [256].

### 3.9. Synthesis of Nanoscale and Thin Film Structures of TiO<sub>2</sub>

It is obvious that the use of nanosized TiO<sub>2</sub> particles leads to a significant increase in its photocatalytic activity. An undoubted advantage of nanoparticles compared to microparticles is the greater probability of charge release on the catalyst surface. Due to the fact that the penetration depth of UV light of TiO<sub>2</sub> particles is limited (~100nm), only the outer surface is active [246]. Figure 14B shows a diagram of light absorption by TiO<sub>2</sub> nano- and microparticles.

As can be seen from Figure 14B, reducing the size of the photocatalyst particles to nanoscale values promotes light absorption by the entire volume of particles. In this regard, the use of TiO<sub>2</sub> in heterogeneous photocatalysis processes is associated with the need to obtain nanosized particles. To date, TiO<sub>2</sub> nanoparticles are obtained with various morphologies, mainly nanotubes, nanowires, nanorods and mesoporous structures [247].

Thus, the properties and applications of TiO<sub>2</sub> nanostructures largely depend on the particle size, structure, effective surface area, and surface properties. Since these properties are in turn influenced with synthesis methods, in this section we will have an overview of different methods of synthesis of nanoparticles TiO<sub>2</sub> thin films [248–250]. Chemical reactions for the synthesis of substances can take place in gaseous, liquid or solid forms. The rate of penetration of reactants in the gas or liquid phase is several times faster than in the solid phase. Therefore, the synthesis methods for TiO<sub>2</sub>-based nanostructures are mainly divided into liquid-phase synthesis and vapour-phase synthesis [251–253]. Moreover, nanostructured TiO<sub>2</sub> particles can be obtained by oxidation of metallic titanium using



various chemical oxidants[254].  $\text{TiO}_2$  nanorods were obtained by this method (by oxidation of a titanium metal plate with hydrogen peroxide). Paulose et al.[255] showed that anodic oxidation of titanium in a fluoride-containing electrolyte allows obtaining nanostructured coatings consisting of  $\text{TiO}_2$  tubes, the properties of which can be controlled by varying the oxidation conditions. However, the authors showed that such coatings with a nanotube length of more than  $1\mu\text{m}$  have low adhesion, and their application is still very limited. Then Ali et al.[256] proved that poor adhesion is due to the low packing density of the nanotubes (Figure 14C and 14D[256]).

According to modern concepts, the growth model of  $\text{TiO}_2$  nanotubes during potentiostatic anodizing consists of several stages, and the reactions responsible for the formation of porous aluminum oxide and  $\text{TiO}_2$  nanotubes[254–257] are identical. Despite the similarity of the processes occurring during the anodization of titanium and aluminum, the morphology of the resulting oxides differs greatly. For example, during the anodization of aluminum, a mesoporous structure is formed, whereas during the anodization of titanium, both mesoporous and nanotubular structures can be obtained[257]. At the same time, the use of porous carriers active only under the influence of UV light, inside the pores of which there are particles activated by light with a wavelength of 400-700nm, seems very promising. Such an approach will make it possible to use both visible and UV radiation in photocatalytic processes.

#### 4. Concept of Photocatalysis Using $\text{TiO}_2$

In 1967, while Professor Fujishima and his colleague Honda[22,237,258] were experimenting, they encountered a strange phenomenon. They observed that when  $\text{TiO}_2$  and Pt electrodes were placed in water, the formed circuit is capable of decomposing water into oxygen and hydrogen without an external electricity input, only when exposed to light[259,260]. Following this phenomenon, Honda discovered that  $\text{TiO}_2$  has strong oxidizing properties, and focused his subsequent studies on the effect of this valuable substance on environmental phenomena such as sterilization, disinfection and pollution removal[261–267]. This important discovery, known as the photocatalytic or Honda-Fujishima effect, resulted in antibacterial products, being one of the most advanced tools for disinfection of spaces and one of the main branches studied in the materials industry[264–267].

$\text{TiO}_2$  photocatalysis is a photon-driven reaction process[214], starting with a photoadsorption event on the surface or bulk of  $\text{TiO}_2$  (Figure 15). When  $\text{TiO}_2$  adsorbs photons with energies greater than or equal to its BG, electrons in the filled VB are excited to the vacant CBs, leaving holes in the VB.

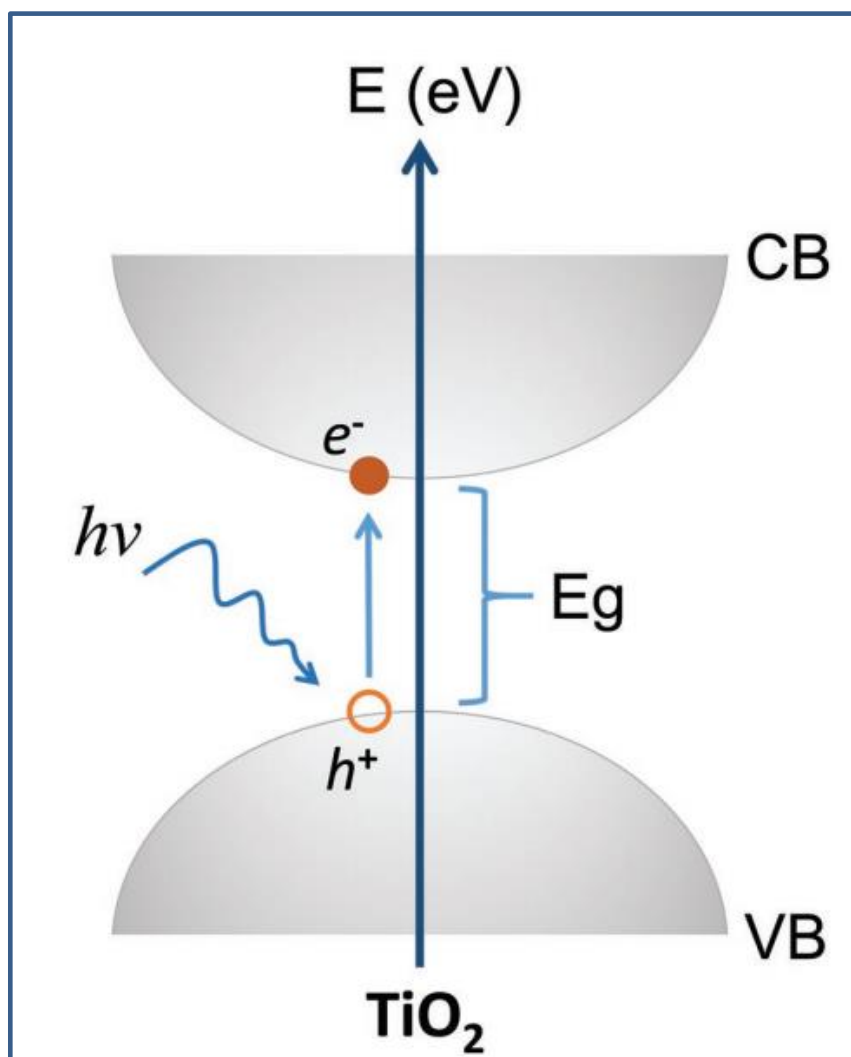


**Figure 15.** Schematic diagram of a typical excitation of electrons from the filled TiO<sub>2</sub> VB to the unoccupied CB via band-to-band excitation. Reprinted with permission from [159]. Copyright 2019, WILEY-VCH Verlag GmbH & Co. KGaA, Weinheim.

The photocatalysts TiO<sub>2</sub> exhibits light absorption property and redox ability based on the position of the VB and CB band edges and the value of  $E_g$ . Essentially, the photocatalytic properties of TiO<sub>2</sub> are based on the generation of electron-hole pairs within the semiconductor particle by electromagnetic radiation. These pairs then interact with adsorbed molecules through redox reactions once they reach the surface of the TiO<sub>2</sub> particle. In this case, a part of the electrons and holes can be subjected to recombination in the volume or on the surface of TiO<sub>2</sub> (Figure 16)[268]. For effective photocatalytic processes, it is necessary that redox reactions involving electron-hole pairs be more efficient than recombination processes. It is known that for most reactions, TiO<sub>2</sub> in the anatase phase state exhibits higher activity than other polymorphic modifications[269]. It has been suggested that the high photoreactivity of anatase is due to the higher location of the Fermi level, which reduces the ability to absorb oxygen and increases the degree of hydroxylation (i.e., the number of hydroxyl groups on the surface)[268]. In general, semiconductor photocatalysis is considered, from this point of view, as a multi-step process, which is illustrated in Figure 15. Such a process is initiated by the photoexcitation with electromagnetic radiation equal to or exceeding  $E_g$  (1) the separation of the charge carrier pairs, (2) the diffusion of  $e^-/h^+$  species within the material towards the surface, and (3) the surface charge transfer for the reduction of adsorbed electron acceptors, and (4) the oxidation of adsorbed electron donors, respectively[270]. Accordingly, the photo-induced electrons and holes should migrate to reach the surface of the material and react with adsorbed chemical species via

surface charge transfer. Therefore, the  $E_g$  of a semiconductor is the minimum thermodynamic requirement for photocatalysis[268].

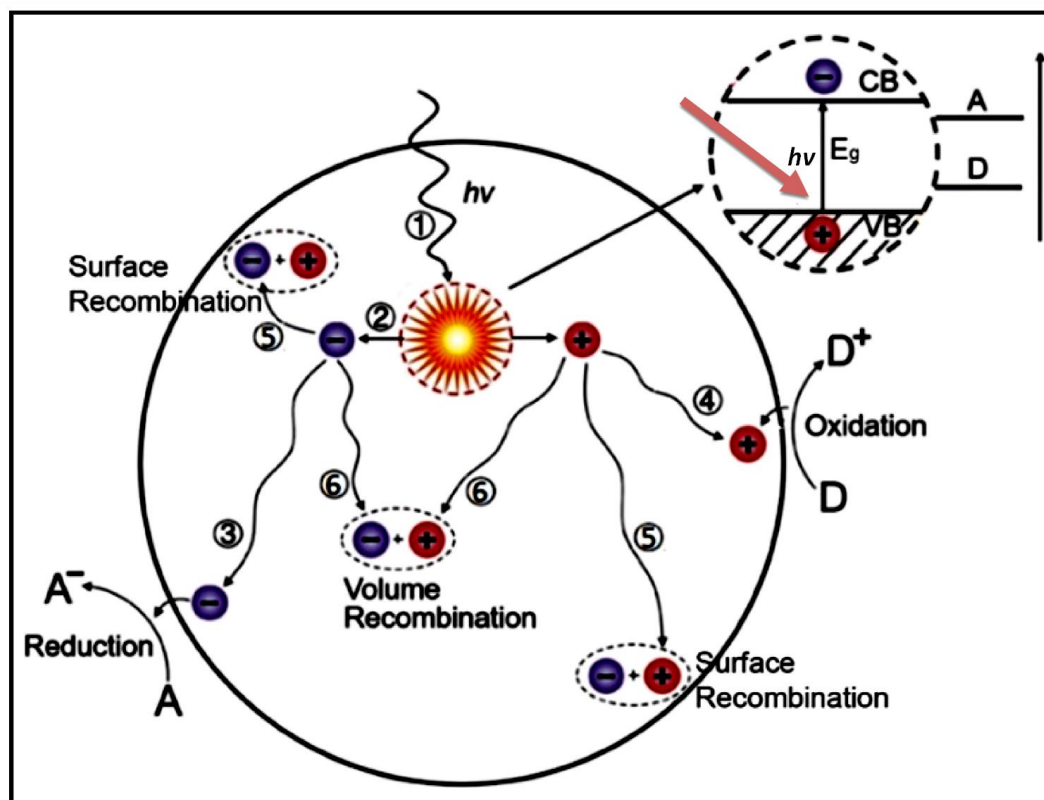


**Figure 16.** Pathways of the photogenerated charge carriers in a semiconductor photocatalyst. Reprinted with permission from [159]. Copyright 2019, WILEY-VCH Verlag GmbH & Co. KGaA, Weinheim.

One of the main limitations of semiconductor photocatalysis is the recombination of the photogenerated charge carriers, dissipating the absorbed energy as heat and affecting negatively the lifetime of the electrons and holes[270]. This undesired recombination occurred either indirectly, i.e., (5) via surface defects, or directly, i.e., by (6) band-to-band recombination. Such phenomena are highly reliant on the crystal structure of the semiconductor. To enhance effectively the redox reactions while minimizing recombination, the photogenerated charge carriers must migrate to the liquid junction through the solid and should react with adsorbed species directly at the semiconductor surface[268]. In the literature, there are data on reactions in which both crystalline phases show the same activity[271], and there are also data on the higher activity of rutile[272]. In addition, there are works in which the authors claim that a mixture of anatase (70-75%) and rutile (30-25%) is a more active photocatalyst than pure anatase[273]. The discrepancy in results may be due to various factors such as specific surface area, pore size, crystallite size, method of preparation, or the form in which the activity is expressed. A commercial  $\text{TiO}_2$  photocatalyst P25 (Evonik Industrials, Germany), consisting of an amorphous phase and an 80/20 mixture of anatase and rutile, shows higher activity in some reactions than pure crystalline phases[274]. The enhanced activity of the catalyst results from the efficient separation of charge carriers due to the multiphase nature of the particles[275]. Another commercial  $\text{TiO}_2$  photocatalyst is Hombikat UV 100 ("Sachtlebem", Germany), which consists only of anatase and has high activity due to the high rate of interfacial electron transfer. For example, it is known that the deposition of platinum on the surface of  $\text{TiO}_2$  can lead to both an increase and a decrease in activity[275]. In most cases, this is explained by different ways of depositing Pt particles.

## 5. Growing Interest in the Application Of $\text{TiO}_2$ Photocatalysis

In recent years, photocatalytic processes have found increasing applications in a variety of fields. Heterogeneous photocatalysis has already established itself as an inexpensive and sustainable technology for purifying water and air from a variety of hazardous pollutants, including organic substances and heavy metals[276]. The most active development of this technology is in Japan, USA, India and China. Figure 17 shows the number of scientific publications devoted to this field from 1967 to 2024, where it can be seen that in the last decade the interest in this field is steadily increasing[277]. According to the statistics on publications in the National Library of Medicine from 1967 to 2000, from 3 to 7 publications were published annually, but from 2001 to 2013 and 2014 to 2024 there is a high growth of interest in research in the field of photocatalysis.

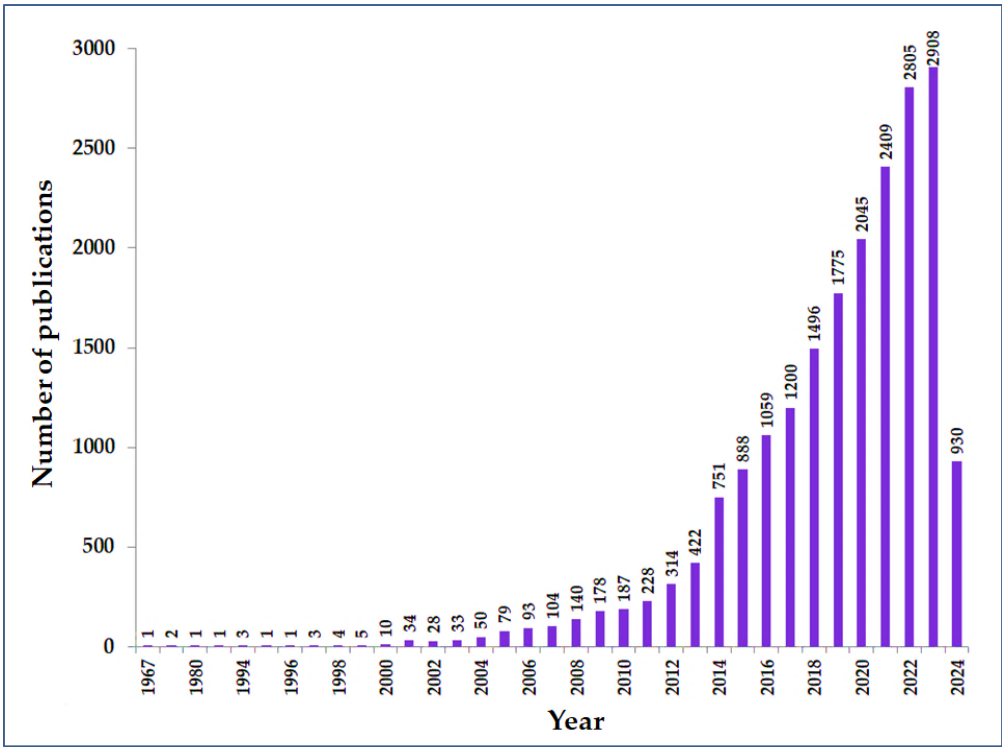


**Figure 17.** Annual statistics of scientific publications on photocatalysis.

The growing interest in this field is due to the fact that, unlike other processes such as reverse osmosis, nanofiltration, and ultrafiltration, photocatalysis is a cheap and potentially “stand-alone” water purification technology. At the same time, TiO<sub>2</sub>, as a low-cost photocatalytic material, is prominent among other solid materials. In fact, according to Figure 18, the number of scientific publications dealing with TiO<sub>2</sub>-based photocatalysis accounts for the bulk of publications in the field of photocatalysis. A total of 127 out of the total number (930) articles on photocatalysis have been published on the topic of TiO<sub>2</sub> photocatalysis in the first trimester of 2024, of which TiO<sub>2</sub> can be noted as the most sought-after material in this field of photocatalysis.



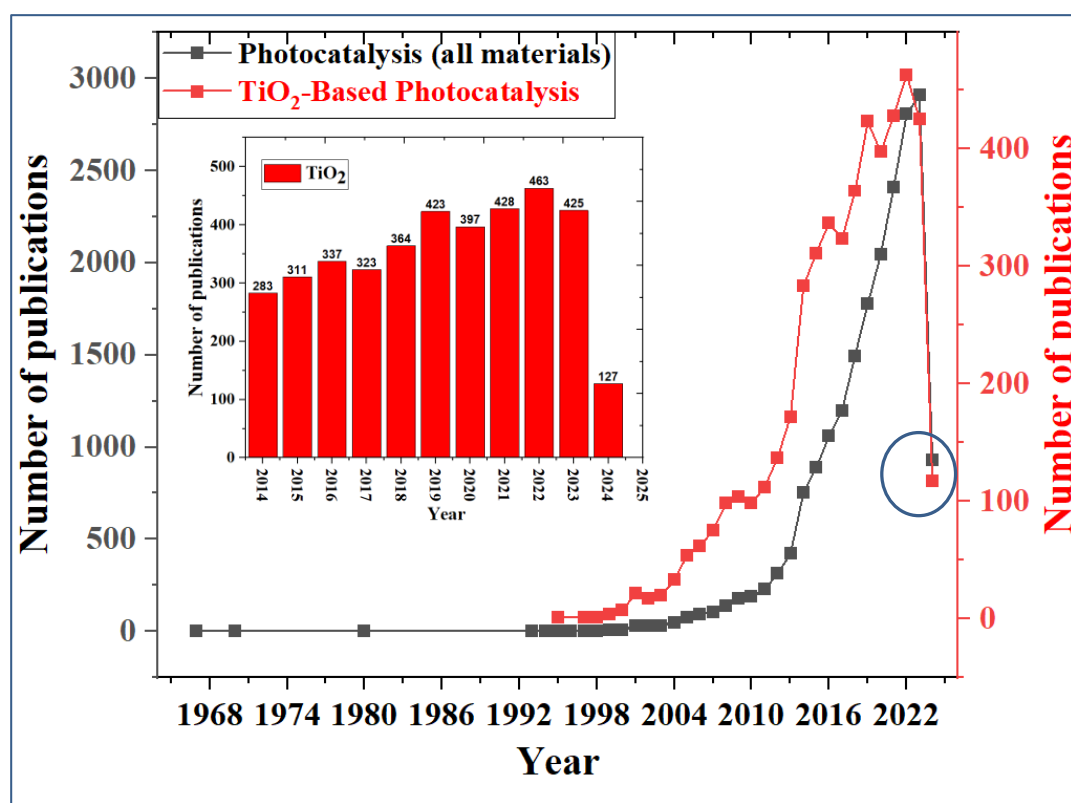


**Figure 18.** Comparison of the total number of scientific publications on photocatalysis with those on TiO<sub>2</sub>-based photocatalysis.

The use of sunlight or UV radiation makes photocatalytic purification technology inexpensive, environmentally friendly, and possible to use worldwide. The use of photocatalysis processes requires minimal equipment and is suitable for developing countries as well as remote sites without access to electricity. TiO<sub>2</sub> photocatalysis has been successfully used in many developing countries for fresh water disinfection and decolorization[278]. Future environmental purification technologies also involve the use of TiO<sub>2</sub> as a photocatalyst capable of utilizing organic pollutants from water, air, and other media due to the formation of free OH radicals during the transformation reaction[278]. It is known that TiO<sub>2</sub> dust particles can act bactericidally[279] and even inhibit cancer cells[280] under the influence of UV light. Those or other properties of TiO<sub>2</sub> depend on its structural and morphological features and chemical varieties. This in turn depends on the technological conditions of synthesis and surface modifications. Specific examples of photocatalysis applications are given below.

### 5.1. Purification of Water and Air from Organic Pollutants

Recently, considerable attention has been paid to the use of photocatalysis for the oxidation of organic pollutants in wastewater, in particular because of its ability to oxidize almost any toxic organic substance to CO<sub>2</sub> and H<sub>2</sub>O[281]. The essence of the photocatalytic process of oxidation of organic compounds is as follows: under the action of light energy, electron-hole pairs are formed in TiO<sub>2</sub> particles. Holes, when coming to the surface of the particle, interact with the electron donor in solution or with hydroxyl ions to form strong oxidizing agents such as hydroxyl or superoxide radicals. In turn, the conduction electrons reaching the surface of TiO<sub>2</sub> interact with oxygen[282], which leads to the formation of superoxide anion radical, electron can interact with organic substances that can act as electron acceptors. The formation of such particles makes the TiO<sub>2</sub> surface a very strong oxidizer, which allows the mineralization of harmful substances by their photocatalytic oxidation to H<sub>2</sub>O and CO<sub>2</sub>. Figure 19 shows the scheme of formation of such oxidants on the surface of TiO<sub>2</sub> under the action of light energy.

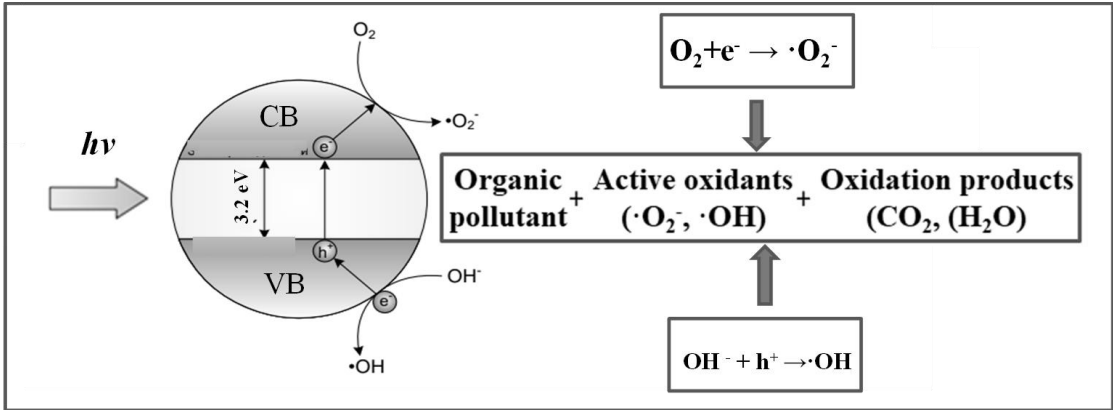


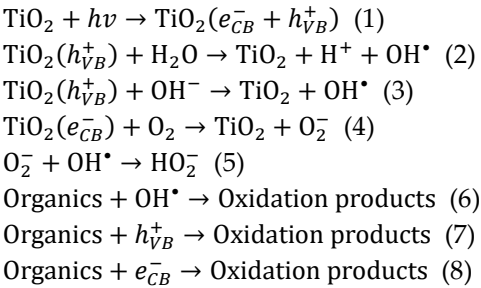
**Figure 19.** Scheme of formation of OH•, and O<sub>2</sub><sup>•-</sup> particles on the surface of TiO<sub>2</sub> under the action of light.

Redox potentials (relative to the standard hydrogen electrode) for a number of the strongest oxidizing agents are presented in Table 3.

**Table 3.** Oxidizing Potentials of Various Chemical Agents.

| Oxidizing Agent                                     | Oxidizing Potential (V) |
|---|-------------------------|
| Hydroxyl radical, HO•                               | +2.80                   |
| Electron hole in VB, h <sup>+</sup>                 | +2.70                   |
| Ozone, O <sub>3</sub>                               | +2.07                   |
| Hydrogen peroxide, H <sub>2</sub> O <sub>2</sub>    | +1.78                   |
| Permanganate ion, (MnO <sub>4</sub> ) <sup>2-</sup> | +1.70                   |
| Chlorine dioxide, ClO <sub>2</sub>                  | +1.15                   |
| Chlorine, Cl <sub>2</sub>                           | +1.40                   |
| Oxygen, O <sub>2</sub>                              | +1.20                   |
| Superoxide radical, O <sub>2</sub> <sup>•-</sup>    | -0.33                   |
| Electron in the CB, e <sup>-</sup>                  | -0.50                   |

As can be seen from Table 3, the HO• - particle is a very strong oxidizing agent (standard redox potential of 2.8V), which allows the oxidation of most organic substances to CO<sub>2</sub> and H<sub>2</sub>O. The processes occurring on the TiO<sub>2</sub> surface as a result of the oxidation of organic pollutants can be expressed by the following reactions:



Photocatalytic water and air purification systems with artificial UV radiation have been on the market for several years, while solar photocatalytic purification plants are at the stage of demonstration and pilot projects. In addition, the combination of photocatalysis and membrane treatment can reduce the fouling of the filter membrane and thus significantly increase the efficiency of water treatment. Nitrogen oxides in tunnels are a serious problem during the summer months, especially in dense and large cities with high traffic levels. Japan and a number of European countries

are actively using cement with TiO<sub>2</sub> additives for tunnel construction. The installation of UV lamps in such tunnels allows controlling exhaust gas emissions, mainly NO and NO<sub>2</sub>[283].

### 5.2. TiO<sub>2</sub> and Water Photolysis

Hydrogen is an environmentally friendly source of energy. Currently, hydrogen is produced from various primary sources such as natural gas, fuel oil, CH<sub>3</sub>OH, biomass, and coal[284–289]. Among these sources, photolysis of water, using solar energy, has attracted the most attention because of its potential. Direct photocatalytic using sunlight is the most efficient way to produce hydrogen because it avoids energy losses in the process of electricity transmission. Interest in this process intensified after the work of Japanese scientists Honda and Fujishima in 1972[286], who were able to obtain hydrogen by irradiating aqueous suspension of TiO<sub>2</sub> with UV light. From the thermodynamic point of view, the reaction of water photolysis proceeds with a significant positive change in the Gibbs free energy ( $\Delta G=237.2\text{kJ/mol}$ , 1.23eV per electron)[287]. For water splitting, the absorbed photon energy must overcome this energy. From the electrochemical point of view, the process of water decomposition into hydrogen and oxygen is stepwise and two electrons take part in it. To overcome the Gibbs free energy, a semiconductor photocatalyst must have a forbidden zone width with an energy greater than 1.23eV. In addition, the CB must be located higher than the water reduction potential, and the VB ceiling must be located lower than the water oxidation potential.

### 5.3. Treatment of Water from Inorganic Compounds

In addition to organic compounds, wastewater contains a wide range of inorganic compounds that are sensitive to photochemical transformations on the catalyst surface. Bromate, chlorate, azide, halide ions, and oxidazote can be photodegraded on the TiO<sub>2</sub> surface. Metal salts such as AgNO<sub>3</sub>, HgCl, and organometallic compounds (e.g., CH<sub>3</sub>HgCl) can be removed from water[289–291]. The content of metals in water, such as mercury (Hg), chromium (Cr), and lead (Pb), is very hazardous to human health. Removal of these toxic metals is a fundamental task in obtaining quality water. With the help of heterogeneous photocatalysis, it is possible to remove heavy metals from wastewater through their reduction by TiO<sub>2</sub>. The authors of [292,293] demonstrated the possibility of photoreduction of metals from industrial wastewater, such as gold (Au), platinum (Pt), and silver (Ag).

### 5.4. Medical Applications of TiO<sub>2</sub>

Hospitals and medical equipment are the only places where climate-controlled treatment and disinfection are required. However, in other environments where plants and animals grow and reproduce, making them susceptible to contamination, microbes and pests must be removed from surfaces, water and air[294]. A basic method of eradicating these microbes must be developed because microbial, viral and fungal structures are becoming increasingly resistant to the use of chemical disinfectants, and these chemicals themselves are dangerous and lethal to human life[295]. DNA damage can affect any biological structure. Therefore, one effective method of getting rid of them is to create proteins that disrupt DNA cell division cycles[296]. On the other hand, the increase in oxygen gas pressure is harmful and deadly for all types of life[297]. Thus, titanium surfaces, along with their photocatalytic properties, produce oxygen free radicals and create an oxygen poisoning for microorganisms[298]. Japanese scientists have found that adding TiO<sub>2</sub> to fabrics helps create an antibactericidal material. Thus, gowns sewn from this fabric can be treated with UV for disinfection after working hours[299]. In their works[299,300], the authors managed to find an application of the photocatalysis effect of TiO<sub>2</sub> nanoparticles in photodynamic therapy to destroy cancer cells. The researchers managed to remove cancerous tumors from the colon in mice using photo-catalytic oxidation[300]. TiO<sub>2</sub> nanoparticles were injected at the site of the cancerous tumor, and illumination was performed using a fiber optic cable. As a result, the light produced reactive oxygen species that oxidized the tumor cells.

Cancer is considered one of the greatest challenges for modern medicine. Despite the continuous development of modern cancer therapies, the first line of therapy is surgical removal of the tumour

and / or radiation therapy. Chemotherapy is usually an adjunctive therapy, but its use is limited by many factors[301,302]. First of all, chemotherapeutic drugs are extremely toxic to rapidly proliferating, both cancerous and healthy, tissues of the human body. Therefore, new delivery systems are still being sought to increase the tissue specificity of therapy and reduce systemic effects. Many chemotherapeutic drugs are also ineffective due to the multidrug resistance mechanism exhibited by cancer cells, which is related to the overexpression of some members of the ABC efflux transporter superfamily, which perceive the drug as a poison and eliminate it from the matrix. Currently, one of the most frequently studied chemotherapeutic drugs is doxorubicin. Although it offers many advantages in the therapy of various cancers, the use of doxorubicin is associated with side effects, among which cardiotoxicity is the most severe and dangerous[302,303]. The use of nanoparticles and the combination of chemotherapy with photodynamic or photothermal therapy could be a potential solution to both problems [302]. Titanium nanoparticles have significant advantages in this field, providing efficient delivery of drug molecules, hence better pharmacokinetics, and targeted delivery.

The potential application of one-dimensional TiO<sub>2</sub> whiskers for drug delivery in cancer therapy and their synergistic effect on the internalization and accumulation of daunorubicin in SMMC-7721 cells were first investigated by Li et al[304]. In addition, conjugation of doxorubicin to TiO<sub>2</sub> nanoparticles was reported to induce a synergistic response in breast cancer cell lines[305]. For blood-contacting medical materials, it is important to minimize the tendency of their surface to adsorb blood proteins and enhance blood coagulability to reduce the risk of thrombosis. TiO<sub>2</sub>s are known to be highly compatible with blood, so they are often proposed as coatings for blood-contacting implants. The conducted study of the interaction of blood plasma proteins with TiO<sub>2</sub> will allow a better understanding of the nature of the interaction of foreign surfaces with blood, as well as their integration into tissues, starting from the first meeting with blood during surgery and then in the subsequent process of wound healing. Research in this area is being carried out at an accelerating pace and in recent years, optimization of the properties of TiO<sub>2</sub> nanoparticles for photodynamic therapy with excitation by UV or visible light after doping with organic photosensitizers has been developing.

Applications of TiO<sub>2</sub> in medicine are going further than the design of drug delivery systems or applications as vehicles for chemotherapeutics. TiO<sub>2</sub> Nanoparticles have been applied in pharmacy, especially in pharmaceutical chemistry and technology, as well as medicine, including growing areas related to dentistry and surgery[306].

### 5.5. Photocatalytic Reduction of CO<sub>2</sub>

The process of direct conversion of CO<sub>2</sub> and water vapour into hydrocarbon fuel using sunlight is aimed at solving two main global problems: ecological - reduction of CO<sub>2</sub> content in the atmosphere and energetic - obtaining high-energy fuel using the energy of sunlight. In Woolerton et al's study[307], the process of CO<sub>2</sub> reduction by H<sub>2</sub>O vapor on the surface of various semiconductor compounds (in the form of TiO<sub>2</sub>, ZnO, CdS, SiC, and WO<sub>3</sub> powders) under xenon lamp illumination was studied. American scientists have developed a composite photocatalyst that acts selectively with respect to the process of reducing CO<sub>2</sub> to CO under the influence of visible light. The main components of this photocatalyst are an enzyme (catalyst), sensitizer, and nanoparticles of TiO<sub>2</sub>[308]. The enzyme included in the composite photocatalyst catalyzes exclusively the two-electron reduction of CO<sub>2</sub> to CO, bypassing the undesirable one-electron radical pathway. In contrast to other TiO<sub>2</sub>-based systems, the investigated system is characterized by selectivity and allows obtaining the target product without impurities.

The greatest success in this direction was achieved by American scientists, who, as a photocatalyst, used TiO<sub>2</sub> nanotubes obtained by anodic oxidation of titanium modified with Cu or Pt nanoparticles[309]. The total productivity for all hydrocarbons obtained in the laboratory was 160 μL/hour per gram of nanotubes. These results are 20 times higher than all previously described methods, but they are still too low for direct practical application. At present, there is an extensive search for new photocatalysts for CO<sub>2</sub> reduction, but despite the abundance of different



photocatalysts, the main preference is still given to  $\text{TiO}_2$ , the surface of which is doped with metal nanoparticles[310]. Thus, water photolysis and carbon dioxide reduction are among the promising areas that have both scientific and applied significance for mankind.

## 6. Current Challenges

Despite intensive research over the past decades, the desired photocatalytic efficiency of  $\text{TiO}_2$  has not yet been achieved at a level suitable for large-scale practical applications. For example, a survey of more than 80 major global water treatment companies showed that only about 4% have utilized photocatalysis on a pilot scale[311]. This is a clear sign of lack of patronage of the technology. If  $\text{TiO}_2$  is chosen for the application of such technology, the effect of anions on the lifetime of  $\text{TiO}_2$  reactor layers cannot be adequately addressed until the electronic, structural and optical properties of  $\text{TiO}_2$  nanoparticles and their interactions in aqueous media are addressed in detail, both theoretically and experimentally. The approach will focus on modifying the model of research methods and presentation and discussion of results. The style of research methods and discussion in reported cases of  $\text{TiO}_2$  deactivation in aqueous suspensions does not reflect differences in the lattices or phase stability of  $\text{TiO}_2$ , while these differences (in lattices) play an important role in computational and experimental analysis. Early thermodynamic analyses of the phase stability of nanocrystalline anatase and rutile were performed by Zhang and Banfield[312]. They concluded that when the particle size is reduced to 14 nm, the structure of anatase becomes more stable than that of rutile. Penn and Banfield[313] indicated that anatase clusters dominate on 101 surfaces while rutile clusters usually dominate on 110 surfaces according to the results of Ramamurthy, Vanderbilt and King-Smith calculations[314]. The reason for the change in phase stability is the higher free energy of rutile arising from the energetics of the dominant surface facet types in such small particles[315]. These minute details should be taken into account in future modeling and experiments.

The behavior in volume also deserves consideration. In the case of bulk quantities, rutile is the most stable crystalline structure of  $\text{TiO}_2$ . For nanoparticles, however, the anatase structure becomes more favorable for medical applications[315]. This has been observed experimentally, for example, in the case of thin layers of  $\text{TiO}_2$ [316]. The driving force behind this phase transformation is the surface energetics of the different surfaces of  $\text{TiO}_2$ . A nanoparticle is a closed object bounded by surface boundaries and the surface-to-volume ratio increases dramatically compared to larger particles, and the various surface energies begin to play an increasingly important role in particle energetics.

In addition, reports on the deactivation of  $\text{TiO}_2$  in aqueous media often do not specify the reaction conditions (except pH and opacity), despite the fact that photoreactions are sensitive to reaction conditions. The phenomenon of photo-induced hydrophilic effect and its conditions are often ignored, and it is a well-known phenomenon in surface science research, describing a process in which UV irradiation in air causes water droplets to wet the surface of a  $\text{TiO}_2$  film, resulting in a decrease in contact angle over time. Although temperature is also a factor when molecules or atoms come into contact with a surface, numerous analyses of temperature dependence, especially in gas- $\text{TiO}_2$  photocatalysis, have been published in Temperature Programmed Desorption (TPD)[317] as it provides information on how reaction temperature affects the binding energy of the adsorbate and surface, but its influence is often ignored when discussing aqueous photodegradation. Among the various materials that have been studied for photocatalytic  $\text{CO}_2$  reduction,  $\text{TiO}_2$  is of great interest because of its high photocatalytic activity, high physical and chemical stability, non-toxicity and low cost[318,319]. But also in this area, there are two major problems faced by  $\text{TiO}_2$ -based photocatalysts for conventional applications. Thus, the large forbidden band width (3.3eV), which limits its photoabsorption to UV light only, and the rapid recombination of electron-hole pairs that limits the photocatalytic efficiency negatively affect the yield fraction in  $\text{CO}_2$  photoreduction. Regarding the problem of medical applications, studies have shown that exposure to  $\text{TiO}_2$  can reduce cell viability and increase caspase-3 levels, indicating the possibility of inducing cell cytotoxicity and apoptosis. One study found that only particles smaller than 100nm at doses of 50 and 100g/mL could induce apoptosis of Caco-2 cells[320], which prompts a comprehensive investigation into the cause and

solution of this problem. The toxicity of  $\text{TiO}_2$  depends on factors such as particle size, shape, exposure scenario, dose, crystal structure and surface charge. It is crucial to thoroughly investigate the combined cytotoxic effect of doped  $\text{TiO}_2$ .  $\text{TiO}_2$  is a common pigment in the plastic industry that may pose a threat to aquatic life due to the potential leaching of  $\text{TiO}_2$  and other toxic plastic additives during environmental weathering of large pigmented plastic wastes[321]. In the former case, the surface functions of pigmented  $\text{TiO}_2$  or  $\text{TiO}_2$  nanoparticles differ between the two particle types and within each size class. In the latter case, the exposure pathway for human or environmental exposure differs between studies, with results showing that particle efficacy and biological model sensitivity differ between published reports. Although the knowledge base on industrially significant  $\text{TiO}_2$  and its environmental health effects is large, the fine details of the physicochemical properties of the particles combined with the design of the toxicology study add notable differences in the types and extent of adverse health effects observed[321]. However, despite the existing barriers, the development and understanding of a highly efficient  $\text{TiO}_2$ -based photocatalyst will continue, so the challenges of large-scale application of  $\text{TiO}_2$  for water disinfection, cancer eradication, and carbon dioxide reduction are only a matter of time. Further work in this area should focus on optimizing the properties of this material by tuning and engineering its structure.

## 7. Opportunities

To date, most of the fundamental processes in  $\text{TiO}_2$  photocatalysis can be studied on model  $\text{TiO}_2$  surfaces by ensemble-averaged experimental methods, including STM, TPD, PSD, IRAS, etc. However, detailed dynamical information on the transient structure of adsorbates, reaction intermediates, bond breaking / formation, and changes in the electronic structures of adsorbates cannot yet be obtained using these methods. Fortunately, the development of ultrafast time-resolved methods gives us the ability to follow these dynamic processes in the photocatalysis of  $\text{TiO}_2$ . For example, the dynamic processes of bond breaking and bond formation during CO desorption and CO oxidation on Ru (0001) have been successfully tracked by Nilsson and co-workers[322] using time-resolved femtosecond emission spectroscopy and X-ray absorption spectroscopy techniques. In addition, time-resolved UPS and 2PPE techniques have been successfully utilized to monitor electron transfer dynamics and VB changes associated with electron-mediated surface reactions[314–322]. In addition, time-resolved SFG can monitor the transition structures of adsorbates in photocatalysis by tracking molecular vibrations. With the advent of new methodology and high-knockdown technology, it may provide opportunities to further deepen the understanding of  $\text{TiO}_2$  photocatalysis and shed light on the fundamental photochemical mechanisms and basic principles of  $\text{TiO}_2$  photocatalysis[322–328].

## 8. Summary and Future Perspectives

Photocatalysis is an environmentally friendly technological process in which solar energy is converted into useful chemical reactions. In claiming the most efficient photocatalytic activity of  $\text{TiO}_2$ , challenges and limitations arise, which are mainly related to the synthesis methods of functionalized  $\text{TiO}_2$ -based materials. Therefore, researchers aim to propose and / or modify various methods to overcome the existing barriers in  $\text{TiO}_2$  photocatalysis applications and thereby enhance the further development of photocatalytic applications using  $\text{TiO}_2$ . In this review, the known methods for the synthesis of  $\text{TiO}_2$  are reviewed and summarized, and the advantages and challenges related to the properties and morphology of  $\text{TiO}_2$ -based functional materials obtained by these methods are discussed. Great importance in this context is given to the use of nanoparticles, which improve the expected results by modifying the size, shape and physicochemical properties of the particles. It is revealed that poor recombination of charge carriers is one of the main limitations in the photocatalytic process involving  $\text{TiO}_2$ , which can be solved by doping, metals and non-metallic modifiers that have the ability to suppress the recombination of photogenerated electrons and holes, providing charge carrier separation. At the same time, it can improve the photoenergy capture by narrowing the forbidden band of  $\text{TiO}_2$ . The applications of  $\text{TiO}_2$  photocatalysis are based on environmental decontamination, biomedical, pharmaceutical and energy applications. Thus,  $\text{TiO}_2$  photocatalysis

plays a crucial role in achieving higher technological development while maintaining a balance with environmental sustainability, which is in line with some of the main goals of the UN sustainable development strategy.

Consideration of future perspectives is important to fill the gaps in the development process of TiO<sub>2</sub>-based photocatalysis, which requires gradual development towards practical applications in different scenarios. Future research should focus on theoretical (DFT, machine learning predictions) and experimental studies based on the electron capture mechanism, to study in detail and precisely modify the process to achieve higher photocatalytic efficiency and extend the lifetime of photoexcited electrons and holes in TiO<sub>2</sub>.

**Acknowledgments:** This work was supported by the International Science and Technology Center (grant no. TJ-2726).

**Conflicts of Interest:** The author declared no conflicts of interest.

**Author Contributions:** Nematov D was responsible for the collection, compilation and summary of all data for articles.

### Abbreviation List

BG, Bandgap  
 CB, Conduction band  
 CH<sub>3</sub>OH, Methanol  
 CVD, Chemical vapor deposition  
 EtOH, Ethanol  
 OR, Alkoxy groups  
 STM, Scanning tunneling microscopy  
 TiCl<sub>4</sub>, Titanium tetrachloride  
 TiO<sub>2</sub>, Titanium dioxide  
 TNB, Titanium n-butoxide  
 TPD, Temperature programmed desorption  
 TTIP, Titanium tetraisopropoxide  
 UV, Ultraviolet  
 VB, Valence bands  
 VOCs, Volatile organic compounds

### References

1. Wang J, Azam W. Natural resource scarcity, fossil fuel energy consumption, and total greenhouse gas emissions in top emitting countries. *Geosci Front*, 2024; 15: 101757.[DOI]
2. Schneider J, Matsuoka M, Takeuchi M et al. Understanding TiO<sub>2</sub> Photocatalysis: Mechanisms and Materials. *Chem Rev*, 2014; 114: 9919-9986.[DOI]
3. Xuan VN, Hoa PX, Thu NTP et al. Factors affecting environmental pollution for green economy: The case of ASEAN countries. *Environ Chall*, 2024; 14: 100827.[DOI]
4. Kabir M, Habiba UE, Khan W et al. Climate change due to increasing concentration of carbon dioxide and its impacts on environment in 21st century; a mini review. *J King Saud Univ Sci*, 2023; 35: 102693.[DOI]
5. Bordet A, Leitner W. Adaptive Catalytic Systems for Chemical Energy Conversion. *Angew Chem Int Edit*, 2023; 62: e202301956.[DOI]
6. Hassan Q, Tabar V, Sameen AZ et al. A review of green hydrogen production based on solar energy; techniques and methods. *Energ Harvesting Sys*, 2024; 11: 20220134.[DOI]
7. Dang VH, Nguyen TA, Le MV et al. Photocatalytic hydrogen production from seawater splitting: Current status, challenges, strategies and prospective applications. *Chem Eng J*, 2024; 484: 149213.[DOI]
8. Zhang C, Li N, An G. Review of Concentrated Solar Power Technology Applications in Photocatalytic Water Purification and Energy Conversion: Overview, Challenges and Future Directions. *Energies*, 2024 ; 17: 463.[DOI]
9. Mohtaram S, Mohtaram MS, Sabbaghi S et al. Enhancement strategies in CO<sub>2</sub> conversion and management of biochar supported photocatalyst for effective generation of renewable and sustainable solar energy. *Energ Convers Manage*, 2024; 300: 117987.[DOI]

10. Worku AK, Ayele DW, Deepak DB et al. Recent Advances and Challenges of Hydrogen Production Technologies via Renewable Energy Sources. *Adv Energy Sustain Res*, 2024; 5: 2300273.[DOI]
11. Kumar A, Rana S, Dhiman P et al. Current progress in heterojunctions based on Nb<sub>2</sub>O<sub>5</sub> for photocatalytic water treatment and energy applications. *J Mol Liq*, 2024; 399: 124360.[DOI]
12. Albini A, Fagnoni M. 1908: Giacomo Ciamician and the Concept of Green Chemistry. *Chem Sus Chem*, 2008; 1: 63-66.[DOI]
13. Zhu S, Wang D. Photocatalysis: Basic Principles, Diverse Forms of Implementations and Emerging Scientific Opportunities. *Adv Energy Mater*, 2017; 7: 1700841.[DOI]
14. Bruner L, Kozak J. On the knowledge of photocatalysis. I. The light reaction in mixtures: uranium salt + oxalic acid [In German]. *J Electroche Appl Phys Chem*, 1911; 17: 354-360.[DOI]
15. Eibner A. Action of light on pigments I. *Chem-Ztg*, 1911; 35: 753-755.
16. Baur E, Perret A. On the effect of light on dissolved silver salts in the presence of zinc oxide [In German]. *Helv Chim Acta*, 1924; 7: 910-915.[DOI]
17. Renz C. On the effect of oxides on silver nitrate and gold chloride in light [In German]. *Helv Chim Acta*, 1932; 15: 1077-1084.[DOI]
18. Goodeve CF, Kitchener JA. The mechanism of photosensitisation by solids. *Trans Faraday Soc*, 1938; 34: 902.[DOI]
19. Ravelli D, Dondi D, Fagnoni M et al. Photocatalysis. A multi-faceted concept for green chemistry. *Chem Soc Rev*, 2009; 38: 1999.[DOI]
20. Lotfabadi P. Analyzing passive solar strategies in the case of high-rise building. *Renew Sust Energ Rev*, 2015; 52: 1340-1353.[DOI]
21. Boddy PJ. Oxygen Evolution on Semiconducting TiO<sub>2</sub>. *J Electrochem Soc*, 1968; 115: 199.[DOI]
22. Fujishima A, Honda K. Electrochemical photolysis of water at a semiconductor electrode. *Nature*, 1972; 238: 37-38.[DOI]
23. Tuntithavornwat S, Saisawang C, Ratvijitvech T et al. Recent development of black TiO<sub>2</sub> nanoparticles for photocatalytic H<sub>2</sub> production: An extensive review. *Int J Hydrogen Energ*, 2024; 55: 1559-1593.[DOI]
24. Schrauzer G, Guth T. Photolysis of water and photoreduction of nitrogen on titanium dioxide. *J Am Chem Soc*, 2002; 99: 7189-7193.[DOI]
25. Aldosari OF, Hussain I. Unlocking the potential of TiO<sub>2</sub>-based photocatalysts for green hydrogen energy through water-splitting: Recent advances, future perspectives and techno feasibility assessment. *Int J Hydrogen Energ*, 2024; 59: 958-981.[DOI]
26. Dai W, Wang H, Xiao M et al. Visible Photocatalytic Hydrogen Production from CH<sub>3</sub>OH Over CuO/WO<sub>3</sub>: The Effect of Electron Transfer Behavior of the Adsorbed CH<sub>3</sub>OH. *Chem Eng J*, 2023; 459: 141616.[DOI]
27. Arora I, Garg S, Sapi A et al. Insights into photocatalytic CO<sub>2</sub> reduction reaction pathway: Catalytic modification for enhanced solar fuel production. *J Ind Eng Chem*, 2024; 137: 1-28.[DOI]
28. Alli YA, Oladoye PO, Onawole AT et al. Photocatalysts for CO<sub>2</sub> reduction and computational insights. *Fuel*, 2023; 344: 128101.[DOI]
29. Chen Z, Zhang G, Cao S et al. Advanced semiconductor catalyst designs for the photocatalytic reduction of CO<sub>2</sub>. *Mat R: Energy*, 2023; 3: 100193.[DOI]
30. Fang S, Rahaman M, Bharti J et al. Photocatalytic CO<sub>2</sub> reduction. *Nature Reviews Methods Primers*, 2023; 3: 61.[DOI]
31. Wang Z, Seo J, Hisatomi T et al. Efficient visible-light-driven water oxidation by single-crystal Ta<sub>3</sub>N<sub>5</sub> nanoparticles. *Nano Res*, 2023; 16: 4562-4567.[DOI]
32. Zhan X, Lei T, Wang L et al. Enhanced photocatalytic removal of tetracycline and methyl orange using Ta<sub>3</sub>N<sub>5</sub>@ZnIn<sub>2</sub>S<sub>4</sub> nanocomposites. *J Photoch Photobio A*, 2024; 451: 115538.[DOI]
33. Zhao T, Ye Z, Zeng M et al. Molten Salt Synthesis of Mg-Doped Ta<sub>3</sub>N<sub>5</sub> Nanoparticles with Optimized Surface Properties for Enhanced Photocatalytic Hydrogen Evolution. *Energy Fuels*, 2023; 37: 18194-18203.[DOI]
34. Liu Z, Fan S, Li X et al. Synergistic effect of single-atom Cu and hierarchical polyhedron-like Ta<sub>3</sub>N<sub>5</sub>/CdIn<sub>2</sub>S<sub>4</sub> S-scheme heterojunction for boosting photocatalytic NH<sub>3</sub> synthesis. *Appl Catal B-Environ*, 2023; 327: 122416.[DOI]
35. Dong Y, Ai F, Sun-Waterhouse D et al. Optical and Photocatalytic Properties of Three-Dimensionally Ordered Macroporous Ta<sub>2</sub>O<sub>5</sub> and Ta<sub>3</sub>N<sub>5</sub> Inverse Opals. *Chem Mater*, 2023; 35: 8281-8300.[DOI]
36. Li S, Cai M, Wang C et al. Ta<sub>3</sub>N<sub>5</sub>/CdS Core-Shell S-scheme Heterojunction Nanofibers for Efficient Photocatalytic Removal of Antibiotic Tetracycline and Cr(VI): Performance and Mechanism Insights. *Adv Fiber Mater*, 2023; 5: 994-1007.[DOI]
37. Zhao T, Ye Z, Zeng M et al. Molten Salt Synthesis of Mg-Doped Ta<sub>3</sub>N<sub>5</sub> Nanoparticles with Optimized Surface Properties for Enhanced Photocatalytic Hydrogen Evolution. *Energy Fuels*, 2023; 37: 18194-18203.[DOI]



38. Akter J, Hanif MdA, Islam MdA et al. Visible-light-active novel  $\alpha$ -Fe<sub>2</sub>O<sub>3</sub>/Ta<sub>3</sub>N<sub>5</sub> photocatalyst designed by band-edge tuning and interfacial charge transfer for effective treatment of hazardous pollutants. *J Env Chem Eng*, 2021; 9: 106831.[DOI]
39. Jia X, Wang C, Li Y et al. All-Solid-State Z-scheme Ta<sub>3</sub>N<sub>5</sub>/Bi/CaTaO<sub>2</sub>N photocatalyst transformed from perovskite CaBi<sub>2</sub>Ta<sub>2</sub>O<sub>9</sub> for efficient overall water splitting. *Chem Eng J*, 2022; 431: 134041.[DOI]
40. Hussain E, Ishaq A, Abid MZ et al. Sunlight-Driven Hydrogen Generation: Acceleration of Synergism between Cu-Ag Cocatalysts on a CdS System. *ACS Appl Energ Mater*, 2024; 7: 1914-1926.[DOI]
41. Li M, Zhang J, Wang L et al. Direct Z-Scheme Oxygen-vacancy-rich TiO<sub>2</sub>/Ta<sub>3</sub>N<sub>5</sub> heterojunction for degradation of ciprofloxacin under visible light: Degradation pathways and mechanism insight. *Appl Surf Sci*, 2022; 583: 152516.[DOI]
42. Lim KL, Sin JC, Lam SM et al. Controlled solvothermal synthesis of self-assembled SrTiO<sub>3</sub> microstructures for expeditious solar-driven photocatalysis dye effluents degradation. *Environ Res*, 2024; 251: 118647.[DOI]
43. Sakthivel S, Paramasivam S, Velusamy P et al. Experimental investigation of structural, morphological, and optical characteristics of SrTiO<sub>3</sub> nanoparticles using a shock tube for photocatalytic applications. *Z Phys Chem*, 2024.[DOI]
44. Liu M, Xu X, Xiao W et al. Au nanoparticles decorated SrTiO<sub>3</sub>-x hollow structure for plasmonic enhanced hydrogen production in UV-visible and near-infrared region. *J Alloy Compd*, 2024; 983: 173859.[DOI]
45. Zhuang H, Chen X, Xia J et al. State-of-the-art progress in Ag<sub>3</sub>PO<sub>4</sub>-based photocatalysts: Rational design, regulation and perspective. *Appl Mater Today*, 2023; 31: 101742.[DOI]
46. Hamrouni A, Azzouzi H, Rayes A et al. Enhanced Solar Light Photocatalytic Activity of Ag Doped TiO<sub>2</sub>-Ag<sub>3</sub>PO<sub>4</sub> Composites. *Nanomaterials-Basel*, 2020; 10: 795.[DOI]
47. Madanu TL, Mouchet SR, Deparis O et al. Tuning and transferring slow photons from TiO<sub>2</sub> photonic crystals to BiVO<sub>4</sub> nanoparticles for unprecedented visible light photocatalysis. *J Colloid Interf Sci*, 2023; 634: 290-299.[DOI]
48. Heckel S, Wittmann M, Reid M et al. An Account on BiVO<sub>4</sub> as Photocatalytic Active Matter. *Accounts Mater Res*, 2024; 5: 400-412.[DOI]
49. Zhang X, Puttaswamy M, Bai H et al. CdS/ZnS core-shell nanorod heterostructures co-deposited with ultrathin MoS<sub>2</sub> cocatalyst for competent hydrogen evolution under visible-light irradiation. *J Colloid Interf Sci*, 2024; 665: 430-442.[DOI]
50. Suresh M, Pravina R, Sivasamy A. Facile synthesis of MoS<sub>2</sub> nanoparticles anchored graphene nanocomposite for enhanced photocatalytic activity under solar irradiation. *J Mol Struct*, 2024; 1305: 137760.[DOI]
51. Panchal D, Sharma A, Pal S. Engineered MoS<sub>2</sub> nanostructures for improved photocatalytic applications in water treatment. *Mater Today Sustain*, 2023; 21: 100264.[DOI]
52. Balan B, Xavier MM, Mathew S. MoS<sub>2</sub> - Based Nanocomposites for Photocatalytic Hydrogen Evolution and Carbon Dioxide Reduction. *ACS Omega*, 2023; 8: 25649-25673.[DOI]
53. Xu Y, Liu K, Zhang J et al. NH<sub>4</sub>Cl-assisted synthesis of TaON nanoparticle applied to photocatalytic hydrogen and oxygen evolution from water. *J Energy Chem*, 2024; 94: 541-550.[DOI]
54. Jiang H, Shi Y, Zang S. Pd/PdO and hydrous RuO<sub>2</sub> difunction-modified SiO<sub>2</sub>@TaON@Ta<sub>3</sub>N<sub>5</sub> nano-photocatalyst for efficient solar overall water splitting. *Int J Hydrogen Energ*, 2023; 48: 17827-17837.[DOI]
55. Maekawa T, Huang Y, Tateishi N et al. Slow photon photocatalytic enhancement of H<sub>2</sub> production in TaON inverse opal photonic crystals. *J Solid State Chem*, 2024; 329: 124404.[DOI]
56. Qu H, Yang S, Zhou X. Theoretical insights into the effect of surface structure and anion ordering on the properties of SrTaO<sub>2</sub>N for photocatalytic water splitting. *Int J Quantum Chem*, 2024; 124: e27321.[DOI]
57. Tao X, Tsugawa T, Hatakeyama K et al. Synthesis and photocatalytic activity of LaTiO<sub>2</sub>N using titanium oxide nanosheet/La<sup>3+</sup> hybrids as a precursor. *Sustain Energy Fuels*, 2024; 8: 1269-1279.[DOI]
58. Xia Z, Wang X, Liu K et al. Preparation and photocatalytic properties of WSe<sub>2</sub>/BiVO<sub>4</sub> p-n heterojunction photocatalytic materials. *Catal Commun*, 2024; 187: 106857.[DOI]
59. Rengifo-Herrera J, Pulgarin C. Why five decades of massive research on heterogeneous photocatalysis, especially on TiO<sub>2</sub>, has not yet driven to water disinfection and detoxification applications? Critical review of drawbacks and challenges. *Chem Eng J*, 2023; 477: 146875.[DOI]
60. Sohail M, Rauf S, Irfan M et al. Recent developments, advances and strategies in heterogeneous photocatalysts for water splitting. *Nanoscale Adv*, 2024; 6: 1286-1330.[DOI]
61. Qahtan TF, Owolabi TO, Olubi OE et al. State-of-the-art, challenges and prospects of heterogeneous tandem photocatalysis. *Coordin Chem Rev*, 2023; 492: 215276.[DOI]
62. Lotfi S, Ouairi ME, Ahsaine HA et al. Recent progress on the synthesis, morphology and photocatalytic dye degradation of BiVO<sub>4</sub> photocatalysts: A review. *Catal Rev*, 2024; 66: 214-258.[DOI]
63. Low J, Zhang C, Ma J et al. Heterogeneous photocatalysis: what is being overlooked? *Trends Chem*, 2023; 5: 121-132.[DOI]

64. Okab AA, Jabbar ZH, Graimed BH et al. A comprehensive review highlights the photocatalytic heterojunctions and their superiority in the photo-destruction of organic pollutants in industrial wastewater. *Inorg Chem Commun*, 2023; 158: 111503.[DOI]
65. Sohail M, Rauf S, Irfan M et al. Recent developments, advances and strategies in heterogeneous photocatalysts for water splitting. *Nanoscale Adv*, 2024; 6: 1286-1330.[DOI]
66. Masri M, Girisha KB, Hezam A et al. Metal halide perovskite-based photocatalysts for organic pollutants degradation: Advances, challenges, and future directions. *Colloid Surface A*, 2024; 687: 133387.[DOI]
67. Baaloudj O, Vu N, Assadi A et al. Recent advances in designing and developing efficient sillenite-based materials for photocatalytic applications. *Adv Colloid Interface Sci*, 2024; 327: 103136.[DOI]
68. Kumar A, Rana S, Dhiman P et al. Current progress in heterojunctions based on Nb<sub>2</sub>O<sub>5</sub> for photocatalytic water treatment and energy applications. *J Mol Liq*, 2024; 399: 124360.[DOI]
69. Anucha CB, Altin I, Bacaksiz E et al. Titanium dioxide (TiO<sub>2</sub>)-based photocatalyst materials activity enhancement for contaminants of emerging concern (CECs) degradation: In the light of modification strategies. *Chem Eng J Adv*, 2022; 10: 100262.[DOI]
70. Dharma HNC, Jaafar J, Widiastuti N et al. A Review of Titanium Dioxide (TiO<sub>2</sub>)-Based Photocatalyst for Oilfield-Produced Water Treatment. *Membranes-Basel*, 2022; 12: 345.[DOI]
71. Gatou M, Syrrakou A, Lagopati N et al. Photocatalytic TiO<sub>2</sub>-Based Nanostructures as a Promising Material for Diverse Environmental Applications: A Review. *Reactions-Basel*, 2024; 5: 135-194.[DOI]
72. Sangeeta O, Sandhu N, Kumar C et al. Critical Review on Titania-Based Nanoparticles: Synthesis, Characterization, and Application as a Photocatalyst. *Chem Afr*, 2024; 7: 1749-1768.[DOI]
73. Rashid A, Hossain KT, Mondal S et al. Synthesis, characterization, and photocatalytic performance of methyl orange in aqueous TiO<sub>2</sub> suspension under UV and solar light irradiation. *S Afr J Chem Eng*, 2022; 40: 113-125.[DOI]
74. Ahmadpour N, Nowrouzi M, Madadi Avargani V et al. Design and optimization of TiO<sub>2</sub>-based photocatalysts for efficient removal of pharmaceutical pollutants in water: Recent developments and challenges. *J Water Process Eng*, 2024; 57: 104597.[DOI]
75. Yao Y, Han Y, Qi S et al. Metal-free thiophene-based covalent organic frameworks achieve efficient photocatalytic hydrogen evolution by accelerating interfacial charge transfer. *Int J Hydrogen Energ*, 2024; 63: 184-192.[DOI]
76. Liu X, Jing X, Liu R et al. Plasmon-Enhanced Perovskite Photocatalysts for CO<sub>2</sub> Reduction: A Mini Review. *Energ Fuel*, 2024; 38: 4966-4679.[DOI]
77. Rawat J, Sharma H, Dwivedi C. Microwave-assisted synthesis of carbon quantum dots and their integration with TiO<sub>2</sub> nanotubes for enhanced photocatalytic degradation. *Diam Relat Mater*, 2024; 144: 111050.[DOI]
78. Puri N, Gupta A. Water remediation using titanium and zinc oxide nanomaterials through disinfection and photo catalysis process: A review. *Environ Res*, 2023; 227: 115786.[DOI]
79. Chen X, Ren Y, Qu G et al. A review of environmental functional materials for cyanide removal by adsorption and catalysis. *Inorg Chem Commun*, 2023; 157: 111298.[DOI]
80. Ibhaddon A, Fitzpatrick P. Heterogeneous Photocatalysis: Recent Advances and Applications. *Catalysts*, 2013; 3: 189-218.[DOI]
81. Hossain R, Uddin MA, Khan MA. Mechanistic Understanding in Manipulating Energetics of TiO<sub>2</sub> for Photocatalysis. *J Phys Chem C*, 2023; 127: 10897-10912.[DOI]
82. Eder M, Tschurl M, Heiz U. Toward a Comprehensive Understanding of Photocatalysis: What Systematic Studies and Alcohol Surface Chemistry on TiO<sub>2</sub> (110) Have to Offer for Future Developments. *J Phys Chem Lett*, 2023; 14: 6193-6201.[DOI]
83. Sumaria V, Rawal TB, Li Y et al. Machine Learning, Density Functional Theory, and Experiments to Understand the Photocatalytic Reduction of CO<sub>2</sub> by CuPt/TiO<sub>2</sub>. *Cond mat*, 2024; 1: 1-16.[DOI]
84. Henderson MA. A surface science perspective on photocatalysis. *Surf Sci Rep*, 2011; 66: 185-297. [DOI]
85. Hyunwoo Y, Eunsoo K, Sung H et al. Hole trap, charge transfer and photoelectrochemical water oxidation in thickness-controlled TiO<sub>2</sub> anatase thin films. *Appl Surf Sci*, 2020; 529: 147020. [DOI]
86. Ali S, Ismail PM, Khan M et al. Charge transfer in TiO<sub>2</sub> - based photocatalysis: fundamental mechanisms to material strategies. *Nanoscale*, 2024; 16: 4352-4377.[DOI]
87. Aldosari OF, Hussain I. Unlocking the potential of TiO<sub>2</sub>-based photocatalysts for green hydrogen energy through water-splitting: Recent advances, future perspectives and techno feasibility assessment. *Int J Hydrogen Energ*, 2024; 59: 958-981.[DOI]
88. Yin S, Liu L, Li J et al. Mesoporous TiO<sub>2</sub> Single-Crystal Particles from Controlled Crystallization-Driven Mono-Micelle Assembly as an Efficient Photocatalyst. *J Am Chem Soc*, 2024; 146: 1701-1709.[DOI]
89. Alamoudi M, Katsiev K, Idriss H. Monitoring the Lifetime of Photoexcited Electrons in a Fresh and Bulk Reduced Rutile TiO<sub>2</sub> Single Crystal Possible Anisotropic Propagation. *J Phys Chem Lett*, 2023; 14: 9238-9244.[DOI]

90. Li C, Shen S, Niu J et al. Mesoporous single-crystal-based TiO<sub>2</sub> microspheres decorated by carbon nitride for obviously improved photocatalytic performance and recyclability. *Inorg Chem Commun*, 2023; 150: 110524.[DOI]
91. He T, Wang D, Xu Y et al. The Facile Construction of Anatase Titanium Dioxide Single Crystal Sheet-Connected Film with Observable Strong White Photoluminescence. *Coat*, 2024; 14: 292.[DOI]
92. Petrik NG, Baer MD, Mundy CJ et al. Mixed Molecular and Dissociative Water Adsorption on Hydroxylated TiO<sub>2</sub> (110): An Infrared Spectroscopy and Ab Initio Molecular Dynamics Study. *J Phys Chem C*, 2022; 126: 21616-21627.[DOI]
93. Jiménez-Calvo P, Caps V, Keller V. Plasmonic Au-based junctions onto TiO<sub>2</sub>, gC<sub>3</sub>N<sub>4</sub>, and TiO<sub>2</sub>-gC<sub>3</sub>N<sub>4</sub> systems for photocatalytic hydrogen production: Fundamentals and challenges. *Renew Sust Energ Rev*, 2021; 149: 111095.[DOI]
94. Qasim M, Arif MI, Naseer A et al. Biogenic Nanoparticles at the Forefront: Transforming Industrial Wastewater Treatment with TiO<sub>2</sub> and Graphene. *Sch J Agric Vet Sci*, 2024. [DOI]
95. Barakat NAM, Irfan OM, Mohamed OA. TiO<sub>2</sub> NPs-immobilized silica granules: New insight for nano catalyst fixation for hydrogen generation and sustained wastewater treatment. *PLoS One*, 2023; 18: e0287424.[DOI]
96. Azizi ZL, M Qasim, MI Arif, A Naseer,. Biogenic Nanoparticles at the Forefront: Transforming Industrial Wastewater Treatment with TiO<sub>2</sub> and Graphene. *Appl Biochem Biotech*, 2024.[DOI]
97. Suhan MdBK, Al-Mamun MdR, Farzana N et al. Sustainable pollutant removal and wastewater remediation using TiO<sub>2</sub>-based nanocomposites: A critical review. *Nano-Struct Nano-Objects*, 2023; 36: 101050.[DOI]
98. Ariaeinezhad F, Mohammadnezhad G, Zare M et al. Controllable and facile one-pot synthesis of high surface area amorphous, crystalline, and triphasic TiO<sub>2</sub> : Catalytic and photocatalytic applications. *J Mater Chem A*, 2024; 12: 6488-6506.[DOI]
99. Chen Z, Chen H, Wang K et al. Enhanced TiO<sub>2</sub> Photocatalytic 2 e<sup>-</sup> Oxygen Reduction Reaction via Interfacial Microenvironment Regulation and Mechanism Analysis. *ACS Catal*, 2023; 13: 6497-6508.[DOI]
100. Eder M, Tschurl M, Heiz U. Toward a Comprehensive Understanding of Photocatalysis: What Systematic Studies and Alcohol Surface Chemistry on TiO<sub>2</sub> (110) Have to Offer for Future Developments. *J Phys Chem Lett*, 2023; 14: 6193-6201.[DOI]
101. Jabraoui H, Rouhani MD, Rossi C et al. Towards H<sub>2</sub> production from water and ethanol interactions on hydrated TiO<sub>2</sub>(101): Insights from ReaxFF molecular dynamics. *Appl Surf Sci*, 2024; 656: 159692.[DOI]
102. Patidar A, Dugyala VR, Chakma S et al. Reactive oxygen species aided photocatalytic degradation of tetracycline using non-metal activated carbon doped TiO<sub>2</sub> nanocomposite under UV-light irradiation. *Res Chem Intermediat*, 2024; 50: 1035-1063.[DOI]
103. Zhang R, Luo T, Zeng W et al. Methanol Adsorption and Reaction on TiO<sub>2</sub> (110) at Near Ambient Pressure. *J Phys Chem C*, 2023; 127: 1049-1056.[DOI]
104. Lin Y, Bocharov D, Isakoviča I et al. Chlorine Adsorption on TiO<sub>2</sub>(110)/Water Interface: Nonadiabatic Molecular Dynamics Simulations for Photocatalytic Water Splitting. *Electron Mater*, 2023; 4: 33-48.[DOI]
105. Abbas M. Factors influencing the adsorption and photocatalysis of direct red 80 in the presence of a TiO<sub>2</sub>: Equilibrium and kinetics modeling. *J Chem Res*, 2021; 45: 694-701.[DOI]
106. Lang X, Liang Y, Zhang J et al. Structure and reactivity of a water-covered anatase TiO<sub>2</sub> (001) surface. *Phys Chem Chem Phys*, 2020; 22: 1371-1380.[DOI]
107. Guo Q, Zhou C, Ma Z et al. Fundamentals of TiO<sub>2</sub> Photocatalysis: Concepts, Mechanisms, and Challenges. *Adv Mater*, 2019; 31: 1901997.[DOI]
108. Ali S, Ismail PM, Khan M et al. Charge transfer in TiO<sub>2</sub> -based photocatalysis: fundamental mechanisms to material strategies. *Nanoscale*, 2024; 16: 4352-4377.[DOI]
109. Lettieri S, Pavone M, Fioravanti A et al. Charge Carrier Processes and Optical Properties in TiO<sub>2</sub> and TiO<sub>2</sub>-Based Heterojunction Photocatalysts: A Review. *Mater*, 2021; 14: 1645.[DOI]
110. Rosa D, Abbasova N, Di Palma L. Titanium Dioxide Nanoparticles Doped with Iron for Water Treatment via Photocatalysis: A Review. *Nanomaterials*, 2024; 14: 293.[DOI]
111. Vorontsov AV, Valdés H, Smirniotis PG et al. Recent Advancements in the Understanding of the Surface Chemistry in TiO<sub>2</sub> Photocatalysis. *Surface*, 2020; 3: 72-92.[DOI]
112. Jeon JP, Kweon DH, Jang BJ et al. Enhancing the photocatalytic activity of TiO<sub>2</sub> catalysts. *Adv Sustain Syst*, 2020; 4: 2000197.[DOI]
113. Mohsin M, Bhatti IA, Zeshan M et al. Prospects, challenges, and opportunities of the metals-modified TiO<sub>2</sub> based photocatalysts for hydrogen generation under solar light irradiation: A review. *Flatchem*, 2023; 42: 100547.[DOI]
114. Kirk CH, Wang P, Chong CYD et al. TiO<sub>2</sub> photocatalytic ceramic membranes for water and wastewater treatment: Technical readiness and pathway ahead. *J Mater Sci Technol*, 2024; 183: 152-164.[DOI]
115. Linsebigler AL, Lu G, Yates JT. Photocatalysis on TiO<sub>2</sub> Surfaces: Principles, Mechanisms, and Selected Results. *Chem Rev*, 1995; 95: 735-758.[DOI]

116. Wang C, Liu H, Qu Y. TiO<sub>2</sub> - Based Photocatalytic Process for Purification of Polluted Water: Bridging Fundamentals to Applications. *J Nanomater*, 2013; 2013: 319637.[DOI]
117. Henderson MA, Lyubinetsky I. Molecular-Level Insights into Photocatalysis from Scanning Probe Microscopy Studies on TiO<sub>2</sub> (110). *Chem Rev*, 2013; 113: 4428-4455.[DOI]
118. Guo Q, Zhou C, Ma Z et al. Fundamentals of TiO<sub>2</sub> Photocatalysis: Concepts, Mechanisms, and Challenges. *Adv Mater*, 2019; 31: 1901997.[DOI]
119. Henderson MA, Shen M, Wang ZT. Characterization of the Active Surface Species Responsible for UV-Induced Desorption of O<sub>2</sub> from the Rutile TiO<sub>2</sub>(110) Surface. *The J of Phyl Che C*, 2013; 17: 5774-5784. [DOI]
120. Guo Q, Zhou C, Ma Z et al. Elementary Chemical Reactions in Surface Photocatalysis. *Annu Rev Phys Chem*, 2018; 69: 451-472.[DOI]
121. Waghmode MS, Gunjal AB, Mulla JA et al. Studies on the titanium dioxide nanoparticles: biosynthesis, applications and remediation. *SN Appl Sci*, 2019; 1: 310.[DOI]
122. Kang X, Liu S, Dai Z et al. Titanium dioxide: from engineering to applications. *Catalysts*, 2019; 9: 191.[DOI]
123. Bai J, Zhou B. Titanium Dioxide Nanomaterials for Sensor Applications. *Chem Rev*, 2014; 114: 10131-10176.[DOI]
124. Ghosh S, Das AP. Modified titanium oxide (TiO<sub>2</sub>) nanocomposites and its array of applications: a review. *Toxicol Environ Chem*, 2015; 97: 491-514.[DOI]
125. Hsu CY, Mahmoud ZH, Abdullaev S et al. Nano titanium oxide (nano-TiO<sub>2</sub>): A review of synthesis methods, properties, and applications. *Case Stud Chem Environ Eng*, 2024; 9: 100626.[DOI]
126. Qamar OA, Jamil F, Hussain M et al. Advances in synthesis of TiO<sub>2</sub> nanoparticles and their application to biodiesel production: A review. *Chem Eng J*, 2023; 460: 141734.[DOI]
127. Anisonian KG. Physico-chemical bases of magnetizing roasting of leucoxene ores and concentrates for separation of leucoxene and quartz by magnetic separation. Novosibirsk, IA: Baikov Institute of Metallurgy and Materials Science, Russian Academy of Sciences, 2015.
128. Zhang W, Zhu Z, Cheng CY. A literature review of titanium metallurgical processes. *Hydrometallurgy*, 2011; 108: 177-188.[DOI]
129. Umar M, Aziz HA. Photocatalytic degradation of organic pollutants in water. *Intech*, 2013; 8: 196-197.[DOI]
130. Wu J, Zhong L. Predictive modeling for VOC adsorption on TiO<sub>2</sub> filters: Implications for enhanced photocatalytic oxidation in indoor air quality management. *Chem Eng J*, 2024; 480: 148222.[DOI]
131. Zhou W, Chen F, Li M et al. Facet-Dependent Photocatalytic Behavior of Rutile TiO<sub>2</sub> for the Degradation of Volatile Organic Compounds: In Situ Diffuse Reflectance Infrared Fourier Transform Spectroscopy and Density Functional Theory Investigations. *Langmuir*, 2024; 40: 2120-2129.[DOI]
132. Lin Z, Jiang X, Xu W et al. The effects of water, substrate, and intermediate adsorption on the photocatalytic decomposition of air pollutants over nano-TiO<sub>2</sub> photocatalysts. *Phys Chem Chem Phys*, 2024; 26: 662-678.[DOI]
133. Kharouf M, Zyoud AH, Zyoud SH et al. Enhanced photocatalytic degradation of phenazopyridine using rutile TiO<sub>2</sub>/clay composite: catalyst recovery and environmental implications. *Int J Environ Sci Technol*, 2024; 21: 7491-7508.[DOI]
134. Pavel M, Anastasescu C, State RN et al. Photocatalytic Degradation of Organic and Inorganic Pollutants to Harmless End Products: Assessment of Practical Application Potential for Water and Air Cleaning. *Catalysts*, 2023; 13: 380.[DOI]
135. Kanan S, Moyet MA, Arthur RB et al. Recent advances on TiO<sub>2</sub>-based photocatalysts toward the degradation of pesticides and major organic pollutants from water bodies. *Catal Rev*, 2020; 62: 1-65.[DOI]
136. Badr P, Sajjadnejad M, Haghshenas SM. Influence of incorporating B4C nanoparticles and pulse electrodeposition parameters on the surface morphology and wear behavior of nickel based nanocomposite coatings. *Prog Chem Biochem Res*, 2023; 6: 292-313.[DOI]
137. Belhachem A, Amara N, Belmekki H et al. Synthesis, characterization and anti-inflammatory activity of an alginate-zinc oxide nanocomposite. *Asian J Nanosci Mater*, 2023; 3: 173-185.[DOI]
138. Puri J, Dhuldhaj U, Abdulbasit S. Nano-biochar production and its characteristics: overview. *Int J Adv Biol Biom Res*, 2023; 11: 206-220.[DOI]
139. Eddy DR, Nur Sheha GA, Permana MD et al. Study on triphase of polymorphs TiO<sub>2</sub> (anatase/rutile/brookite) for boosting photocatalytic activity of metformin degradation. *Chemosphere*, 2024; 351: 141206.[DOI]
140. Zahra Z, Habib Z, Chung S et al. Exposure Route of TiO<sub>2</sub> NPs from Industrial Applications to Wastewater Treatment and Their Impacts on the Agro-Environment. *Nanomaterials*, 2020; 10: 1469.[DOI]
141. Berardinelli A, Parisi F. Introduction: TiO<sub>2</sub> in the food industry and cosmetics. In *Titanium Dioxide (TiO<sub>2</sub>) and Its Applications*. Publishing: Elsevier, Netherlands, 2021; 353-371.
142. Janczarek M, Klapiszewska I, Jesionowski T et al. Progress of functionalized TiO<sub>2</sub>-based nanomaterials in the construction industry: A comprehensive review. *Chem Eng J*, 2022; 430: 132062.[DOI]
143. Ziental D, Czarzynska-Goslinska B, Mlynarczyk DT et al. Titanium Dioxide Nanoparticles: Prospects and Applications in Medicine. *Nanomaterials*, 2020; 10: 387.[DOI]



144. Samuel HS, Maraizu UN, Emmanuel EE. Supercritical fluids: Properties, formation and applications. *J Eng Ind Res*, 2023; 4: 176-188.[DOI]
145. Taheri A, Rezayati-Zad Z. Characterization of tribological and electrochemical corrosion behavior of GO coatings formed on 6061 Al alloy processed by plasma electrolytic oxidation. *Prog Chem Biochem Res*, 2023; 6: 261-276.
146. Asaad Mahdi M, Farhan MA, Mahmoud ZH et al. Direct sunlight photodegradation of congo red in aqueous solution by TiO<sub>2</sub>/rGO binary system: Experimental and DFT study. *Arab J Chem*, 2023; 16: 104992.[DOI]
147. Mahmoud ZH, Hamrouni A, Kareem AB et al. Synthesis and characterization of chitosan sheet modified by varied weight ratio of anatase (TiO<sub>2</sub>) nano mixture with Cr(VI) adsorbing. *Kuwait J Sci*, 2023; 50: 290-299.[DOI]
148. Eddy DR, Nur Sheha GA, Permana MD et al. Study on triphase of polymorphs TiO<sub>2</sub> (anatase/rutile/brookite) for boosting photocatalytic activity of metformin degradation. *Chemosphere*, 2024; 351: 141206.[DOI]
149. Simons PY, Dachille F. The structure of TiO<sub>2</sub> II, a high-pressure phase of TiO<sub>2</sub>. *Acta Cryst*, 1967; 23: 334-336.[DOI]
150. Latroche M, Brohan L, Marchand R et al. New hollandite oxides: TiO<sub>2</sub>(H) and K<sub>0.06</sub>TiO<sub>2</sub>. *J Solid State Chem*, 1989; 81: 78-82.[DOI]
151. Cromer DT, Herrington K. The Structures of Anatase and Rutile. *J Am Chem Soc*, 1955; 77: 4708-4709.[DOI]
152. Mo SD, Ching WY. Electronic and optical properties of three phases of titanium dioxide: Rutile, anatase, and brookite. *Phys Rev B*, 1995; 51: 13023-13032.[DOI]
153. Kandiel TA, Robben L, Alkaima A et al. Brookite versus anatase TiO<sub>2</sub> photocatalysts: phase transformations and photocatalytic activities. *Photoch Photobio Sci*, 2013; 12: 602-609.[DOI]
154. Samat M, Ali A, Taib M et al. Hubbard U calculations on optical properties of 3d transition metal oxide TiO<sub>2</sub>. *Results in Physics*, 2016; 6: 891-896.[DOI]
155. Landmann M, Rauls E, Schmidt WG. The electronic structure and optical response of rutile, anatase and brookite TiO<sub>2</sub>. *J Phys-Condens Mat*, 2012; 24: 195503.[DOI]
156. Thompson TL, Yates JT. Surface Science Studies of the Photoactivation of TiO<sub>2</sub> - New Photochemical Processes. *Chem Rev*, 2023; 106: 4428-4453.[DOI]
157. Tang H, Prasad K, Sanjines R et al. Electrical and optical properties of TiO<sub>2</sub> anatase thin films. *J Appl Phys*, 1994; 75: 2042-2047.[DOI]
158. Yang HG, Sun CH, Qiao SZ et al. Anatase TiO<sub>2</sub> single crystals with a large percentage of reactive facets. *Nature*, 2008; 453: 638-641.[DOI]
159. Guo Q, Zhou C, Ma Z et al. Fundamentals of TiO<sub>2</sub> Photocatalysis: Concepts, Mechanisms, and Challenges. *Adv Mater*, 2019; 31: 1901997.[DOI]
160. Wang Z, Wen B, Hao Q et al. Localized Excitation of Ti<sup>3+</sup> Ions in the Photoabsorption and Photocatalytic Activity of Reduced Rutile TiO<sub>2</sub>. *J Am Chem Soc*, 2015; 137: 9146-9152.[DOI]
161. Yin WJ, Wen B, Zhou C et al. Excess electrons in reduced rutile and anatase TiO<sub>2</sub>. *Surf Sci Rep*, 2018; 73: 58-82.[DOI]
162. Hardman PJ, Raikar GN, Muryn CA et al. Valence-band structure of TiO<sub>2</sub> along the  $\Gamma$ - $\Delta$ -X and  $\Gamma$ - $\Sigma$ -M directions. *Phys Rev B*, 1994; 49: 7170.[DOI]
163. Lindan PJD, Harrison NM, Gillan MJ et al. First-principles spin-polarized calculations on the reduced and reconstructed TiO<sub>2</sub> (110) surface. *Phys Rev B*, 1997; 55: 15919-15927.[DOI]
164. Diebold U. The surface science of titanium dioxide. *Surf Sci Rep*, 2003; 48: 53-229.[DOI]
165. Li G, Chen L, Graham ME et al. A comparison of mixed phase titania photocatalysts prepared by physical and chemical methods: The importance of the solid-solid interface. *J Mol Catal A-Chem*, 2007; 275: 30-35.[DOI]
166. Morrison SR. Electrochemistry at Semiconductor and Oxidized Metal Electrodes. Plenum Press: New York, USA, 1980.
167. Zhao Y, Li C, Liu X et al. Synthesis and optical properties of TiO<sub>2</sub> nanoparticles. *Mater Lett*, 2007; 61: 79-83.[DOI]
168. Ma J, Li W, Le N, et al. Red-shifted absorptions of cation-defective and surface-functionalized anatase with enhanced photoelectrochemical properties. *ACS omega*, 2019; 4(6): 10929-10938. [DOI]
169. Shon H, Phuntsho S, Okour Y et al. Visible light responsive titanium dioxide (TiO<sub>2</sub>). *J Korean Ind Eng Chem*, 2008; 19: 1-16.
170. Mathew RM, Jose J, Zachariah ES et al. Defect Induced Ultrafast Organic Dye Adsorption by Amorphous Titanium Dioxide/Phosphorus-Doped Carbon Nanodot Hybrid. *J Clust Sci*, 2024; 35: 1045-1062.[DOI]
171. Ahad A, Podder J, Saha T et al. Effect of chromium doping on the band gap tuning of titanium dioxide thin films for solar cell applications. *Heliyon*, 2024; 10: e23096.[DOI]
172. Kuranov D, Grebenkina A, Bogdanova A et al. Effect of Donor Nb(V) Doping on the Surface Reactivity, Electrical, Optical and Photocatalytic Properties of Nanocrystalline TiO<sub>2</sub>. *Materials*, 2024; 17: 375.[DOI]

173. Devi LG, Kumar SG. Influence of physicochemical - electronic properties of transition metal ion doped polycrystalline titania on the photocatalytic degradation of Indigo Carmine and 4-nitrophenol under UV/solar light. *Appl Surf Sci*, 2011; 257: 2779-2790.[DOI]
174. Basavarajappa PS, Patil SB, Ganganagappa N et al. Recent progress in metal-doped TiO<sub>2</sub>, non-metal doped/codoped TiO<sub>2</sub> and TiO<sub>2</sub> nanostructured hybrids for enhanced photocatalysis. *Int J Hydrogen Energ*, 2020; 45: 7764-7778.[DOI]
175. Kuriechen SK, Murugesan S, Paul RS. Mineralization of Azo Dye Using Combined Photo-Fenton and Photocatalytic Processes under Visible Light. *J Catalysts*, 2013; 2013: 1-6.[DOI]
176. Chakraborty AK, Ganguli S, Sabur MA. Nitrogen doped titanium dioxide (N-TiO<sub>2</sub>): Electronic band structure, visible light harvesting and photocatalytic applications. *J Water Process Eng*, 2023; 55: 104183.[DOI]
177. Ishikawa T, Sahara R, Ohno K et al. Electronic structure analysis of light-element-doped anatase TiO<sub>2</sub> using all-electron GW approach. *Comp Mater Sci*, 2023; 220: 112059.[DOI]
178. Gao C, Guo M, Liu Y et al. Surface modification methods and mechanisms in carbon nanotubes dispersion. *Carbon*, 2023; 212: 118133.[DOI]
179. Yang J, Mei S, Ferreira JMF. Hydrothermal synthesis of TiO<sub>2</sub> nanopowders from tetraalkylammonium hydroxide peptized sols. *Mat Sci Eng C*, 2001; 15: 183-185.[DOI]
180. Wang D, Yu B, Zhou F et al. Synthesis and characterization of anatase TiO<sub>2</sub> nanotubes and their use in dye-sensitized solar cells. *Mater Chem Phys*, 2009; 113: 602-606.[DOI]
181. Wahi RK, Liu Y, Falkner JC et al. Solvothermal synthesis and characterization of anatase TiO<sub>2</sub> nanocrystals with ultrahigh surface area. *J Colloid Interf Sci*, 2006; 302: 530-536.[DOI]
182. Kobayashi M, Kato H, Miyazaki T et al. Hydrothermal Synthesis of Pseudocubic Rutile-Type Titania Particles. *Ceramics*, 2019; 2: 56-63.[DOI]
183. Govindaraj R, Santhosh N, Senthil Pandian M et al. Synthesis of nanocrystalline TiO<sub>2</sub> nanorods via hydrothermal method: An efficient photoanode material for dye sensitized solar cells. *J Cryst Growth*, 2017; 468: 125-128.[DOI]
184. Rajamanickam G, Narendhiran S, Muthu SP et al. Hydrothermally derived nanoporous titanium dioxide nanorods / nanoparticles and their influence in dye-sensitized solar cell as a photoanode. *Chem Phys Lett*, 2017; 689: 19-25.[DOI]
185. Wang F, Shi Z, Gong F, Jiu J, Adachi M. Morphology Control of Anatase TiO<sub>2</sub> by Surfactant-assisted Hydrothermal Method. *Chinese J Chem Eng*, 2007; 15: 754-759.[DOI]
186. Lei L, Yuming C, Bo L et al. Study on the surface erosion route to the fabrication of TiO<sub>2</sub> hollow spheres. *Appl Surf Sci*, 2010; 256: 2596-2601.[DOI]
187. Liu Z, Sun DD, Guo P et al. One-Step Fabrication and High Photocatalytic Activity of Porous TiO<sub>2</sub> Hollow Aggregates by Using a Low-Temperature Hydrothermal Method Without Templates. *Chem A Eur J*, 2007; 13: 1851-1855.[DOI]
188. Xue B, Sun T, Mao F et al. Facile synthesis of mesoporous core-shell TiO<sub>2</sub> nanostructures from TiCl<sub>3</sub>. *Materials Research Bulletin*, 2011; 46: 1524-1529.[DOI]
189. Yan XM, Kang J, Gao L et al. Solvothermal synthesis of carbon coated N-doped TiO<sub>2</sub> nanostructures with enhanced visible light catalytic activity. *Appl Surf Sci*, 2013; 265: 778-783.[DOI]
190. Kang M, Lee SY, Chung CH et al. Characterization of a TiO<sub>2</sub> photocatalyst synthesized by the solvothermal method and its catalytic performance for CHCl<sub>3</sub> decomposition. *J Photoch Photobio A*, 2001; 144: 185-191.[DOI]
191. Nam WS, Han GY. Characterization and photocatalytic performance of nanosize TiO<sub>2</sub> powders prepared by the solvothermal method. *Korean J Chem Eng*, 2003; 20: 1149-1153.[DOI]
192. Yang HG, Liu G, Qiao SZ et al. Solvothermal Synthesis and Photoreactivity of Anatase TiO<sub>2</sub> Nanosheets with Dominant {001} Facets. *J Am Chem Soc*, 2009; 131: 4078-4083.[DOI]
193. Sencer S, Annabella S. Surface Structure and Reactivity of Anatase TiO<sub>2</sub> Crystals with Dominant {001} Facets. *Phys. Chem. C* 2013, 117, 12, 6358–6362.[DOI]
194. Li X, Peng Q, Yi J et al. Near Monodisperse TiO<sub>2</sub> Nanoparticles and Nanorods. *Chem A Eur J*, 2006; 12: 2383-2391.[DOI]
195. Lü X, Ding S, Xie Y et al. Non-Aqueous Preparation of High-Crystallinity Hierarchical TiO<sub>2</sub> Hollow Spheres with Excellent Photocatalytic Efficiency. *Eur J Inorg Chem*, 2011; 2011: 2879-2883.[DOI]
196. Liu Z, Sun DD, Guo P et al. One-Step Fabrication and High Photocatalytic Activity of Porous TiO<sub>2</sub> Hollow Aggregates by Using a Low-Temperature Hydrothermal Method Without Templates. *Chem A Eur J*, 2007; 13: 1851-1855.[DOI]
197. Liu C, Sun H, Yang S. From Nanorods to Atomically Thin Wires of Anatase TiO<sub>2</sub>: Nonhydrolytic Synthesis and Characterization. *Chem A Eur J*, 2010; 16: 4381-4393.[DOI]
198. Supphasirongjaroen P, Praserttham P, Panpranot J et al. Effect of quenching medium on photocatalytic activity of nano-TiO<sub>2</sub> prepared by solvothermal method. *Chem Eng J*, 2008; 138: 622-627.[DOI]
199. Dinh C, Nguyen T, Kleitz F et al. A solvothermal single-step route towards shape-controlled titanium dioxide nanocrystals. *Can J Chem Eng*, 2012; 90: 8-17.[DOI]

200. Kim CS, Moon BK, Park JH et al. Solvothermal synthesis of nanocrystalline TiO<sub>2</sub> in toluene with surfactant. *J Cryst Growth*, 2003; 257: 309-315.[DOI]
201. Gong D, Grimes CA, Varghese OK et al. Titanium oxide nanotube arrays prepared by anodic oxidation. *J Mater Res*, 2001; 16: 3331-3334.[DOI]
202. Zhang P, Yin S, Sato T. Synthesis of high-activity TiO<sub>2</sub> photocatalyst via environmentally friendly and novel microwave assisted hydrothermal process. *Appl Catal B-Environ*, 2009; 89: 118-122.[DOI]
203. Zhang QH, Han WD, Hong YJ et al. Photocatalytic reduction of CO<sub>2</sub> with H<sub>2</sub>O on Pt-loaded TiO<sub>2</sub> catalyst. *Catal Today*, 2009; 148: 335-340.[DOI]
204. Zhang Y, Zheng H, Liu G et al. Synthesis and electrochemical studies of a layered spheric TiO<sub>2</sub> through low temperature solvothermal method. *Electrochim Acta*, 2009; 54: 4079-4083.[DOI]
205. Fattakhova-Rohlfing D, Zaleska A, Bein T. Three-Dimensional Titanium Dioxide Nanomaterials. *Chem Rev*, 2014; 114: 9487-9558.[DOI]
206. Attar AS, Ghamsari MS, Hajiesmaeilbaigi F et al. *J Am Chem Soc*, 1981; 103: 6116.[DOI]
207. Oskam G, Nellore A, Penn RL et al. The Growth Kinetics of TiO<sub>2</sub> Nanoparticles from Titanium(IV) Alkoxide at High Water/Titanium Ratio. *J Phys Chem B*, 2003; 107: 1734-1738.[DOI]
208. Mehrotra RC, Singh A. ChemInform Abstract: Recent Trends in Metal Alkoxide Chemistry. *J Cheminformatics*, 1997; 28: 12869 [DOI]
209. Livage J, Henry M, Sanchez C. Sol-gel chemistry of transition metal oxides. *Prog Solid State Ch*, 1988; 18: 259-341.[DOI]
210. Rahman I, Mostafa M, Kazem M et al. An inclusive review on inorganic gels: classifications, synthesis methods and applications. *J Ir Cheml Soc*, 2023; 20: 1757-1779.[DOI]
211. Yu JC, Yu J, Ho W et al. Preparation of highly photocatalytic active nano-sized TiO<sub>2</sub> particles via ultrasonic irradiation. *Chem Commun*, 2001; 19: 1942-1943.[DOI]
212. Chen X. Titanium Dioxide Nanomaterials and Their Energy Applications. *Chinese J Catal*, 2009; 30: 839-851.[DOI]
213. Zhu YJ, Chen F. Microwave-Assisted Preparation of Inorganic Nanostructures in Liquid Phase. *Chem Rev*, 2014; 114: 6462-6555.[DOI]
214. Collins MJ. Future Trends in Microwave Synthesis. *Future Med Chem*, 2010; 2: 151-155.[DOI]
215. Jacob J, Chia LHL, Boey FYC. Thermal and non-thermal interaction of microwave radiation with materials. *J Mater Sci*, 1995; 30: 5321-5327.[DOI]
216. De La Hoz A, Díaz-Ortiz Á, Moreno A. Microwaves in organic synthesis. Thermal and non-thermal microwave effects. *Chem Soc Rev*, 2005; 34: 164-178.[DOI]
217. Gressel-Michel E, Chaumont D, Stuerger D. From a microwave flash-synthesized TiO<sub>2</sub> colloidal suspension to TiO<sub>2</sub> thin films. *J Colloid Interf Sci*, 2005; 285: 674-679.[DOI]
218. Corradi AB, Bondioli F, Focher B et al. Conventional and Microwave-Hydrothermal Synthesis of TiO<sub>2</sub> Nanopowders. *J Am Ceram Soc*, 2005; 88: 2639-2641.[DOI]
219. Shang J, Zhou Y, Yan H, et al. Atom layer deposited TiO<sub>2</sub> electron transport layer for silicon heterojunction solar cells to achieve high performance. *Langmuir*, 2011; 27: 10191-10196.[DOI]
220. Baldassari S, Komarneni S, Mariani E et al. Rapid Microwave - Hydrothermal Synthesis of Anatase Form of Titanium Dioxide. *J Am Ceram Soc*, 2005; 88: 3238-3240.[DOI]
221. Kang J, Gao L, Zhang M et al. Synthesis of rutile TiO<sub>2</sub> powder by microwave-enhanced roasting followed by hydrochloric acid leaching. *Adv Powder Technol*, 2020; 31: 1140-1147.[DOI]
222. Kim H, Noh K, Choi C et al. Extreme Superomniphobicity of Multiwalled 8 nm TiO<sub>2</sub> Nanotubes. *Langmuir*, 2011; 27: 10191-10196.[DOI]
223. Malekshahi BM, Nemati KA, Fathollahi L et al. A review on synthesis of nano-TiO<sub>2</sub> via different methods. *J Nanostructures*, 2013; 3: 1-9.[DOI]
224. Chen X, Mao SS. Titanium Dioxide Nanomaterials: Synthesis, Properties, Modifications, and Applications. *Chem Rev*, 2007; 107: 2891-2959.[DOI]
225. Seifried S, Winterer M, Hahn H. Nanocrystalline Titania Films and Particles by Chemical Vapor Synthesis. *Chem Vap Depos*, 2000; 6: 239-244.[DOI]
226. Oh SM, Ishigaki T. Preparation of pure rutile and anatase TiO<sub>2</sub> nanopowders using RF thermal plasma. *Thin Solid Films*, 2004; 457: 186-191.[DOI]
227. Gablenz S, Voltzke D, Abicht HP et al. Preparation of fine TiO<sub>2</sub> powders via spray hydrolysis of titanium tetraisopropoxide. *J Mater Sci Lett*, 1998; 17: 537-539.[DOI]
228. Yu J, Zhao X. Effect of substrates on the photocatalytic activity of nanometer TiO<sub>2</sub> thin films. *Mater Res Bull*, 2000; 35: 1293-1301.[DOI]
229. Zhang Q, Li C. High Temperature Stable Anatase Phase Titanium Dioxide Films Synthesized by Mist Chemical Vapor Deposition. *Nanomaterials*, 2020; 10: 911.[DOI]
230. Sedky NK, Mahdy NK, Abdel-kader NM et al. Facile sonochemically-assisted bioengineering of titanium dioxide nanoparticles and deciphering their potential in treating breast and lung cancers: Biological, molecular, and computational-based investigations. *RSC Adv*, 2024; 14: 8583-8601.[DOI]

231. Aswini R, Murugesan S, Kannan K. Bio-engineered TiO<sub>2</sub> nanoparticles using *Ledebouria revoluta* extract: Larvicidal, histopathological, antibacterial and anticancer activity. *Int J Environ An Ch*, 2021; 101: 2926-2936.[DOI]
232. Danyliuk NV, Tatarchuk TR, Shyichuk AV. Batch microreactor for photocatalytic reactions monitoring. *PCSS*, 2020; 21: 338-346.[DOI]
233. Mbonyiriyivu A, Zongo S, Diallo A et al. Titanium dioxide nanoparticles biosynthesis for dye sensitized solar cells application: Review. *Phys Mater Chem*, 2015; 3: 12-17.[DOI]
234. Saikumari N, Preethi T, Abarna B et al. Ecofriendly, green tea extract directed sol - gel synthesis of nano titania for photocatalytic application. *J Mater Sci: Mater Electron*, 2019; 30: 6820-6831.[DOI]
235. Sundrarajan M, Bama K, Bhavani M et al. Obtaining titanium dioxide nanoparticles with spherical shape and antimicrobial properties using *M. citrifolia* leaves extract by hydrothermal method. *J Photoch Photobio B*, 2017; 171: 117-124.[DOI]
236. Hariharan D, Jegatha CA, Mayandi J et al. Visible light active photocatalyst: Hydrothermal green synthesized TiO<sub>2</sub> NPs for degradation of picric acid. *Mater Lett*, 2018; 222: 45-49.[DOI]
237. Thandapani K, Kathiravan M, Namasivayam E et al. Enhanced larvicidal, antibacterial, and photocatalytic efficacy of TiO<sub>2</sub> nanohybrids green synthesized using the aqueous leaf extract of *Parthenium hysterophorus*. *Environ Sci Pollut Res*, 2018; 25: 10328-10339.[DOI]
238. Gurrappa I, Binder L. Electrodeposition of nanostructured coatings and their characterization - A review. *Sci Technol Adv Mat*, 2008; 9: 043001.[DOI]
239. Hanaor D, Michelazzi M, Leonelli C et al. The effects of carboxylic acids on the aqueous dispersion and electrophoretic deposition of ZrO<sub>2</sub>. *J Eur Ceram Soc*, 2012; 32: 235-244.[DOI]
240. Jiang LC, Zhang WD. Electrodeposition of TiO<sub>2</sub> nanoparticles on multiwalled carbon nanotube arrays for hydrogen peroxide sensing. *Electroanal*, 2019; 21: 988-993.[DOI]
241. Wasserscheid P, Keim W. Ionic Liquids - New "Solutions" for Transition Metal Catalysis. *Angew Chem Int Ed*, 2000; 39: 3772-3789.[DOI]
242. Wasserscheid P, Welton T. Ionic liquids in synthesis. Wiley Vch Press: New Jersey, USA, 2008.
243. Ma Z, Yu J, Dai S. Preparation of Inorganic Materials Using Ionic Liquids. *Adv Mater*, 2010; 22: 261-285.[DOI]
244. Hong K, Yoo KS. Synthesis of TiO<sub>2</sub> hollow spheres using binary ionic liquids as an electrocatalyst. *Res Chem Intermed*, 2011; 37: 1325-1331.[DOI]
245. Mali SS, Betty CA, Bhosale PN et al. Hydrothermal synthesis of rutile TiO<sub>2</sub> nanoflowers using Brønsted Acidic Ionic Liquid [BAIL]: Synthesis, characterization and growth mechanism. *Cryst Eng Comm*, 2012; 14: 1920.[DOI]
246. He Z, Yue G, Gao Y et al. Efficient flexible dye-sensitized solar cells from rear illumination based on different morphologies of titanium dioxide photoanode. *J Semicond*, 2024; 45: 022801.[DOI]
247. Kakihana M, Kobayashi M, Tomita K et al. Application of Water-Soluble Titanium Complexes as Precursors for Synthesis of Titanium-Containing Oxides via Aqueous Solution Processes. *B Chem Soc Jpn*, 2010; 83: 1285-1308.[DOI]
248. Younus LA, Mahmoud ZH, Hamza AA et al. Photodynamic therapy in cancer treatment: properties and applications in nanoparticles. *Braz J Biol*, 2024; 84: e268892.[DOI]
249. Abdul-Reda HU, Mahmoud ZH, Alaziz KMA et al. Antimicrobial finishing of textiles using nanomaterials. *Braz J Biol*, 2024; 84: e264947.[DOI]
250. Mohammadkhani A, Mohammadkhani F, Farhadyar N et al. Novel nanocomposite zinc phosphate / polyvinyl alcohol / carboxymethyl cellulose: Synthesis, characterization and investigation of antibacterial and anticorrosive properties. *Case Stud Chem Environ Eng*, 2024; 9: 100591.[DOI]
251. Kianfar E. A review of recent advances in carbon dioxide absorption-stripping by employing a gas - liquid hollow fiber polymeric membrane contactor. *Polym Bull*, 2023; 80: 11469-11505.[DOI]
252. Yi Hsu C, Mahmoud ZH, Abdullaev S et al. Nanocomposites based on Resole / graphene / carbon fibers: A review study. *Case Stud Chem Environ Eng*, 2023; 8: 100535.[DOI]
253. AL-Salman HNK, Hsu CY, Nizar JZ et al. Graphene oxide-based biosensors for detection of lung cancer: A review. *Results Chem*, 2024; 7: 101300.[DOI]
254. Gong D, Grimes CA, Varghese OK et al. Titanium oxide nanotube arrays prepared by anodic oxidation. *J Mater Res*, 2001; 16: 3331-3334.[DOI]
255. Paulose M, Shankar K, Yoriya S et al. Anodic Growth of Highly Ordered TiO<sub>2</sub> Nanotube Arrays to 134µm in Length. *J Phys Chem B*, 2006; 110: 16179-16184.[DOI]
256. Ali G, Chen C, Yoo SH et al. Fabrication of complete titania nanoporous structures via electrochemical anodization of Ti. *Nanoscale Res Lett*, 2011; 6: 332.[DOI]
257. Parmon VN. Development of physico-chemical foundations of transformation solar energy by decomposing water into molecular photocatalytic systems [doctor's thesis]. *Novosibirsk*, 1984.
258. Shijubo N, Honda Y, Fujishima T et al. Lung surfactant protein-A and carcinoembryonic antigen in pleural effusions due to lung adenocarcinoma and malignant mesothelioma. *Eur Respir J*, 1995; 8: 403-406.[DOI]



259. Jasim SA, Ali MH, Mahmood ZH et al. Role of Alloying Composition on Mechanical Properties of CuZr Metallic Glasses During the Nanoindentation Process. *Met Mater Int*, 2022; 28: 2075-2082.[DOI]
260. Bokov DO, Mustafa YF, Mahmoud ZH et al. Cr-SiNT, Mn-SiNT, Ti-C<sub>70</sub> and Sc-CNT as Effective Catalysts for CO<sub>2</sub> Reduction to CH<sub>3</sub>OH. *Silicon*, 2022; 14: 8493-8503.[DOI]
261. Krakowiak R, Musial J, Bakun P et al. Titanium Dioxide-Based Photocatalysts for Degradation of Emerging Contaminants including Pharmaceutical Pollutants. *Appl Sci*, 2021; 11: 8674.[DOI]
262. Magaña-López R, Zaragoza-Sánchez PI, Jiménez-Cisneros BE et al. The Use of TiO<sub>2</sub> as a Disinfectant in Water Sanitation Applications. *Water*, 2021; 13: 1641.[DOI]
263. Yang X, Zhao R, Zhan H et al. Modified Titanium dioxide-based photocatalysts for water treatment: Mini review. *Environ Funct Mater* 2024 [Epub ahead of print].[DOI]
264. Khan M. Principles and mechanisms of photocatalysis. *Photocatalytic Syst Des*, 2021; 1: 1-22.[DOI]
265. Yadav HM, Kim JS, Pawar SH. Developments in photocatalytic antibacterial activity of nano TiO<sub>2</sub>: A review. *Korean J Chem Eng*, 2016; 33: 1989-1998.[DOI]
266. Hassan SA, Ghadam P. Introduction: Photocatalytic Properties of Metal-Based Nanoparticles. In: Handbook of Green and Sustainable Nanotechnology. Springer Publishing: New York, 2022; 1-25.
267. Sedita SR, Yasunori B, Naohiro S. Introduction: Pasteur scientists meet the market: An empirical illustration of the innovative performance of university-industry relationships. In: Innovation, Alliances, and Networks in High-Tech Environments. Routledge Publishing: London, 2015; 263-281.
268. Mills A, Le HS. An overview of semiconductor photocatalysis. *J Photoch Photobio A*, 1997; 108: 1-35.[DOI]
269. Munuera G, Gonzalez-Elipe AR, Rives-Arnau V et al. Photo-adsorption of oxygen on acid and basic TiO<sub>2</sub> surfaces. *Sud Surf Sci Catal*, 1985; 21: 113-126.[DOI]
270. Linsebigler AL, Lu G, Yates JT. Photocatalysis on TiO<sub>2</sub> Surfaces: Principles, Mechanisms, and Selected Results. *Chem Rev*, 1995; 95: 735-758.[DOI]
271. Watson SS, Beydoun D, Scott JA et al. The effect of preparation method on the photoactivity of crystalline titanium dioxide particles. *Chem Eng J*, 2003; 95: 213-220.[DOI]
272. Ohno T, Sarukawa K, Tokieda K et al. Morphology of a TiO<sub>2</sub> Photocatalyst (Degussa, P-25) Consisting of Anatase and Rutile Crystalline Phases. *J Catal*, 2001; 203: 82-86.[DOI]
273. Gerischer H, Heller A. Photocatalytic Oxidation of Organic Molecules at TiO<sub>2</sub> Particles by Sunlight in Aerated Water. *J Electro chem Soc*, 1992; 139: 113-118.[DOI]
274. Gao L, Zhang Q. Effects of amorphous contents and particle size on the photocatalytic properties of TiO<sub>2</sub> nanoparticles. *Scripta Mater*, 2001; 44: 1195-1198.[DOI]
275. Mohd Raub AA, Bahru R, Mohamed MA et al. Photocatalytic activity enhancement of nanostructured metal-oxides photocatalyst: A review. *Nanotechnol*, 2024; 35: 242004.[DOI]
276. Ahmed SN, Haide W. Heterogeneous photocatalysis and its potential applications in water and wastewater treatment: a review. *Nanotechnology*, 2018; 29: 342001. [DOI]
277. Tanos F, Razzouk A, Lesage G et al. A Comprehensive Review on Modification of Titanium Dioxide-Based Catalysts in Advanced Oxidation Processes for Water Treatment. *Chem Sus Chem*, 2024; 17: e202301139.[DOI]
278. Hamad TG, Salman TA. Green synthesis of titanium oxide nanoparticles using pomegranate leaf extract: Characterization and antibacterial activity evaluation: Proceedings of the AIP Conference. Baghdad, Iraq, 26-27 August 2023.[DOI]
279. Kubota Y, Shuin T, Kawasaki C et al. Photokilling of T-24 human bladder cancer cells with titanium dioxide. *Clin Oncol*, 1994; 70: 1107-1111.[DOI]
280. Sun S, Vikrant K, Kim KH et al. Titanium dioxide-supported mercury photocatalysts for oxidative removal of hydrogen sulfide from the air using a portable air purification unit. *J Hazard Mater*, 2024; 470: 134089.[DOI]
281. Shang H, Jia H, Zhang W et al. Surface Hydrogen Bond-Induced Oxygen Vacancies of TiO<sub>2</sub> for Two-Electron Molecular Oxygen Activation and Efficient NO Oxidation. *Environ Sci Technol*, 2023; 57: 20400-20409.[DOI]
282. Serpone N. Heterogeneous Photocatalysis and Prospects of TiO<sub>2</sub>-Based Photocatalytic DeNO<sub>x</sub>ing the Atmospheric Environment. *Catal*, 2018; 8: 553.[DOI]
283. Safni S, Patricia EO, Ollinovela T et al. Degradation of Phenol Using Sonolysis and Photolysis by TiO<sub>2</sub> / RHAC Catalyst and Analysis with Spectrophotometer UV-VIS and HPLC. *Al Kimiya*, 2023; 10: 50-56.[DOI]
284. Yamaguti K, Sato S. Photolysis of water over metallized powdered titanium dioxide. *J Chem Soc*, 1985; 81: 1237.[DOI]
285. Stevens CG, Wessman NJ, Bowman JE et al. Photolysis of water vapor on titanium / TiO<sub>2</sub> surfaces. *Chem Phys Lett*, 1982; 91: 335-338.[DOI]
286. Fujishima A, Honda K. Electrochemical Photolysis of Water at a Semiconductor Electrode. *Nature*, 1972; 238: 37-38.[DOI]
287. Nosaka Y. Water Photo-Oxidation over TiO<sub>2</sub> - History and Reaction Mechanism. *Catal*, 2022; 12: 1557.[DOI]
288. Bentouba S, Vajeeston P, Yohi S et al. TiO<sub>2</sub> as a Photocatalyst for Water Splitting - An Experimental and Theoretical Review. *Molecules*, 2021; 26: 1687.[DOI]

289. Ni M, Leung MKH, Leung DYC et al. A review and recent developments in photocatalytic water-splitting using TiO<sub>2</sub> for hydrogen production. *Renew Sust Energ Rev*, 2007; 11: 401-425.[DOI]
290. Al-Rasheed RA. Water Treatment by Heterogeneous Photocatalysis: An overview. 2005; 14: 1-15.
291. Jafari S, Mahyad B, Hashemzadeh H et al. Biomedical applications of TiO<sub>2</sub> nanostructures: recent advances. *Int J Nanomed*, 2020; 3447-3470.[DOI]
292. Lee SY, Park SJ. TiO<sub>2</sub> photocatalyst for water treatment applications. *J Ind Eng Chem*, 2013; 19: 1761-1769.[DOI]
293. Dharma HNC, Jaafar J, Widiastuti N et al. A Review of Titanium Dioxide (TiO<sub>2</sub>)-Based Photocatalyst for Oilfield-Produced Water Treatment. *Membranes*, 2022; 12: 345.[DOI]
294. Raya I, Mansoor AS, Widjaja G et al. ZnMoO<sub>4</sub> nanoparticles: Novel and facile synthesis, characterization, and photocatalytic performance. *J Nanostruct*, 2022; 12: 446-454.[DOI]
295. Mahmood ZH, Jarosova M, Kzar HH et al. Synthesis and characterization of Co<sub>3</sub>O<sub>4</sub> nanoparticles: Application as performing anode in Li-ion batteries. *J Chinese Chem Soc*, 2022; 69: 657-662.[DOI]
296. Bahadoran A, Jabarabadi M, Mahmood Z et al. Quick and sensitive colorimetric detection of amino acid with functionalized-silver / copper nanoparticles in the presence of cross linker, and bacteria detection by using DNA-template nanoparticles as peroxidase activity. *Spectrochim Acta A*, 2022; 268: 120636.[DOI]
297. Mahmoud ZH, AL-Bayati RA, Khadom AA. Electron transport in dye-sanitized solar cell with tin-doped titanium dioxide as photoanode materials. *J Mater Sci: Mater Electron*, 2022; 33: 5009-5023.[DOI]
298. Raya I, Widjaja G, Mahmood ZH et al. Kinetic, isotherm, and thermodynamic studies on Cr (VI) adsorption using cellulose acetate / graphene oxide composite nanofibers. *Appl Phys A*, 2022; 128: 167.[DOI]
299. Çeşmeli S, Biray Avci C. Application of titanium dioxide (TiO<sub>2</sub>) nanoparticles in cancer therapies. *J Drug Target*, 2019; 27: 762-766.[DOI]
300. Li Q, Wang X, Lu X et al. The incorporation of daunorubicin in cancer cells through the use of titanium dioxide whiskers. *Biomaterials*, 2009; 30: 4708-4715.[DOI]
301. Rivankar S. An overview of doxorubicin formulations in cancer therapy. *J Can Res Ther*, 2014; 10: 853.[DOI]
302. Wang Q, Huang JY, Li HQ et al. TiO<sub>2</sub> nanotube platforms for smart drug delivery: a review. *Int J Nanomed*, 2016; 11: 4819-4834.[DOI]
303. Raja G, Cao S, Kim DH et al. Mechanoregulation of titanium dioxide nanoparticles in cancer therapy. *Mat Sci Eng C*, 2020; 107: 110303.[DOI]
304. Akram MW, Raziq F, Fakhar-e-Alam M et al. Tailoring of Au-TiO<sub>2</sub> nanoparticles conjugated with doxorubicin for their synergistic response and photodynamic therapy applications. *J Photoch Photobio A*, 2019; 384: 112040.[DOI]
305. Inoue T, Fujishima A, Konishi S et al. Photoelectrocatalytic reduction of carbon dioxide in aqueous suspensions of semiconductor powders. *Nature*, 1979; 277: 637-638.[DOI]
306. Kurzmann C, Verheyen J, Coto M et al. In vitro evaluation of experimental light activated gels for tooth bleaching. *Photoch Photobio Sci*, 2019; 18: 1009-1019.[DOI]
307. Woolerton TW, Sheard S, Reisner E et al. Efficient and Clean Photoreduction of CO<sub>2</sub> to CO by Enzyme-Modified TiO<sub>2</sub> Nanoparticles Using Visible Light. *J Am Chem Soc*, 2010; 132: 2132-2133.[DOI]
308. Roy SC, Varghese OK, Paulose M et al. Toward Solar Fuels: Photocatalytic Conversion of Carbon Dioxide to Hydrocarbons. *ACS Nano*, 2010; 4: 1259-1278.[DOI]
309. Thampi KR, Kiwi J, Grätzel M. Methanation and photo-methanation of carbon dioxide at room temperature and atmospheric pressure. *Nature*, 1987; 327: 506-508.[DOI]
310. Kaya S, Krupin O, LaRue J et al. Real-time observation of surface bond breaking with an x-ray laser. *Science*, 2013; 339: 1302-1305.[DOI]
311. Farouk HU, Raman AAA, Daud WMAW. Surface transformations of TiO<sub>2</sub> anatase deactivated in methylene blue solution with Cl<sup>-</sup> ions in the colloid. *J of the Taiwan Inst of Chem Engin*, 2017; 80: 203-214.[DOI]
312. Zhang H, Banfield JF. Structural Characteristics and Mechanical and Thermodynamic Properties of Nanocrystalline TiO<sub>2</sub>. *Chem Rev*, 2014; 114: 9613-9644.[DOI]
313. Penn RL, Banfield JF. Morphology development and crystal growth in nanocrystalline aggregates under hydrothermal conditions: Insights from titania. *Geochim Cosmochim Ac*, 1999; 63: 1549-1557.[DOI]
314. Rahimi N, Pax RA, Gray EMacA. Review of functional titanium oxides. I: TiO<sub>2</sub> and its modifications. *Prog Solid State Ch*, 2016; 44: 86-105.[DOI]
315. Farouk HU, Raman AAA, Daud WMAW. TiO<sub>2</sub> catalyst deactivation in textile wastewater treatment: Current challenges and future advances. *J Ind Eng Chem*, 2016; 33: 11-21.[DOI]
316. Kääriäinen ML, Kääriäinen TO, Cameron DC. Titanium dioxide thin films, their structure and its effect on their photoactivity and photocatalytic properties. *Thin Solid Films*, 2009; 517: 6666-6670.[DOI]
317. Ta N, Liu J, Shen W. Tuning the shape of ceria nanomaterials for catalytic applications. *Chinese J Catal*, 2013; 34: 838-850.[DOI]
318. Lee K, Yoon H, Ahn C et al. Strategies to improve the photocatalytic activity of TiO<sub>2</sub>: 3D nanostructuring and heterostructuring with graphitic carbon nanomaterials. *Nanoscale*, 2019; 11: 7025-7040.[DOI]

319. Nakata K, Fujishima A. TiO<sub>2</sub> photocatalysis: Design and applications. *J. Photochem Photobiol C Photochem Rev*, 2012; 13: 169-189.[DOI]
320. Yang S, Xiong F, Chen K et al. Impact of Titanium Dioxide and Fullerenol Nanoparticles on Caco-2 Gut Epithelial Cells. *J nanosci nanotechnol*, 2018; 18: 2387-2393.[DOI]
321. Ayorinde T, Sayes CM. An updated review of industrially relevant titanium dioxide and its environmental health effects. *J Hazard Mater Lett*, 2023; 4: 100085.[DOI]
322. Bauer M, Lei C, Read K et al. Direct Observation of Surface Chemistry Using Ultrafast Soft-X-Ray Pulses. *Phys Rev Lett*, 2001; 87: 025501.[DOI]
323. Nematov, D. (2021). Investigation optical properties of the orthorhombic system CsSnBr<sub>3</sub>-xI<sub>x</sub>: application for solar cells and optoelectronic devices. *Journal of Human, Earth, and Future*, 2(4), 404-411.[DOI]
324. Nematov, D. D., Burhonzoda, A. S., Khusenov, M. A., Kholmurodov, K. T., & Ibrahim, M. A. (2019). The quantum-chemistry calculations of electronic structure of boron nitride nanocrystals with density Functional theory realization. *Egyptian Journal of Chemistry*, 62(The First International Conference on Molecular Modeling and Spectroscopy 19-22 February, 2019), 21-27. [DOI]
325. Dilshod, N., Kholmurzo, K., Aliona, S., Kahramon, F., Viktoriya, G., & Tamerlan, K. (2022). A DFT Study of Structure, Electronic and Optical Properties of Se-Doped Kesterite Cu<sub>2</sub>ZnSnS<sub>4</sub> (CZTSSe).
326. Nematov, D. (2024). Analysis of the optical properties and electronic structure of semiconductors of the Cu<sub>2</sub>NiXS<sub>4</sub> (X= Si, Ge, Sn) family as new promising materials for optoelectronic devices. *Journal of Optics and Photonics Research*, 1(2), 91-97.[DOI]
327. Nematov, D. D., Burhonzoda, A. S., Kholmurodov, K. T., Lyubchyk, A. I., & Lyubchyk, S. I. (2023). A detailed comparative analysis of the structural stability and Electron-Phonon properties of ZrO<sub>2</sub>: mechanisms of water adsorption on T-ZrO<sub>2</sub> (101) and T-YSZ (101) surfaces. *Nanomaterials*, 13(19), 2657.[DOI]
328. Nematov, D. (2023). Bandgap tuning and analysis of the electronic structure of the Cu<sub>2</sub>NiXS<sub>4</sub> (X= Sn, Ge, Si) system: mBJ accuracy with DFT expense. *Chemistry of Inorganic Materials*, 1, 100001.[DOI]

**Disclaimer/Publisher's Note:** The statements, opinions and data contained in all publications are solely those of the individual author(s) and contributor(s) and not of MDPI and/or the editor(s). MDPI and/or the editor(s) disclaim responsibility for any injury to people or property resulting from any ideas, methods, instructions or products referred to in the content.